Chair of Mining Engineering and Mineral Economics

Master's Thesis

Microwave irradiation treatment in the improvement of the performance of a Bucket Wheel Excavator

Elena Folgoso Lozano

February 2020

MONTANUNIVERSITÄT LEOBEN
www.unileoben.ac.at

AFFIDAVIT

I declare on oath that I wrote this thesis independently, did not use other than the specified sources and aids, and did not otherwise use any unauthorized aids.

I declare that I have read, understood, and complied with the guidelines of the senate of the Montanuniversität Leoben for "Good Scientific Practice".

Furthermore, I declare that the electronic and printed version of the submitted thesis are identical, both, formally and with regard to content.

Date 17.02.2020

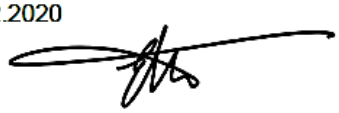

Signature Author
Elena, Folgoso Lozano

PREFACE, DEDICATION, ACKNOWLEDGEMENT

I would like to thank my adviser Mr. Dipl.-Ing. Dr. Mont Philipp Hartlieb, for the advice and suggestions during the time I was involved in this topic.

I also want to thank FL-Smidth for the help they provided me.

Especialmente, a mis padres y mi hermano, por su apoyo incondicional incluso en los peores momentos. No habría llegado hasta aquí sin vosotros.

ZUSAMMENFASSUNG

Der Schaufelradbagger, ist eine mechanische Baggermaschine für den Tagebau. Der Schaufelradbagger kann kontinuierlich arbeiten: Er gräbt, lädt und transportiert das Material gleichzeitig. Das Material, das ein Schaufelradbagger extrahieren kann, ist durch seine FestigKeit begrenzt. In der Regel können nur lose oder weiche Gesteinsarten wirtschaftlich verladen werden. Härtere Gesteine werden oft durch Sprengen vor dem Aushub mit einem Schaufelradbagger vorbehandelt.

Ziel dieser Arbeit ist es, zu zeigen, dass die Bandbreite des Materials, das ein Schaufelradbagger graben kann, durch eine Vorbehandlung des Materials mit Mikrowellenbestrahlung erweitert werden kann, um dessen mechanische FestigKeit zu reduzieren.

Die Demonstrationen bestehen im direkten Vergleich beider Situationen: behandeltes und unbehandeltes Material. Zuerst werden die Simulationen in einer hypothetischen Situation durchgeführt, wobei ein breites Spektrum von Materialeigenschaften basierend auf dem Gebirgsklassifikationssystem verwendet wird. Im zweiten Schritt beinhaltet die Simulationen reale Daten, die von Sensoren gewonnen werden, die auf einem Schaufelradbagger installiert sind. Zusätzlich wird die Energieverbrauchsbilanz berechnet, einschließlich der Daten der Maschinensensoren sowie der Daten aus Labortests zur Mikrowellenbehandlung- durchgeführt in früheren Untersuchungen zur Mikrowellenbestrahlung von Gesteinen.

Die Ergebnisse zeigen, dass nach der Mikrowellenbehandlung an einem bestimmten Material die auf das Schaufelrad ausgeübten Kräfte durch die Verringerung des Schnittwiderstands des Materials reduziert werden. Dadurch wird auch eine konsequente proportionale Reduzierung des Energieverbrauchs erreicht, was bestätigt, dass die Leistung der Schaufelradbagger Extraktion verbessert wird.

ABSTRACT

The Bucket Wheel Excavator, also known as BWE, is a mechanical excavation machine used in open pit mines, widely implemented in open pit coal mines. BWE can continuously work a regime: it digs, loads and hauls the material simultaneously. The material that a BWE can extract is limited by its strength. Normally, only loose or soft rock types can be loaded economically. Harder rocks are often preconditioned by blasting prior to excavation with a BWE.

This research is demonstrating that the range of the material that a BWE is able to dig can be widened by pretreating the material with microwave irradiation, in order to reduce its rock's mechanical strength.

The demonstrations consist of the direct comparison of both situations: treated and non-treated material. At first, the simulations are run in a hypothetical situation, using a wide range of material properties based on the Rock Mass Rating system. In the second step, the simulations include real data obtained by sensors installed on a BWE. Additionally, the energy consumption balance is calculated, including the data from the machine sensors as well as the data obtained in laboratory tests regarding the microwave treatment performed in previous research regarding microwave irradiation tests on rocks.

The results show that after the microwave treatment on a specific material, the forces applied to the bucket wheel are reduced, due to the decrease of the cutting resistance of the material. Therefore, as a consequence, a proportional reduction in energy consumption will be also achieved, which confirms that the performance of the BWE's extraction is improved.

TABLE OF CONTENTS

1 INTRODUCTION: THE BUCKET WHEEL EXCAVATOR

The Bucket Wheel Excavator, also known as BWE, is a mechanical excavation machine used in open pit mines, widely used in open pit coal mines. This machine can work continuous regime: digs, loads and hauls the material. The basic design of the BWE consists in a wheel where several buckets are assembled, and which, due to the rotation of the wheel, can dig into the material. Each machine can be modified depending on the operation and the material dug out. The lifetime of this type of excavator is approximately 20 years.

Figure 1 Bucket Wheel Excavator, model PE100 from FLSmidth. (flsmidth.com)

BWEs have been used in the excavation of shallow mineralization in cyclic operation. In Europe, the coal strata lie deep below the surface and normally they are parted, the direct dumping and striping operations—typically done by draglines and other big mining excavators—are no longer profitable. In these cases, the overburden must be removed first and transported to mined out areas, which may be far away from the active pit, increasing highly the extraction costs. Due to all these reasons and also because of the characteristics of them, BWEs have been used in brown surface coal.

The first sketches and designs of a BWE belong to Leonardo Da Vinci and appeared in a publication of excavating machines. However, the first implementation of this type of excavator took place in Germany, by Peltier. Until 1834 the steam engine was not assembled on the shovel. From 1863 until 1868, primitive bucket wheel excavators were used in the construction of the Suez's Chanel. However the basic layout of a BWE as are known now was unrecognizable until 1936, when a company settled in Leipzig patented it (U.S Department of Energy 1979; Rasper 1975).

1.1 Applicability

The applicability of the bucket wheel excavator is basically determined by the amount of material that must be extracted, which must be reasonably large to be feasible. As an example, in the United States, in the Illinois coal basin, these machines are extensively used due to the large dimensions of the mineralization. Additionally, it must be highlighted that several studies took place in these coal mines such as Bucket Wheel Excavator Study, (U.S Department of Energy 1979).

Generally, the topography is rather flat, which enhances the performance and the exposure of the deposit once the overburden is removed. Furthermore, the bucket wheel excavators need large surfaces of land in order to maneuver due to the large dimensions of their design. Those are the reasons why BWEs are limited to open pit mines as well as big construction sites, which normally are related to motorways, canals or dams.

Bucket wheel excavators can dig out easily loose material and soft rocks and up to now the applicability has been reduced to those situations. However, the ground is never ideal and as it happens in Europe, the soft layers of coal are located among boulders or layers of other harder rocks such as sandstone. Harder and abrasive rocks like sandstone may cause delays in the production or stops due to the incapability of the BWE to excavate those occurrences. The changes in the rock properties are also a large struggle for these machines as they have not been designed for that propose.

On the other hand, the diggable material range enlargement has been a point for long time. The larger the range of materials –regarding abrasiveness and strength— a BWE can get extracted the more efficient and more applicable will become. The

following chapters 1.1.1 and 1.1.2 list all the items regarding the advantages and disadvantages related to the BWE operation and extraction, which define the applicability of this machine and its feasibility.

1.1.1 Advantages of BWE

Among others, the literature describes these as the main advantages against other types of excavators:

- Bucket wheel excavators are the best solution for large tonnage of material; draglines and other type of excavators must be larger than BWE for the same payload.
- The working regime is continuous, not cyclic as draglines or regular excavators.
- Energy consumption per produced unit is approximately 65% of cable excavators.
- The dumping radius is larger.
- BWE works above and below the crawler tracks level, and the material extracted can be delivered at different levels.
- It can work in with different bench heights
- The material, which has been dug out and after hauled, can be dumped in several types of further haulage.
- After the machine has extracted a slice of material, the bench's slope is stable.
- Selective method.

1.1.2 Disadvantages of BWE

- High maintenance costs.
- Problems related to adverse weather conditions, such as snow or low temperatures.
- The material will be difficult to haul by the conveyor belt when the moisture content is rather high.
- BWEs are not flexible due to reduced maneuverability.
- High initial investment.

- The material that can be extracted is limited in terms of abrasiveness and strength.
- The infrastructure of the machine will suffer when the lithology changes dramatically or when there are lenses of hard material
- Depending on the size, the machine will not be able to transport boulders or load them.

1.2 BWE operation

The applicability of the machine is also defined by the type of operation, the movements and the dimensions of the main parts of the machine, such as the BW and the boom.

The basic operation can be split into two main movements:

- Wheel rotation
- Slewing of the arm

During operation the machine performs both movements at the same time, leaving a helical curve behind. A bucket cuts a slice of material from the front face, which width changes as the bucket moves. The literature defines the final movement that the machine describes as an ellipse, whose formula is described as follows:

$$\boldsymbol{ellipse} \rightarrow \ \mathbf{1} = \ (\mathbf{4}\ \ \boldsymbol{D^{-2}}\ \boldsymbol{z^2}) + (\mathbf{4}\ \boldsymbol{D^{-2}}\ \boldsymbol{sin^{-2}}\ \boldsymbol{\alpha_b}\ \ \boldsymbol{y^2}) \qquad \textbf{[1]}$$

Where,

- D = diameter of the BW
- $z\ and\ y$ = dimensions on the plane perpendicular to axis “x”
- α_b = slewed angle

In the Figure 2, the point “1a” corresponds with the pivot axis of the slewing movement. The “α_b “angle corresponds to the angle that the arm has been slewed, and “α_f “is the free space from the pivot point to the end of the working face.

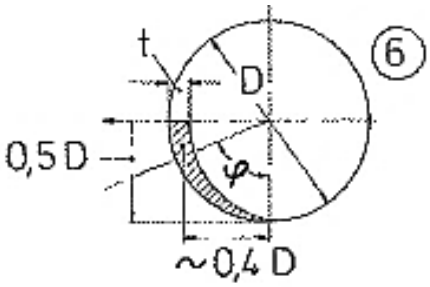

Figure 2 Sickle scheme (Bucket Wheel Excavator, 1988)

1.2.1 Full block operation

Full block method is the most economical mode when operating with a BWE, and basically consists in the total extraction of a block. Once the block is dug out, the BWE continues extracting the following block. The most critical issues is the haulage of the material, if the transportation of the mined out material fails, the operation must stop.

The block's volume is calculated as expressed in equation [2]:

$$\boldsymbol{Vb = H\ B\ L} \qquad \textbf{[2]}$$

Where,

- H = height of the block (m)
- B = block width (m)
- L = block length (m)

1.2.2 Types of operation

The selection of the type of operation depends on the selectivity needed as well as the geometric constrains of the design. In case of high selectivity, it could be possible to perform a mixed operation between terrace cut and drop cut.

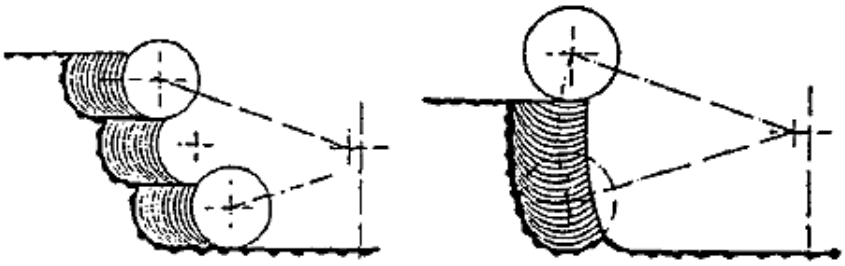

Figure 3 Terrace and drop cut basic scheme comparison (López Jimeno 1995).

1.2.2.1 Terrace cut operation

A terrace is the horizontal level of material in the working area, and it is defined by the block width, the boom length and the inclination of the slope; it is formed as the BWE advances forwards.

The height of the terrace must be optimized, and in any case, it can be larger than the following values show in expression [3]:

$$\mathbf{0.33}\ \boldsymbol{D} \leq \boldsymbol{h} \leq \mathbf{0.67}\ \boldsymbol{D} \qquad \textbf{[3]}$$

Where:

- D = the diameter of the BW

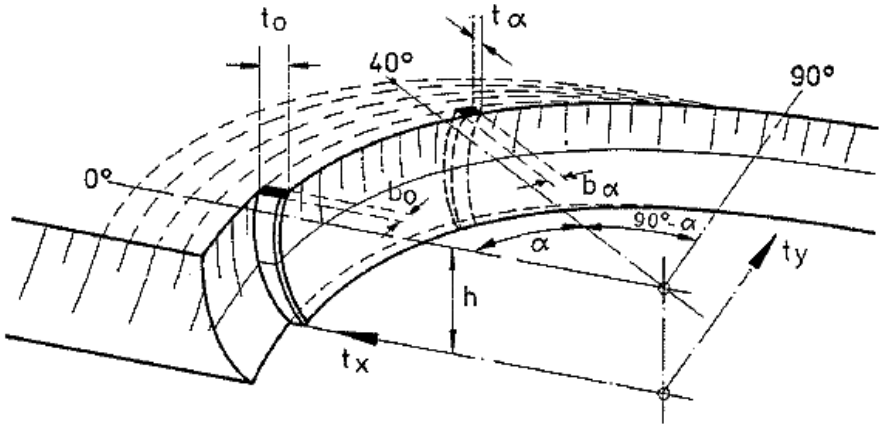

Figure 4 Geometric parameters of the design of a terrace (W. Durst and W. Vogt 1988)

The height of the terraces must be defined in a way that the final height of the block is going to be reached; this is the reason why generally, the “h” is defined as “½ D”. When advancing forwards, the individual cut should not exceed the largest penetration depth of the BW, 90% of the largest cut is usually adopted.

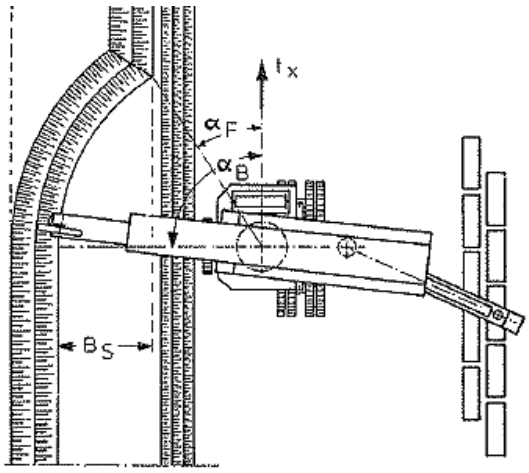

Figure 5 Overview of the terrace operation (W. Durst and W. Vogt 1988)

Each full sliced which is dug out from the terrace has sickle section, basically due to the swelling movement of the arm. The area cut off sickled—shaped is as follows:

$$\boldsymbol{Aa = t\alpha \,.\, h = to \,.\, h \,.\, cos\, \alpha} \qquad \textbf{[4]}$$

Where:

- $t\alpha$ = cutting depth t at α angle from x—axis
- h = cutting height
- to = cutting depth t at 0 angle from x—axis

Once the slice is cut and the limiting angle is reached, the arm must return to the initial position, at 0° from x—axis. Every sickled—shaped slice during the operation in the terrace is done the same. When the terrace is over, the machine must back up, low the arm until reach lower terrace, and then start the cycle again until it reaches the crawler level. Then the machine should advance until reach the new level of the working face.

1.2.2.2 Drop cut operation

This type of extraction consists on extract the material from the upper part of the bench until the lowest elevation. Once the first slice is cut off, the arm lifts the BW and advances to the second slice position.

In order to withdraw the whole sickle, the BWE must repeat the operation, slice by slice. The main issue about this procedure is that the first slices dug out are not that large, and several slices must be dug in order to reach the optimum extraction per cut. The result of this is a significant reduction on the overall performance.

It is possible to enhance the extraction ratio in the first slices by advance forwards—horizontally—in the upper part of the bench and dig the material in order to get the optimum surface for the following slices. However, a reduction in the performance will occur in any case.

However, in any case the arc of the cut can be greater than 2/3 of the diameter. Although many empirical studies claimed that, still nowadays machines dig the overburden with full diameter, in case of gravels and clays (U.S. Dept. of Energy, 1979).

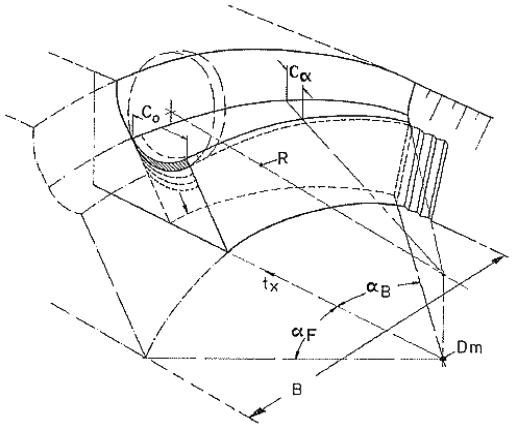

Figure 6 Geometric parameters of a drop cut operation. (W. Durst and W. Vogt 1988)

1.3 Problematic areas during extraction

The disadvantages of BWE's operation which were discussed in 1.1.2 chapter included some of the largest challenges these machines might face in the near future.

The main issues can be grouped in three classes:

1.3.1 Abrasiveness of the material

Abrasiveness is also other parameter that limits the performance of the BWE. A high abrasiveness value determines a higher maintenance cost, due to a larger need of stops to replace the cutting tools, as well as fix the bucket lip. Although those are the major issues during the extraction, an abrasive material may wear and even cut the belt of the conveyor. Replacing the belt may need several days of works, which means a long stop during the production. Edgy fragments may cause the same problems in the belt.

When the overburden contains high level of silica, the wear of the machine elements is rather high even if the material is not consolidated. There are some studies about machines that under these circumstances needed a replacement every 8 hours of work (U.S Department of Energy 1979). It is well known that worn teeth of cutting tools are have a lower performance than brand new ones, since need extra power in order to dig out the same amount of material.

1.3.2 Weather conditions

Open pit operations depend on the climate and ground conditions, especially the ones related to rainfall and snow. Clay lenses in the ground and shale rocks change their consistency and behavior when in contact with water, mainly because they turn tacky and they tend to adhere to the walls of the bucket wheel and other parts of the machine.

The whole operation becomes slower because of the decreased capacity of the bucket to load material. The conveyor may carry less material for the same reason. Furthermore, the extra weight of the clayey material will develop stresses on the system, which are critical for the belt.

1.3.3 Vegetative material

Before the operations start, the hummus layer and the rest of the vegetative matter should be totally removed from the pit. This fibrous material, such as roots, may

entangle around the BWE if the wheel is not able to cut them off. The entanglement of course will reduce the performance; in some cases, the machine should be stopped to clean it.

1.3.4 Hard rock occurrence

As the digging capability of BWE is reduced, in comparison with other machines, when a boulder or a lens or unexpected hard material is hit by the BW, the whole infrastructure of the excavator will suffer; including the cutting tools assemble in the buckets, the gear train, the wheel motor drive shaft. Additionally, these randomly located boulders of lenses cannot be loaded by the BW due to their size, which of course will cause the stop of the production until the boulders are removed from the working face.

The same situation may happen when the lithology changes and some hard strata are placed among the coal—layered deposit. These strata, even if they are hard but not thick, can be removed by the BWE. In this case, hardened cutting tools with special steel or harder coatings, as well as pre—cutters, are needed (U.S Department of Energy 1979).

This can be avoided by studying the geology and geotechnical parameters of the material extracted, reducing the uncertainty of their location. However, in many cases the mines do not have this geological study, and unfortunately, the experience showed that in those cases the mining companies are reluctant to invest money on one.

1.4 Excavate rock with a BWE

Excavating harder rocks with a BWE has always been a goal, as it would mean that the applicability of the BWE operation might be increased. The U.S. Energy Department (1989) suggested some ideas about the future development of a BWE capable of digging rock. For example, a shear wheel must be developed, stronger materials must be used, and the production speed will have to be lowered, in order to achieve this goal.

The reduction in the velocity of advance and extraction has two major reasons:

- Reduce the impacts in the conveyor belt and allow it to evacuate the material properly.
- As the forces needed to extract rock are larger than soil material, more time will be needed to achieve it when the power remains the same.

1.5 Benefits of microwave irradiation

Nowadays, one of the biggest challenges that a BWE faces is the occurrence of hard rocks, as explained in 1.1 Applicability chapter. It is reasonable that if the issues regarding the material properties, abrasiveness and strength, are reduced, the impact of the unexpected harder rocks during the production will be decreased.

It was demonstrated that the microwave irradiation on rock produces cracks in large and small scale which reduce the mechanical properties of it, and therefore the excavation difficulty is reduced. Therefore, microwave irradiation is a plausible solution for this issue and to face the hard rock extraction challenge.

Among other, the following aspects are involved when applying microwaves on the rock:

- **Enhance the applicability of BWE in terms of larger range of material**

The scope of this study is based on this point: enlarge the range of material in terms of strength (UCS) and RMR. The bigger the range of material that the BWE would be able to dig out, the more versatile and adaptable to the surroundings and environment the BWE would turn.

- **Reduction of impacts against boulders or stronger and harder inclusions, such as sandstone strata among the coal seams.**

In Europe, the coal seams generally are associated with sandstone strata inclusions, which make the extraction of the coal more difficult by continuous and large-scale machinery, like draglines and BWE.

The pretreatment by microwave irradiation would reduce the impact of the boom of the machine due to the occurrence of those inclusions of harder material. The

treatment could be used locally on those hard areas to reduce the forces which cause major issues on the structure of the machine.

- **Decrease the installed power in the BWE**

The lowering of the power needed to extract a certain material is a direct consequence of the mitigation of the cutting resistance of the material, Ke. The cutting resistance is parameter which defines the capability of a material to be dug out or diggability. Ke is explained more in detail in the following chapters.

2 MECHANICAL EXCAVATION AND INFLUENCE OF ROCK PARAMETERS

In this chapter, mechanical excavation just related to the bucket wheel and the cutting tools are reported, as the topic of this study is limited to the mechanical behavior of rocks.

2.1 Cutting resistance

The cutting resistance, commonly called Ke, is a term directly related to the capability of digging out material by an excavator, which basically expresses the relation between the force applied by the bucket and its area, in N/cm^2.

The cutting resistance is the main concept of this study, as it relates the RMR conditions of the rock and the productivity of a BWE.

The relation regarding the properties of the ground dug out by a BWE and the cutting resistance of the material has been defined empirically after laboratory tests and the following formulas ([5] and [6])came out (Andras et al. 2016):

$$Es = 0.85830681\ \sigma rc^{2.162328} C^{-0.413209357}\ \varphi^{-1.04675} \quad [5]$$

$$A = 3.72432675\ \sigma rc^{1.592777} C^{0.348245478} \varphi^{-0.98134} \quad [6]$$

Where:

- Es = Specific energy consumption, (MPa)
- A = Specific cutting resistance, (kN/m)
- σrc = unconfined rock strength (MPa)
- C = cohesion (MPa)
- φ = friction angle (°)

Several authors created data bases or wrote reports in other units, N/m or kN/m, which represent the value of the specific cutting resistance, named A. The relation between A and Ke is shown in the equation [7]:

$$Ke = \frac{A}{10 * to} \quad [7]$$

Where:

- Ke: cutting resistance (N/cm^2)
- A**:** specific cutting resistance (kN/m)
- to: cutting depth (cm), depends on the dimensions of the BWE

Commonly, the Oreinstein and Koppel (O&K) laboratory test is used to define the cutting resistance of the cutting tools of a BWE (Bölükbaşsi et al. 1991). The dimensions must follow the strict standards and the tests were carried out from horizontal to vertical set up.

According to the data from the Table 2 it can be defined that the limits of BWE diggability based on Ke values are the following ones:

- Lower limit: 0.8 N/cm2 (Kozlowski)
- Upper limit: 2.64 N/cm2 (Canmet)

The differences between the different authors and procedures, are defined by the material and the size of the specimens used in addition to the anisotropy of the materials.

Table 1 Values of the cutting resistance and class of material regarding different methods (Bölükbaşsi et al. 1991)

Criteria	Class	Cutting resistance from O&K test (N/cm2)	Criteria	Class	Cutting resistance from O&K test (N/cm2)
Highvale	Easy	0 - 0,6	Canmet	Easy	0 - 1
	Diggable	0,6 - 1,1		Diggable	1 - 1,5
	Hard	1,1 - 1,4		Hard	1,5 - 2,4
	Marginal	1,4 - 1,8		Marginal	>2,4
	Undiggable	>1,8		Undiggable	-
Goonyella	Easy	0,15 - 0,45	Kozlowski	Easy	0 - 0,17
	Diggable	0,45 - 0,6		Diggable	0,17 - 0,36
	Hard	0,6 - 0,75		Hard	0,36 - 0,54
	Marginal	0,75 - 1		Marginal	0,54 - 0,8
	Undiggable	>1		Undiggable	>0,8
Neyveli	Easy	-	Krzanowski	Easy	0 - 0,27
	Diggable	<1,1		Diggable	0,27 - 0,9
	Hard	1,1 - 2,3		Hard	0,9 - 1,85
	Marginal	-		Marginal	-
	Undiggable	>2,3		Undiggable	>1,85

2.1.1 Materials cutting resistance

The Ke value, as it was explained before, is really an important parameter to define the diggability of the BWE, which also means its applicability and even the working regime of the machine.

Due to these reasons, there are tables which contain the ranges of A (specific cutting resistance, N/cm) values for materials according to their nature and/or composition, such as Table 2

2.2 Working regime of a BWE and its relation with the Ke

In order to identify how a machine works under certain circumstances, the simplest way is to define a set of formulas, thus the behavior of the machine can be shown in graphs. This is much easier method and more effective to identify problems during production.

Table 2 Specific cutting resistance (A) of different materials (López Jimeno 1995)

Material	N/cm	Material	N/cm
Sand	100 - 400	Soft sandstone	700 - 1600
Silt	200 - 400	Hard sandstone	1600 - 2800
Sandy clay	100 - 500	Gypsum	500 - 1300
Fine gravel	200 - 500	Phosphates	800 - 2000
Coarse gravel	200 - 800	Limestone	1000 - 1800
Sandy silt	200 - 600	Metheorized granite	500 - 1000
Wet clay	300 - 650	Unconsolidadted alluvium	300 - 600
Dry clay	500 - 1200	Medium consolidated alluvium	500 - 800
Schistose clay	350 - 1200	Coal	500 - 1000
Clayey sand	200 - 650	Frozen coal	1000 - 1600
Clayey shale	500 - 1600	Lignite	200 - 700
Shale	700 - 2000	Limonite	1900 - 2100

2.2.1 Description of the method

The formulas [8] and [9] (Marin Silviu et al. 2008) were used to identify the working behavior of the BWE, and are based on the Ke concept.

- Average cutting force Fxm, in the X axis (N):

$$\boldsymbol{\theta = 0} \qquad \boldsymbol{Fxm = Kuz\ Ke\ Stm} \qquad \textbf{[8]}$$

$$\boldsymbol{\theta \neq 0} \qquad \boldsymbol{Fxm\ (\theta) = Kuz\ Ke\ St(\theta)} \qquad \textbf{[9]}$$

Where:

- Kuz = cutting tool wear:
  - New: Kuz = 1
  - Average worn: Kuz = 1.2—1.5
  - Very worn: Kuz = 2
- Ke= specific resistance of the excavated material to the cutting force, (N/cm2)
- Stm = transversal section of the chip dug out
- θ = positioning angle of the bucket when extracting the material, Fxm = 0 when θ = 90°.

- The resultant cutting force FxR on the wheel in the X axis, (N):

$$\boldsymbol{FxR = nca\ \ Fxm} \qquad \textbf{[10]}$$

Where:

- nca = active buckets in a period, defined as follows:

$$\boldsymbol{nca = nc\left(\frac{\alpha 0}{2\pi}\right) = nc\ \frac{arc\ cos\left(1 - \frac{H}{R}\right)}{2\pi}} \qquad \textbf{[11]}$$

Where:

- nc = number of buckets on the wheel
- $\alpha 0$ = chipping angle
- H = height of dug out slice
- R = cutting radius

- Penetration force Fym, in the Y axis, (N):

$$\boldsymbol{Fym = Ky\ Kuz\ Ke\ Stm = \frac{Fy}{Fx}\ Kuz\ \ Ke\ \ Stm} \qquad \textbf{[12]}$$

Ky describes de ratio between the acting force on the Y axis, Fy, and the acting force on the X axis, Fx.

- Resultant penetration force FyR on the Y axis, (N):

$$\boldsymbol{FyR = \ Ky\ Kuz\ Ke\ Stm\ nca} \qquad \textbf{[13]}$$

- Lateral force Fzm, in the Z axis, (N):

$$\boldsymbol{Fzm = \ Kz\ Kuz\ Ke\ Stm} \qquad \textbf{[14]}$$

As well as Ky, Kz is the ratio between the lateral force,Fz and the penetration force Fx.

- Resultant lateral force FzR on the Z axis, (N):

$$\boldsymbol{FzR = Kz\ FxR} \qquad \textbf{[15]}$$

- Power necessary to excavate, *Pex,* there are two ways, (kW):

1. $$\boldsymbol{Pex = 10^{-3}\ FxR\ \ vt} \qquad \textbf{[16]}$$

Where:

- vt = cutting speed of the BW

2. $$\boldsymbol{Pex} = \frac{\mathbf{1}}{\mathbf{360}}\ \boldsymbol{Kuz\ Ke\ Qm} \quad \textbf{[17]}$$

- Qm = excavating capacity of BW

- Required power, P, to operate the BW, (kW):

$$\boldsymbol{P} = (\ \boldsymbol{Ke1\ Ke} + \boldsymbol{Ke2})\ \boldsymbol{Qt} \quad \textbf{[18]}$$

- Cutting capacity, Qt, (m3/h):

$$\boldsymbol{Qt} = \frac{\boldsymbol{P}}{\boldsymbol{Ke1\ Ke} + \boldsymbol{K2}} \quad \textbf{[19]}$$

- $Ke1$, (dimensionless):

$$\boldsymbol{Ke1} = \frac{\boldsymbol{Kuz}}{\mathbf{3.6\ 10^2}\ \boldsymbol{Ka\ nt}} \quad \textbf{[20]}$$

Ke1 describes the maximum value of the cutting resistance that the machine can dig out before the machine performs out from the established working regime.

Above Ke1:

- The extracted volume (Qt) decreases
- The power needed (P) rises beyond the installed (real) power

- $Ke2$, (kWh/m3):

$$\boldsymbol{Ke2} = \boldsymbol{g\ \rho}\frac{\boldsymbol{D} - \frac{\boldsymbol{H}}{\mathbf{2}} - \frac{\mathbf{2}}{\mathbf{3}}\ \boldsymbol{hc}}{\mathbf{3.6\ 10^3}\ \boldsymbol{Ka\ nt}} \quad \textbf{[21]}$$

Where:

- ρ = density of the material
- g = gravity constant
- Ka = bulk coefficient of the material dug out
- nt = performance of the transmission of the rotor to the wheel
- hc = active height of BW
- D = diameter of BW
- H = height of the slice cut off, cutting height

Ke2 defines the minimum power required to extract the maximum material, which is not a restrictive value as Ke1 is, but defines the minimum values of the profitable or minimum performance that the machine should achieve.

2.2.2 Verification of the method

These formulas and parameters have been calculated and compared with the results given by (Marin Silviu et al.) in order to confirm that they work with the machine object of this study. The comparison of the data can be seen in the following graphs: Figure 7, Figure 8 and Figure 9. The input data can be shown in the Annex I: Parameters of the BWE.

In these plots, the volume extracted (right vertical axis) and the power needed (left vertical axis) are plotted for the whole range of the cutting resistance of the material (Ke, horizontal axis). Those graphs represent a simple way to identify if the machine can perform properly, between the limits Ke1 and Ke2, according with the material properties.The volume extracted (Q) and the theoretical extracted volume (Q nominal, determined by the machine working regime) values are referred to the left vertical axis, in m^3/h. The nominal power (Nominal P determined by the machine working regime) and the extraction power (P) are referred to the right axis in kW.

Figure 7, Figure 8 and Figure 9 display the different working regimes of three BWE. All of them show the limits Ke1 and Ke2. Ke1, the upper limit value, is the intersection of the lines of volume extracted and at the same time, the same value corresponds to the intersection of the extraction power lines. It is calculated by using equation [20]. As it has already been described, the Ke1 defines the upper limit of the optimum range of working regime for a specific BWE.

Ke2 on the other hand is the lower limit and defines the minimum amount of material that must be dug out in order to maintain the productivity of the machine. In this case, Ke2 values do not refer to any intersection between the lines: it is directly calculated from the equation [21].

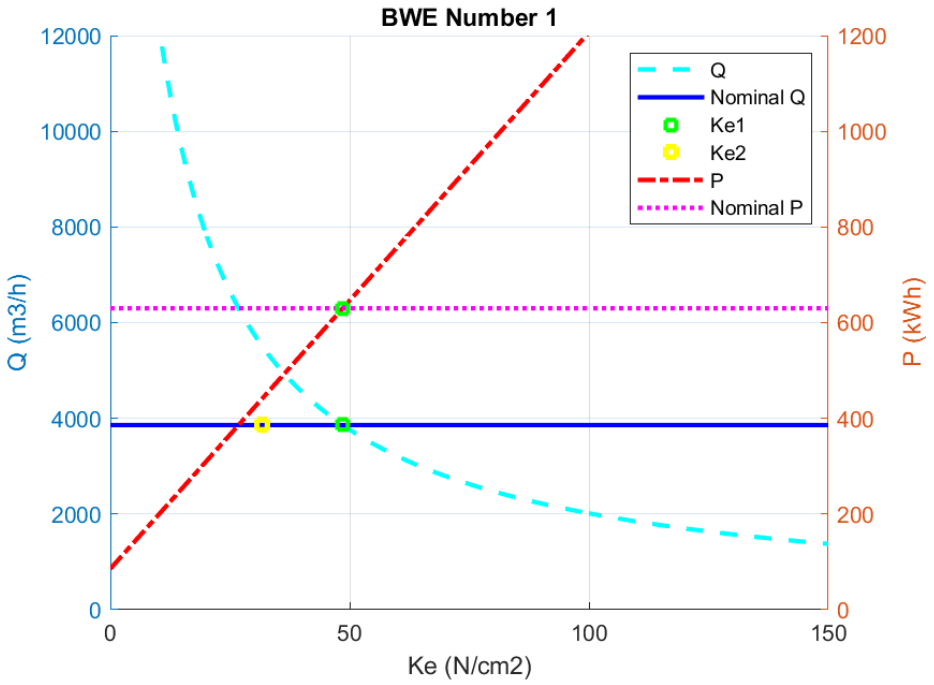

Figure 7 BWE model EsRc 1400·30/7·630. Nominal power 630 kW, BW diameter 14 m (Marin Silviu et al.)

All these graphs (Figure 7, Figure 8 and Figure 9) have the same structure but the values of the limits Ke1 and Ke2 are different. The values of the charts are related to technical and design issues. EsRc 1400·30/7·630 BWE has a bigger diameter than SRs 1300·26/3.5·500, and also EsRc 1400·30/7·630 has a higher nominal power. As a consequence of this differences and according to the equations from [8] to [21], EsRc 1400·30/7·630 shows a larger range of Ke values.

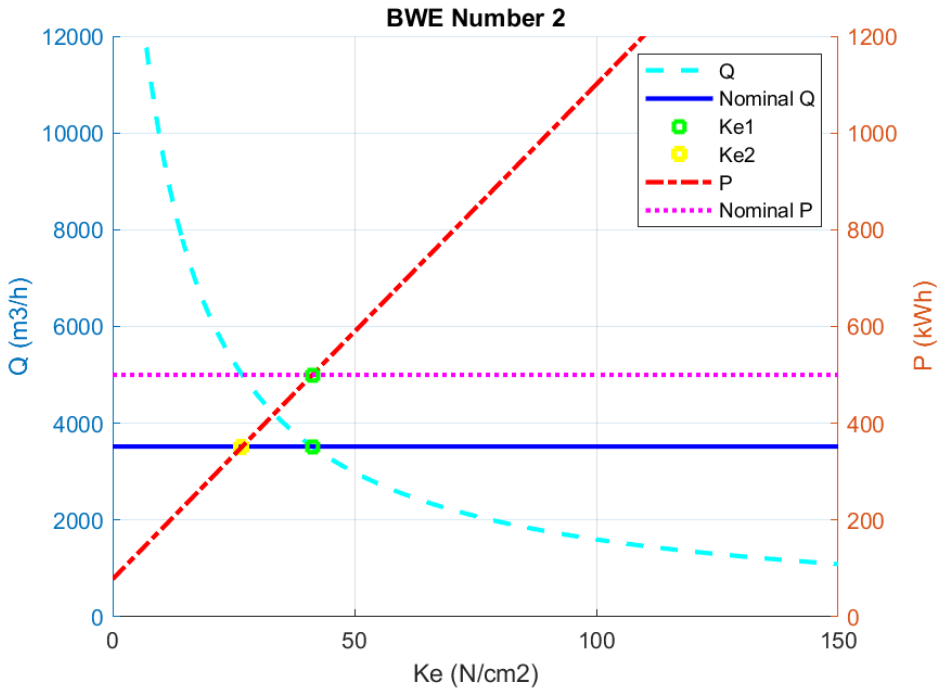

Figure 8 BWE model SRs 1300·26/3,5·500. Nominal power 500 kW. BW diameter 11 m. (Marin Silviu et al.)

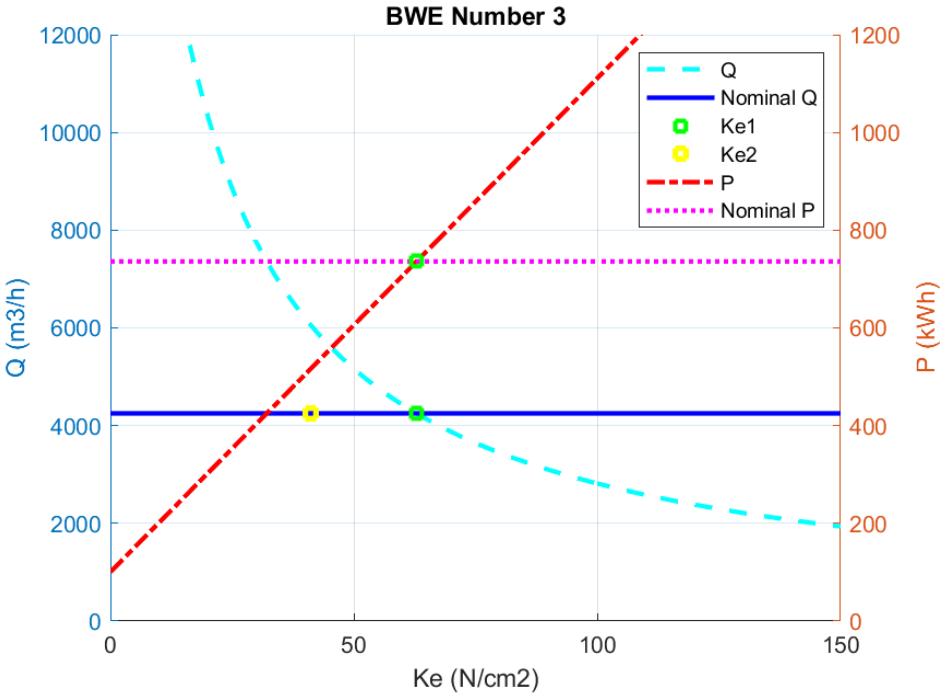

Figure 9 Object BWE of this study working regime attending the method proposed. Nominal power 760 kW.

The same reasons can be applied to the object BWE, which actually has the highest BW diameter and the highest nominal power. In this case, the Ke1 value is 65 N/cm^2 and the Ke2 is 41 N/cm^2. Comparing Figure 7, Figure 8 and Figure 9 is noticeable that the optimum range, thus range between Ke1 and Ke2, is larger in the case of the object BWE.

2.3 Rock mass classifications

The parameters of the rock mass have been widely studied. There are several methods to rate the characteristics of the rock mass. Stress and strain of the rocks and minerals have been also the target of many researchers.

2.3.1 Rock mass rating, RMR_{89}

Bieniawski defined the RMR first in 1973, and over the years it has been modified, and currently the most spread version is RMR_{89}. The RMR classification is divided in five main rock parameters which are rated through in Table 3, and then the sum of all these rates is the final RMR_{89} (Brady and Brown 2004).

Parameters to estimate the RMR_{89}:

- Strength of the intact rock material
- Rock Quality Designation
- Spacing of the joints
- Joint conditions
- Groundwater conditions
- The RMR is a value which goes from 0 to 100, and it gives a description of the rock mass quality, according to the parameters of the Table 3. The column “Rating” in the table indicates the maximum value that can be obtained from each parameter. As the RMR maximum value is 100, it can be said that the maximum “Rating” is also the percentage of influence of each parameter in the final RMR value.

Table 3 Input parameters for the calculation of the initial RMR

	Parameters	Range of values	Rating
a)	**Uniaxial Compressive strength, UCS (MPa)**	30 — 60	15
b)	**Drill core quality, RQD (%)**	25 — 75	20
c)	**Spacing discontinuities (mm)**	50 — 500	20
d)	**Ground water, general conditions**	Dry — flowing	15
e)	**Discontinuity length, persistence or continuity of the joints (m)**	0 — 10	6
f)	**Separation or Aperture of the joints (mm)**	0 — 5	6
g)	**Roughness of the joints**	Very rough —slickensided	6
h)	**Infilling or gouge of the joints**	None —5 mm	6
i)	**Weathering of the joints**	Unweathered —Highly weathered	6

It can be easily seen in the table that, the parameters related to jointing and discontinuities have a high influence on the RMR, the 50% of it. Therefore, it is confirmed that the more fractures on the rock, the lower the RMR will be. This is actually one of the base points of this study. However, the microwave irradiation will only have effects on the spacing of the joints, which means only change the RMR_{89} by 15%. The RMR value is associated with some ranges for the friction angle and cohesion, which must be defined since are necessary for further calculations (see lower part of Figure 10).

2.3.2 RMR_{14}

Some years ago, some modifications on the RMR_{89} were published, which in this case was renamed RMR_{14} (Celada et al. 2014). After more than 2000 study cases, a correlation between RMR_{89} and RMR_{14} was also established. The equation [22]is used in the range of 10 to 80 RMR_{89}.

$$RMR_{14} = 1.1 * RMR_{89} + 2 \quad [22]$$

A. CLASSIFICATION –PARAMETERS AND THEIR RATINGS									
Parameter			Range of values						
1	Strength of intact rock material	Point-load strength index	>10 MPa	4 - 10 MPa	2 - 4 MPa	1 - 2 MPa	For this low range - uniaxial compressive test is preferred		
		Uniaxial comp. strength	>250 MPa	100 - 250 MPa	50 - 100 MPa	25 - 50 MPa	5 - 25 MPa	1 - 5 MPa	< 1 MPa
	Rating		15	12	7	4	2	1	0
2	Drill core Quality *RQD*		90% - –100%	75% - –90%	50% - 75%	25% - 50%	< 25%		
	Rating		20	17	13	8	3		
3	Spacing of discontinuities		> 2 m	0.6 - 2 . m	200 - 600 mm	60 - 200 mm	< 60 mm		
	Rating		20	15	10	8	5		
4	Condition of –discontinuities (See E)		Very rough –surfaces Not continuous No separation Unweathered wall rock	Slightly rough surfaces Separation < 1 mm Slightly weathered walls	Slightly rough surfaces Separation < 1 mm Highly weathered walls	Slickensided surfaces or Gouge < 5 mm thick or Separation 1-5 mm Continuous	Soft gouge >5 mm thick or Separation –> 5 mm Continuous		
	Rating		30	25	20	10	0		
–5	Ground water	Inflow per 10 m tunnel length (l/m)	None	< 10	10 - 25	25 - 125	> 125		
		(Joint water press)/ (Major principal σ)	0	< 0.1	0.1, - 0.2	0.2 - 0.5	> 0.5		
		General conditions	Completely dry	Damp	Wet	Dripping	Flowing		
	Rating		15	10	7	4	0		

B. RATING ADJUSTMENT FOR DISCONTINUITY ORIENTATIONS (See F)						
Strike –and dip orientations		Very favourable	Favourable	Fair	Unfavourable	Very Unfavourable
Ratings	Tunnels & mines	0	-2	-5	-10	-12
	Foundations	0	-2	-7	-15	-25
	Slopes	0	-5	-25	-50	

C. ROCK MASS CLASSES DETERMINED FROM TOTAL RATINGS					
Rating	100 ← 81	80 ← 61	60 ← 41	40 ← 21	< 21
Class number	I	II	III	IV	V
Description	Very good rock	Good rock	Fair rock	Poor rock	Very poor rock

D. MEANING OF ROCK CLASSES					
Class number	I	II	III	IV	V
Average stand-up time	20 yrs for 15 m span	1 year for 10 m span	1 week for 5 m span	10 hrs for 2.5 m span	30 min for 1 m span
Cohesion of rock mass (kPa)	> 400	300 - 400	200 - 300	100 - 200	< 100
Friction angle of rock mass (deg)	> 45	35 - 45	25 - 35	15 - 25	< 15

E. GUIDELINES FOR CLASSIFICATION OF DISCONTINUITY conditions					
Discontinuity length (persistence) Rating	< 1 m 6	1 - 3 m 4	3 - 10 m 2	10 - 20 m 1	> 20 m 0
Separation (aperture) Rating	None 6	< 0.1 mm 5	0.1 - 1.0 mm 4	1 - 5 mm 1	> 5 mm 0
Roughness Rating	Very rough 6	Rough 5	Slightly rough 3	Smooth 1	Slickensided 0
Infilling (gouge) Rating	None 6	Hard filling < 5 mm 4	Hard filling > 5 mm 2	Soft filling < 5 mm 2	Soft filling > 5 mm 0
Weathering Ratings	Unweathered 6	Slightly weathered 5	Moderately weathered 3	Highly weathered 1	Decomposed 0

F. EFFECT OF DISCONTINUITY STRIKE AND DIP ORIENTATION IN TUNNELLING**			
Strike perpendicular to tunnel axis		Strike parallel to tunnel axis	
Drive with dip - Dip 45 - 90°	Drive with dip - Dip 20 - 45°	Dip 45 - 90°	Dip 20 - 45°
Very favourable	Favourable	Very favourable	Fair
Drive against –dip - Dip 45-90°	Drive against –dip - –Dip 20-45°	–Dip 0-20 - Irrespective of strike°	
Fair	Unfavourable	Fair	

* Some conditions are mutually exclusive . –For example, if infilling is present, the roughness of the surface will be overshadowed by the influence of the gouge. –In such cases use A.4 directly.
** Modified after Wickham et al (1972).

Figure 10 Geomechanics classification of jointed rock masses (Z. T. Bieniawski 1989)

2.3.3 Geological Strength index, GSI

GSI rating system for the rock masses was first defined in 1995. It was developed in order to reduce some joint measurement defects. GSI was specifically created for discontinuous rock masses that influence the strength and deformation characteristics (Brady and Brown 2004). The GSI and the RMR_{89} are related, and several researchers proposed different methods and equations to establish a relation between them.

Although both methods consider joint parameters and rock conditions, the further calculations, which will establish a relationship between rock mass structure and BWE performance were done using the RMR_{89}.

The reasons behind the selection of the RMR_{89} are simple:

- It is more well known
- Nowadays is still in use, even when there is a new update version (RMR_{14})
- The researches on this topic still use this system.

2.4 Relation between the RMR and Ke

In this chapter the relation between the rock parameters, which are also involved in the calculation of the RMR, and the Ke is explained. As the formulas to calculate the specific energy consumption and the specific cutting resistance were empirically obtained (formulas [5] and [6]), the behavior of all the parameters was studied, including specific cases and the general case, with all possibilities involved.

The target of this chapter is demonstrated that the reduction of the RMR, due to the increasing number of fractures, has a direct impact on the Ke which can be exploited for higher productivity of the BWE.

- **Calculation of all options possible, regarding the values of RMR:**

At first and in order to evaluate the behavior of the method, the input data describes all the possibilities regarding all the rock parameters which are included in the RMR calculation. As a result, the RMR values, split in different ranges, are linked to friction angle and cohesion values (see Table 4). The RMR is not involved in these first calculations in a direct way but instead the UCS is used.

The range of UCS higher than 200 MPa was omitted, as the values are too large for the application range of BWE and therefore regarded as meaningless for the present study. The main reason to omit the values above 200 MPa is simple: the maximum UCS value that a regular BWE can dug out in a proper working regime is rather small (around 30 MPa, depending on several other parameters). 200 MPa is really far from that limitation and thus, for a first approach, the values above 200 MPa are avoided. At this point, formulas [6] and [7] were used.

Table 4 Relation between UCS, cohesion and friction angle. Input data for the formulas [6] and [7]

UCS (MPa)	Cohesion (KPa)	Friction angle (°)
>250	>400	>45
100—250	300—400	35—45
50—100	200—300	25—35
25—50	100—200	15—25
0—25	0—100	0—15

Figure 11, Figure 12 and Figure 13 describe the current situation. The reason why they seem to have steps is due to the ranges of values of the Table 4. The range 1 defines the behavior of the UCS range of 250 to 100 MPa, which has the highest values and it can be noticed in Figure 11. The range 2 refers to UCS 50-100 MPa which still has rather high values. Ranges 2 and 1 (UCS 25—50 and 0—25 MPa, respectively) show lower values and in a suitable range to be extracted by a BWE.

The ranges are used in the calculations in order to reduce the amount of options possible which go up to millions of choices. Additionally, as the RMR values are linked to those ranges of cohesion and friction angle, more realistic results can be expected.

The results and the comparisons in this chapter are featured by specific cutting resistance A (kN/m) due to the fact that to calculate Ke (N/cm^2) BWE specific design parameters are needed and at this point only the general results, and not the specific

machines, are discussed. In addition, the results shown in this chapter may be compared with data displayed in Table 2.

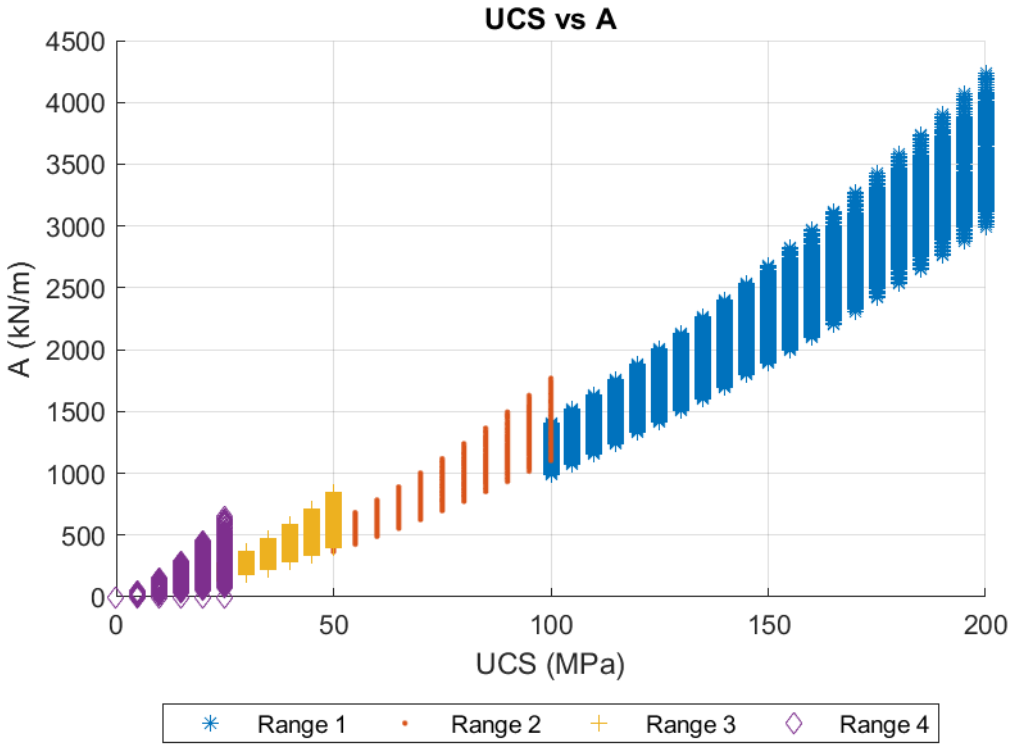

Figure 11 UCS (MPa) ranges show different behavior in the graph and different ranges of A (kN/m)

Figure 11 shows that the cutting resistance enhances rapidly when increasing UCS. The results displayed in Figure 11 were expected since in Table 2 reveals that hard rocks (hard sandstone e.g.), which is expected to have a higher UCS value than a soft one (soft sandstone), features a higher specific cutting resistance (Ke) than a soft one.

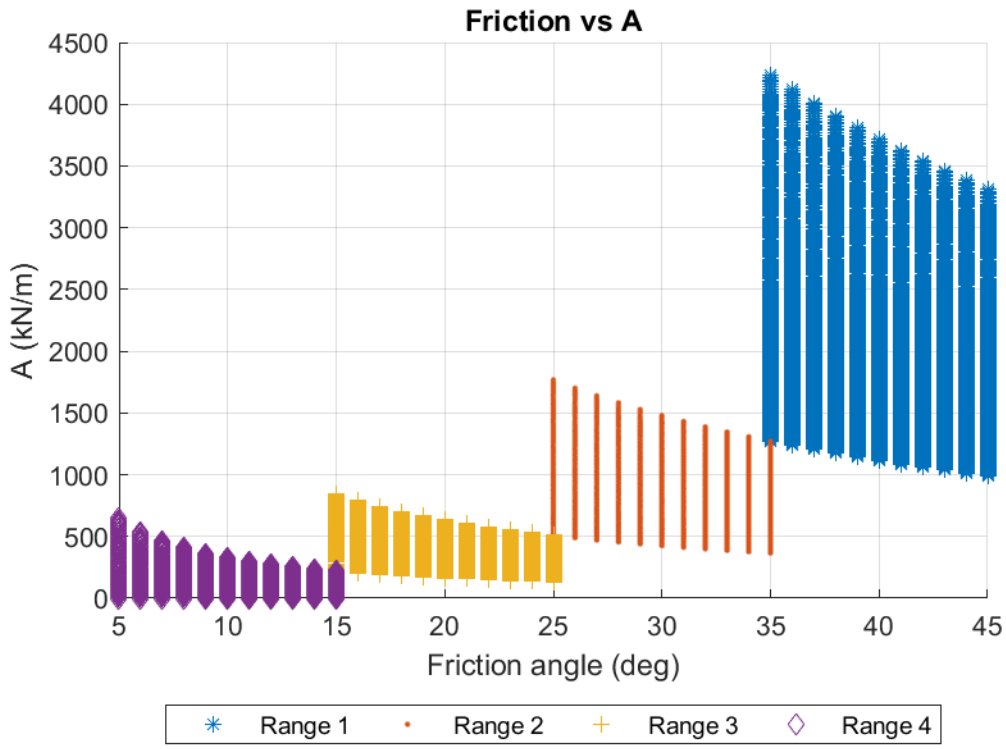

Figure 12 UCS ranges and the consequent ranges of Friction angle (deg) values. The graph shows the values of A refer to Friction angle.

The same features occur with the friction angle (Figure 12) if the different ranges are compared as a total. Due to the relation between the UCS ranges and the ranges of friction angle, the distribution of the values is not surprising. Once again the higher values of UCS (range 1) have the highest values and the lowest values of UCS (range 4) have also the smallest values.

Figure 12 may be also studied in terms of the different ranges (ranges 1 to 4). Then these ranges represent a different behavior: it was claimed that the bigger the UCS values the larger the friction angle and as a direct consequence the higher the cutting resistance values. Although this is true, the tendency of the friction angle in each of the ranges shows something different: the higher the friction angle, the lower the cutting resistance.

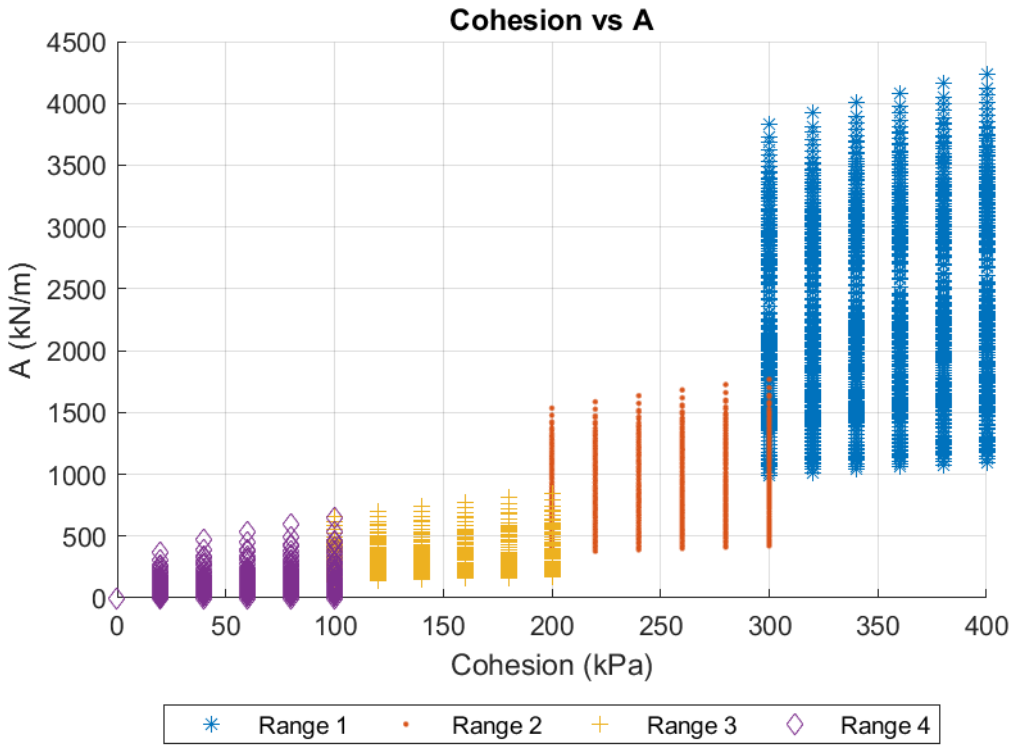

Figure 13 The four ranges of Cohesion, previously defined by the UCS value, show a clear trend referring to the A (kN/m) values.

The cohesion's graph (Figure 13) shows also that the trend of the entire group of results increases when increasing the cohesion value; however, when considering the different ranges, the trend is not easily understandable. Figure 13 defines a clear trend, the higher the cohesion values the larger the cutting resistance. However, as in the case of the friction angle, in each range, there is other trend, which is not that clear. For that reason, the same plots but fixing one of those parameters used in the ranges are plotted and they help to understand the method and the relation of the parameters.

- **Constant UCS values: 100 MPa and 75 MPa**

In order to identify the behavior of these formulas, some of the parameters remain steady. In this case, the UCS keeps a constant value of 100 MPa and 75 MPa (as

intermediate values (UCS range used before goes from 1 to 200 MPa). Both values are used in order to show the influence of different UCS.

The charts (Figure 14 and Figure 15) display the cutting resistance of the material, friction angle and cohesion when the UCS of the rock remains constant. As it can be seen in Figure 14, the lower the friction angle, the higher the cutting resistance.

The most problematic area, as it can be seen in the Figure 12, are values of friction angle below 15°, which make the Ke increase exponentially. However, rocks normally tend to have higher friction angle values, from the range of 15 to 40° and in that range the Ke values are not so high anymore.

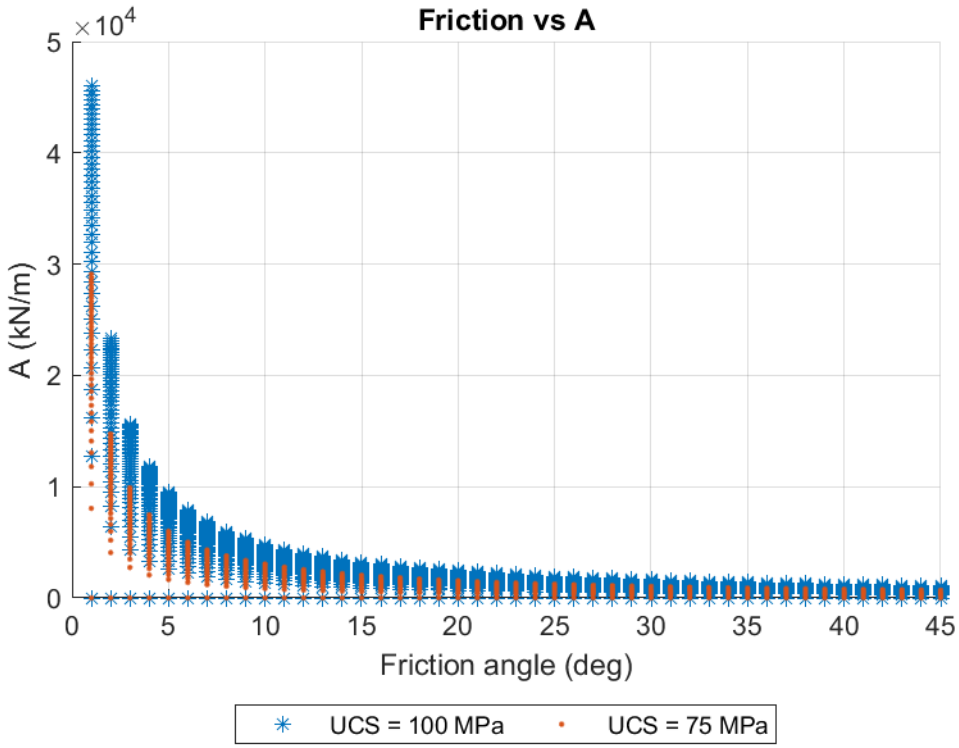

Figure 14 Friction angle values (deg) and A (kN/m) according to the method used. UCS value = 100 MPa and UCS value = 75 MPa.

On the other hand, Figure 15 shows the changing values of the Ke regarding the increasing cohesion, and constant UCS values. It is obvious that the increasing cohesion increases the cutting resistance, and when plotting the results of all the possibilities it was not possible to be seen.

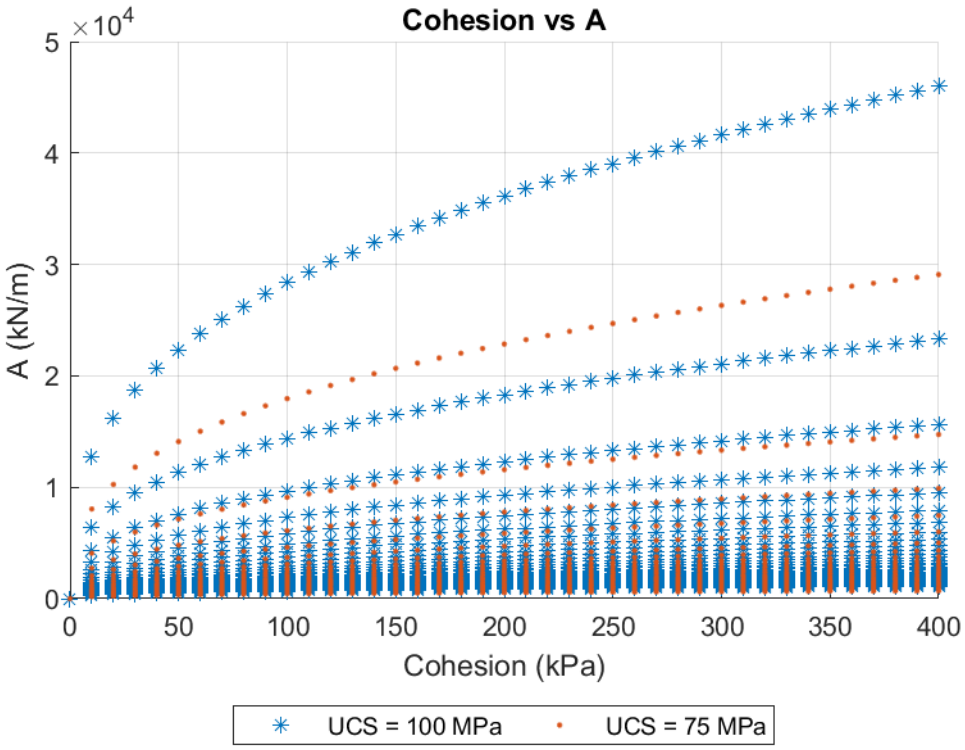

Figure 15 Cohesion values (MPa) and A (kN/m) according to the method used. UCS value = 100 MPa (circles) and UCS value =75 MPa (dots).

As a summary, it was settled that the increasing UCS and cohesion values result in increasing cutting resistance. High friction angle values decrease the cutting resistance.

3 REDUCTION OF RMR BY INDUCING FRACTURES

The reduction of the RMR is based on the development of induced cracks on the rock by irradiating microwaves on the rock surface (see chapter: Rock mass rating, RMR89).

In this chapter the relationship between the microwaves and the fractures is explained and linked to the RMR concept.

3.1 Definition of microwaves and applicability

It was confirmed that the microwave irradiation on the rock reduces the value of spacing of the fractures by developing cracks or fractures in the matrix of the material, which enhances the cutting rate of the machines, such as roadheaders (Hartlieb and Bock 2018).

In this chapter the electromagnetic waves and the microwaves are explained in order to understand their behavior and how they can improve the conditions for a better excavation.

3.1.1 Electromagnetic waves

The electromagnetic waves are a type of waves which are involved in the daily common activities: light, radio waves, Wi-Fi and microwaves belong to this group. Electromagnetic waves are defined as waves which can travel through both vacuum and matter, whereas mechanical waves are only able to travel through matter, and they change the magnetic and electric fields when travelling.

When an electric charge vibrates a wave, which is both electric and magnetic is produce: an electromagnetic wave. The electromagnetic wave is formed by two other waves: an electric and a magnetic, which travel perpendicular to each other, as it is shown in Figure 16.

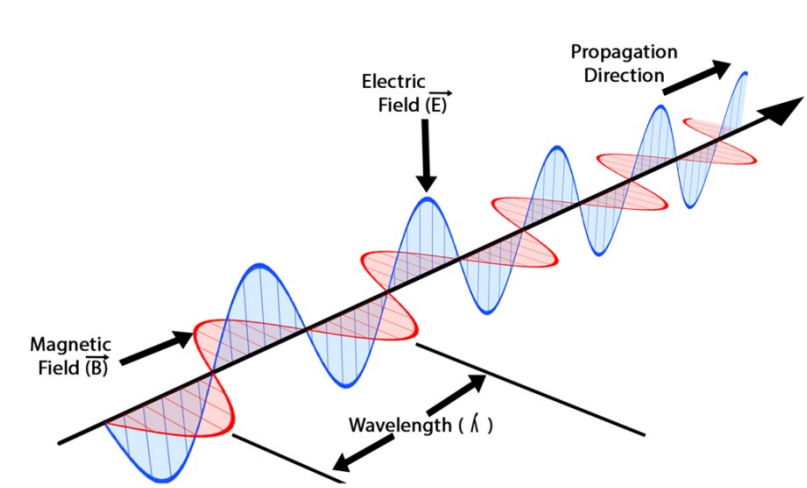

Figure 16 Electromagnetic waves components (https://byjus.com)

Both fields are superimposed, and they can be defined as vector fields. Due to this characteristic, this type of waves can suffer different processes when interacting with matter, such as refraction, absorption, reflection…

Electromagnetic waves propagate their energy at a velocity of $3 \cdot 10^8$ meters/second in the vacuum— e.g. the outer space-, which is the speed of light. However, when the transportation of this energy takes place through matter, that velocity is reduced, due to the absorption and later emission of a part of the energy. The particles of the material that is radiated with electromagnetic waves absorb part of its energy and the atoms start to vibrate or oscillate, and later produce a wave with the same frequency as the initial one which is reemitted.

The absorbed energy is stored in the material as heat: the larger the losses during the conduction of the material, the warmer the material gets.

The reduction of the velocity of the wave depends on the properties of the radiated material, such as the optical density or the packing of the atoms of the material.

The velocity of the electromagnetic waves is directly proportional to their wavelength, lambda, and the universal constant. The formula (Santamarina 1989) is defined as follows:

$$v = \lambda * f \quad \textbf{[23]}$$

Where:

- f: frequency
- λ : wavelength

The energy of these waves is directly proportional to Plank's constant. When this radiating energy—or ionizing radiation—is large, the bonds of the compounds are broken and then, these are not neutral anymore, they will become ions.

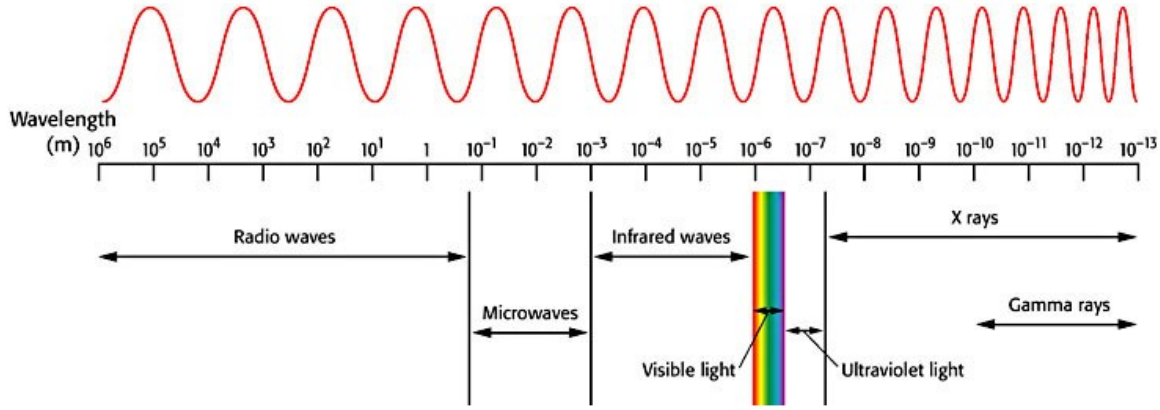

Figure 17 Electromagnetic spectrum and the different types of waves (Google Sites, *Mochebiology*; July 2019)

There are several different types of electromagnetic waves, depending on the range of wavelength. Due to the difference in frequency, the properties change, and so the applications.

3.1.2 Microwaves

Microwaves have always been related to positioning and location monitoring, and this is the reason why they were used in radars. Additionally, the energy generation and the warming up of dielectric compounds were also linked to microwaves.

In the late sixties, new researches about microwave applications in mining and metallurgical fields started. It was confirmed that metal ores were heated up while the hosting rock did not, which can make the difference during separation and sorting between these two (J. W. Walkiewicz, 1988). Other studies related to coal revealed that the sulfur could be removed from it by using microwave heating (Hall and Finch, 1984; Jacobs, 1982). Furthermore, microwaves have been studied to enhance the performance of roadheaders as well as

The microwaves have frequencies in the range from 0.3 GHz to 3 GHz, which correspond with wavelengths between 10 mm up to 1 meter.

For industrial, scientific and medical proposes, the following frequency ranges of microwaves were defined:

- 915 MHz
- 2 450 MHz
- 5 800 MHz
- 22 125 MHz

The powers of the devices are in the range of 3 kW to 200 kW. 2 450 MHz is the most used as the domestic microwave ovens use this range (A. Kemerman; N. Erocevic, 1997), and their power is about 3kW, which is considered low. The conventional microwave ovens have a wavelength (lambda) of 120 mm and travels through 90 mm x 45 mm waveguide (Hassani et al. 2016).

Microwaves are not really energetic if compared with the rest of the electromagnetic range. On the other hand, they are still used for heating proposes due to their high penetration depth, thus, low energy losses when travelling through matter (Scott 2006) in following parts the penetration depth is explained in more detail-.

3.1.3 Dielectric properties

Dielectric substances, which have been mentioned above, are defined as the materials which let the electric current pass through and that have weak bonds, which can be easily polarized by an electric field.

During the exposure, their molecules are repositioned in order to find the equilibrium positions due to the changing electric field: positive charges are placed close to the negative charged field and vice versa. The movement—vibration and rotation—of the molecules during the polarization, generates heat. In addition, the electric current when passing through the material faces contact resistance from the material, called ohmic loss, and which also generates heat (Abdi et al. 2017). This process is called dielectric heating.

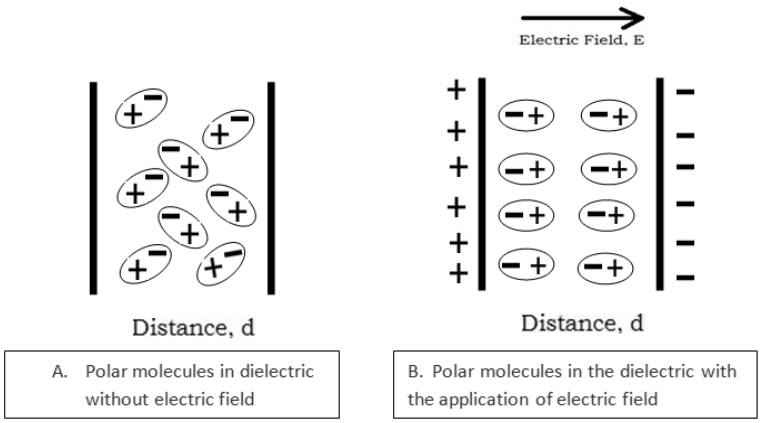

Figure 18 Unpolarized and polarized molecules due to the presence of an electric field (https://www.electrical4u.com)

Dielectric heating can be produced by radio waves spectrum, which includes microwaves:

- 10 kHz—10 THz → Radio waves
- 300 MHz—30 GHz → Microwaves

The dielectric properties of the rocks and minerals determine how the microwave treatment is going to perform, in terms of energy absorption and heat transfer.

J. Carlos Santamarina published a table showing the dielectric properties of intact substances: loss factor k''—includes both polarization and conduction—and the

dielectric constant k'. He concluded that dielectric properties depend on the frequency and the temperature of the material.

$$FzR = Kz\ FxR \quad \textbf{[24]}$$

In addition, he claimed that the water content of a material is an important factor to consider, as well as the content of salts. The water content helps polarization, and as the water molecules are permanent dipoles, these will directly be reoriented during electromagnetic radiation. The orientation of the grains in the rock and how they are displayed in layers is another relevant factor.

3.1.4 Penetration depth

As the microwave radiation wants to be applied to break rock, the energy absorption must be as large as possible, and it is claimed that the distance between de emitter and the objective is related to the reflection of the electromagnetic waves. This relation is periodic, which means that in a good pairing the energy absorbed can reach the 95%, and if the pairing is not well done, the reflection is approximately 80%.

3.1.4.1 Penetration depth calculation

The depth reached into the material by the microwaves is called penetration depth (Dp), when the power is decreased e^{-1} — e refers to the Euler number which has a value of 2.718—at the surface. Depending on the losses during the microwaves conduction through the material, two different equations are available (Santamarina 1989):

Low losses

$$Dp = \frac{\lambda \sqrt{\varepsilon}}{2 * \pi * k''} \quad \textbf{[25]}$$

High losses

$$Dp = \frac{\lambda}{2 * \pi * \sqrt{k''}} \quad \textbf{[26]}$$

Where:

- λ: wavelength (m)
- ε**:** permittivity of the material
- k''**:** losses factor

The penetration depth is directly related to the frequency of the waves and the electrical permittivity of the material, as it was settled in the equations [25] and [26].

3.1.4.2 Issues regarding Dp

Although the penetration depth is a determinant factor for the profitability and the benefits of the microwave irradiation on rocks, unfortunately there is not enough information regarding the optimization and improvement of the penetration of the waves, and therefore the cracks, into the rock.

This must be a target for future research and studies on this field.

3.1.5 Exposure time

The exposure time needed depends on the power and the frequency of the microwaves. Some researchers have done test using 24kW with a frequency of 2450kW during 30 seconds (Hartlieb and Grafe 2017). In other test, the exposure time was 45 seconds, and the power of the magnetron was 30kW which achieved a penetration depth of 200 mm (Hartlieb et al. 2017).

The exposure time is a critical factor for the performance of the microwave irradiation, and it is linked to the power and the frequency of the magnetron. However, the exposure time is out of the scope of this study.

3.2 Rock fracturing using microwave irradiation

During the radiation of a rock, and supposing good energy absorption, the rock will develop differential volumetric expansion, which means that thermal stresses will rise causing the fracture of the grain's boundaries and eventually, the breaking of the grains. The bond work index can be reduced dramatically, up to 90% as Kingman confirmed in 1998.

This process depends on the following factors:

- The uniformity of the grains in the rock fabric
- The thermal expansion coefficient of the material
- The confining and stress situation of the rock
- The hardness of the rock.
- The loss factor, k''
- The exposure time

J. Carlos Santamarina confirmed that increasing frequency, the temperature rate and the penetration depth increases. He also claimed that increasing thermal gradient helps to break the rock, however the total volume obtained is reduced as well as the penetration depth. The selection of the proper parameters in order to optimize the breakage of the by microwave radiation is rather complex and many parameters must be taken into account.

If the penetration depth is rather small for a given lambda, lower frequencies must be used to enhance and optimize de breaking of the rock.

3.3 Fractures patterns on laboratory tests

The definition of the pattern of the induced cracks is one of the main issues to understand the behavior of the irradiation of microwaves in the rocks. Several authors have been researching on this topic and some of the results are explained on this chapter.

3.3.1 Description of the patterns

In the literature, the patterns used in the microwave irradiation tests have a staggered distribution, thus the irradiated spots are distributed uniformly but in an alternating pattern. Figure 19 illustrates the pattern:

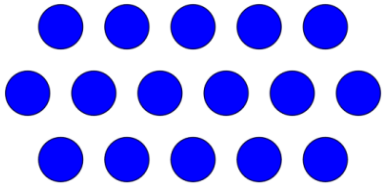

Figure 19 Staggered pattern from previously reported microwave irradiation experiments.

This pattern is used due to the higher covered surface during the microwaving processes, which also allows an easier connection between the different induced cracks, as it can be seen in Figure 20.

Figure 20 Crack pattern of several irradiated spots. (Hartlieb and Grafe 2017)

The sample was exposed to 24kW at 2450 MHz and the cracks were developed due to the thermos—physical properties (differential heating) as well as dielectric properties of the material. The cracks occurred in different areas of the sample and in different directions (Hartlieb and Grafe 2017).

Some of them were sub-horizontal (parallel to the surface), and their aperture was less than 70 microns and the frequency of those was limited to 1 cm under the surface of the sample. The cracks related to the breakage through the grain boundaries the aperture was even less. For this reason, the aperture of the joints is not taken into account when calculating or recalculating the RMR values; it is non-significant for this study's propose.

The penetration depths of the cracks induced in this test were in the range of 1—100mm. The lengths of the cracks on the surface were about 100—300 mm and were connected one to another irradiated spot. About 10 cracks crossed the entire sample (500x500 mm surface). After the test it was claimed that the sequence of the irradiation makes the difference and affects directly the performance of the fracture development.

3.3.2 Pattern selection for further calculations

The large-scale fractures describe an asterisk shape, and these developed 5 cm long cracks from the center. This test and the results are considered as the ideal pattern and are consider for the further calculations and hypothesis. The definition of the pattern is necessary in order to reckon and analyze de number of induced fractures that are needed to reduce a certain amount the RMR or other rock mass properties.

Figure 21 Ideal pattern of the induced cracks, asterisk shaped.

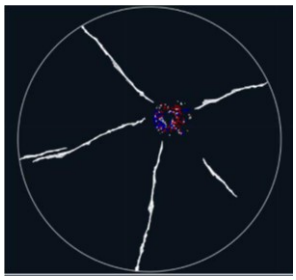

Figure 22 Large- and small-scale microwave induced crack patterns. The circle has a diameter of 10 cm. (Hartlieb and Grafe 2017)

3.3.3 Definition of the patterns according to the fracture density

Fracture density is defined as the number of cracks per area unit. The fracture density must be calculated and defined in order to calculate the number of cracks needed to reach certain reduction of rock mass parameters. It mainly relates the joint spacing when calculating the RMR of the rock mass.The fracture density has been calculated by counting the fractures per 1 m^2 of each of the patterns defined in Figure 23 and the results have been displayed in Figure 26.

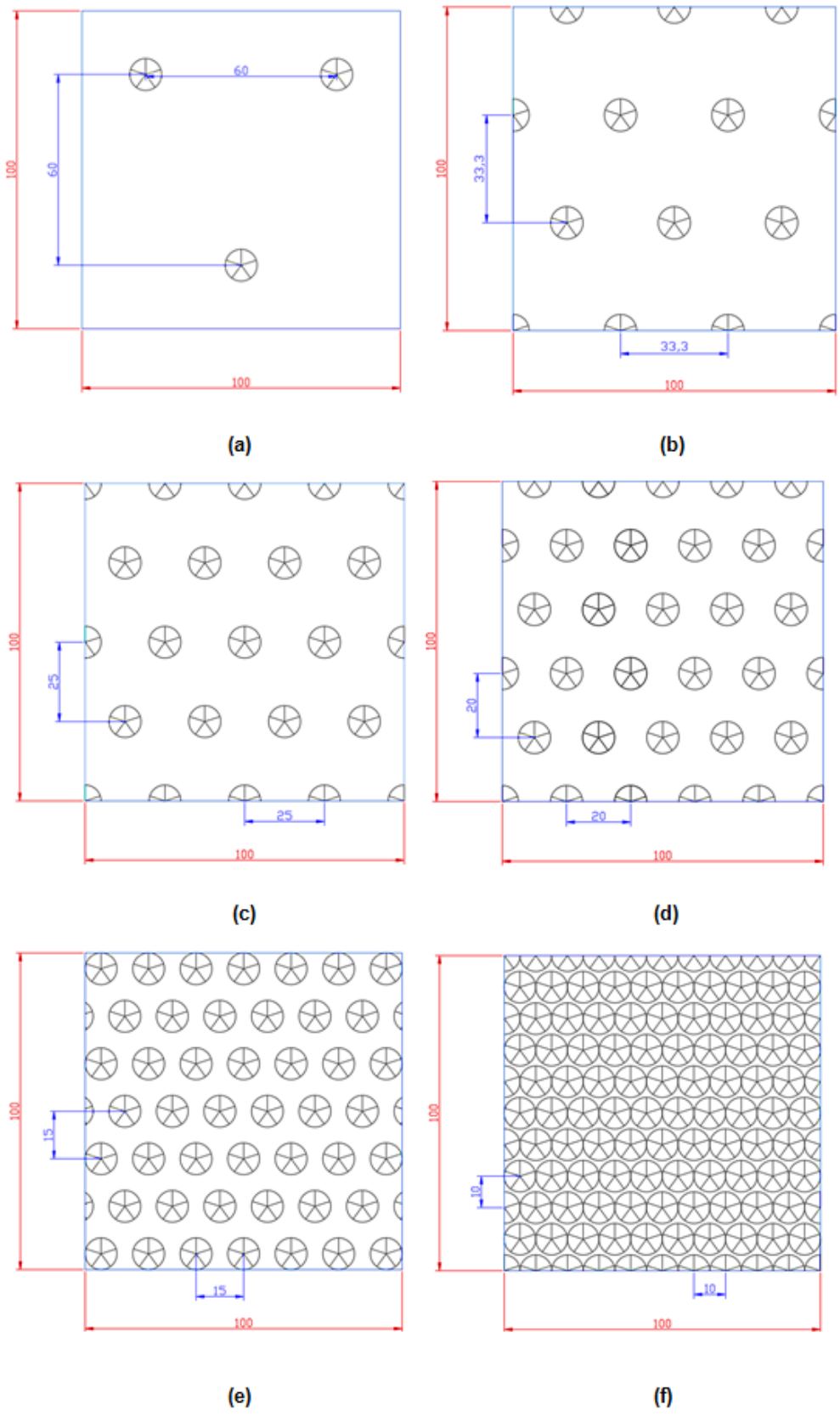

Figure 23 Different patterns of cracks when using different distance between the irradiation spots.

The patterns are then defined for 600 mm until 100 mm, which are included in different ranges and ratings in the RMR rating system. Patterns with larger distances between the irradiated spots are not considered as they might not be seen in a 1 m^2 or just two spots might fit in that surface, which is a low rate of irradiation.

The distribution of the cracks is homogeneous through the surface but in staggered pattern, defined as 1 m^2 surface. The irradiated target spots are defined as the center of an asterisk (see Figure 21).The asterisk actually refers to the fracture pattern and its diameter is 100 mm and the length of the induced cracks is 50 mm. The distance between the edge of each of those cracks to other edge is defined as the spacing. There are many options due to the distribution of the cracks in each pattern, so the average of those distances is calculated. The average distance between the edge of the cracks is defined as the spacing for further calculations.

There are five different patterns defined, which different distributions and as a consequence different crack density (Figure 26) which go from (a) to (e).

3.3.4 Spacing between the induced fractures

The spacing between the cracks is measured from the edges of one irradiated spot's crack to the edge of the nearby cracks. As the pattern and the shapes are regular, the measures are all different in order to cover as many options as possible. Figure 24 illustrates the procedure to measure the distance between the different fractures' edges.

Once all the measures are taken, the average value is calculated, and this value represents the spacing value which is used in the further calculations. The measuring procedure is shown in Figure 24. The results are displayed in Table 5.

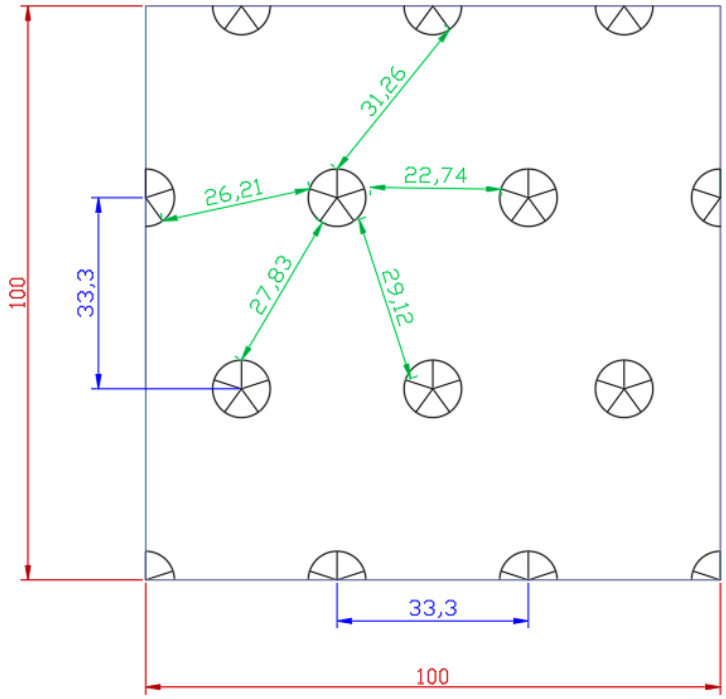

Figure 24 Induced fractures measuring procedure: all possibilities from edge to edge; values in cm.

Table 5 Average spacing values according to the different patterns that were developed

Pattern type	Distance between spots (mm)	Average spacing value (mm)
(a)	600	561.5
(b)	333	274.32
(c)	250	190.8
(d)	200	137.62
(e)	150	85.66
(f)	100	30.8

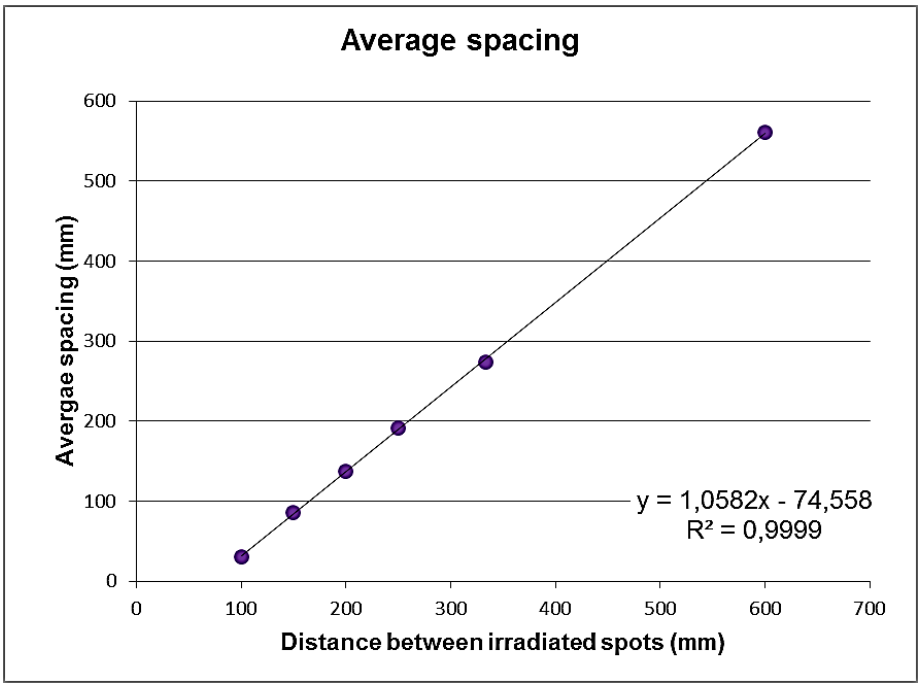

Figure 25 Average spacing (mm) related to the distance between the irradiated spots when applying the microwaves. Trend line included.

3.3.5 Fractures density

The fracture density is defined as the number of cracks in the patterns per area unit. The cracks which are near the border of the defined surface are excluded from further calculations as they cannot be connected to other cracks because they are out of that surface. It must be highlighted at this point, that the union of two or more cracks are not considered, as there is no data available to determine the behavior of them.

Table 6 Distance of the irradiated spots and the fracture density for patterns defined in Figure 23.

Pattern	Distance between irradiated spots (m)	Fracture density (cracks /m^2)
(a)	0.6	15
(b)	0.333	62.5
(c)	0.25	75
(d)	0.2	120
(e)	0.15	230
(f)	0.1	490

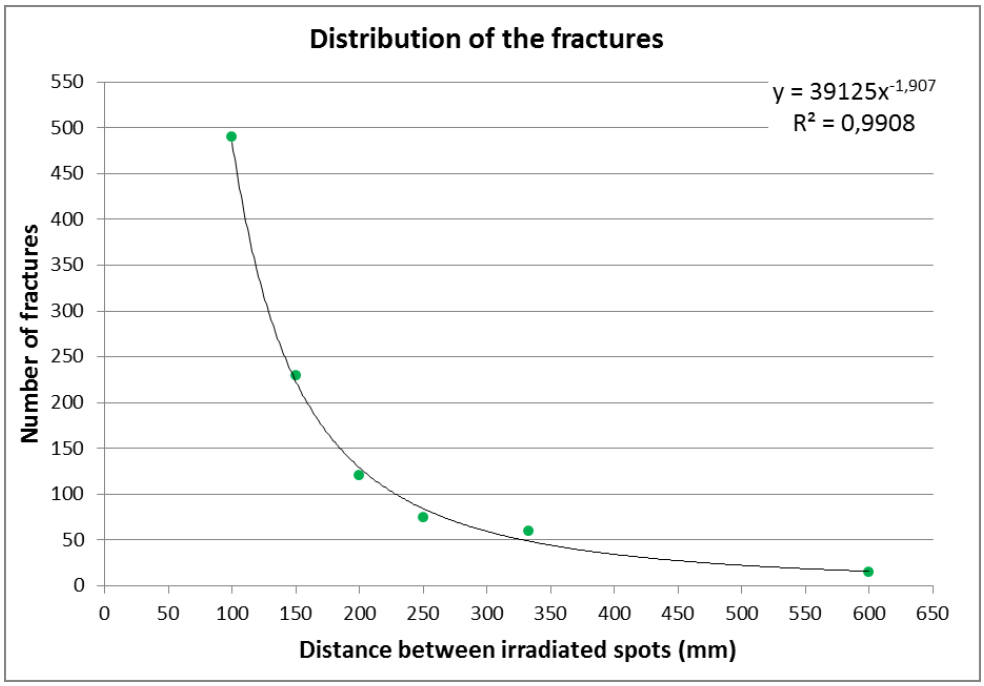

Figure 26 Spots distance v. Number of induced fractures

3.3.6 Relation between pattern fracture density and reduction of the RMR

In order to relate the number of cracks or the density of fractures needed to reach a certain reduction on the overall RMR, the Figure 27 is used.

Figure 27 presents the relation between the spacing and the rating values in a continuous way. Using this graph and its trend line, the ranges that the RMR table shows are removed, Figure 10, and a proper relationship can be calculated.

The RMR can be changed just by modifying the spacing of the fractures 15%. The range of values of the spacing rating go from 5 to 20 and as the RMR is a value over 100 that make the 15%.

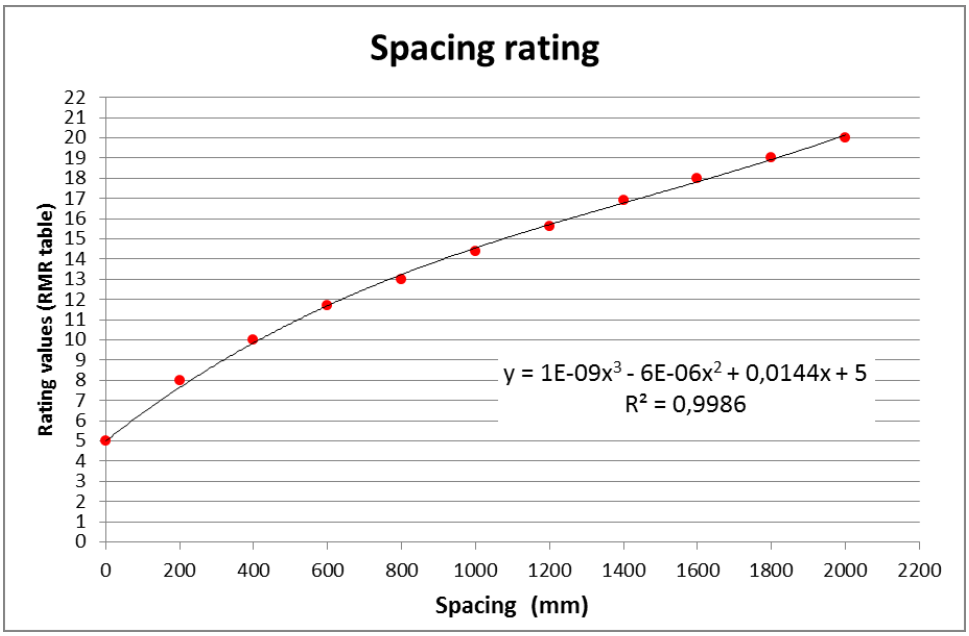

Figure 27 Rating of the spacing (mm), from 5 to 20 after RMR system. Trend line included.

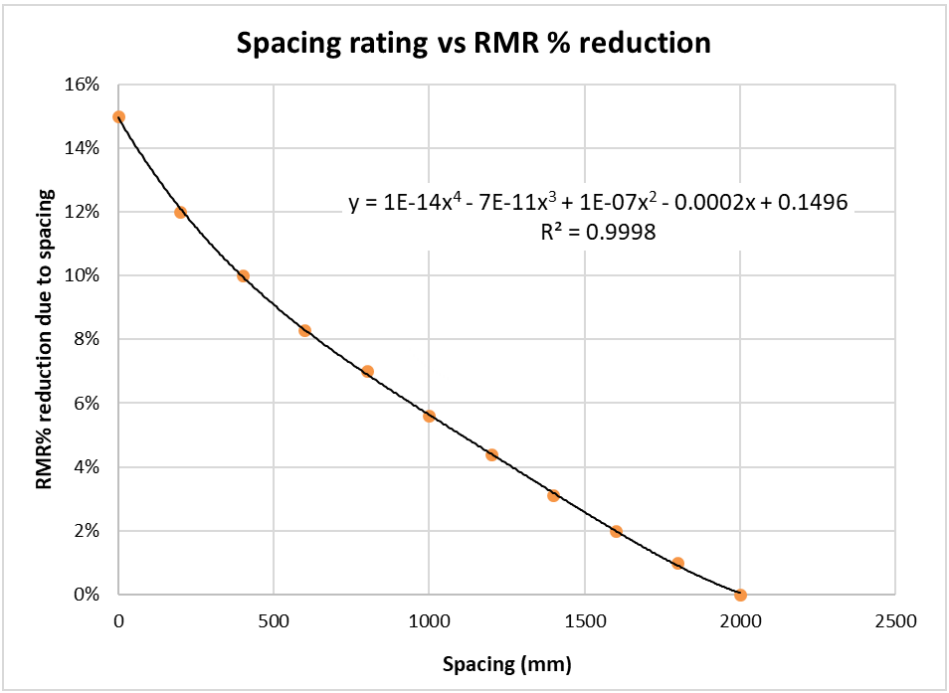

Figure 28 Spacing in mm related to the change of RMR (%) which can be done.

- **Example:**

A non-fractured ideal rock, which has a 100 RMR value, needs to reduce its RMR by 10% in order to reach a certain Ke value. This example excludes other parameters such as UCS and it is only focused on the reduction of the RMR by means of creating fractures in the ideal rock.

If the rating needed is not easy to recognize just by using the graph, the trend line can be used to calculate it.

$$\boldsymbol{Spa_{rat} = 10^{-9} * spa^3 - 6 * 10^{-6} * spa^2 + 0.0144 * spa + 5} \quad \textbf{[27]}$$

Where:

- Spa_{rat}: rating of the spacing
- spa: Spacing in mm between the fractures of the rock (mm)

The percentage of variation of the RMR can also be calculated.

$$\boldsymbol{RMR\ \% = 10^{-11} * spa^3 - 5 * 10^{-8} + 0,0001 * spa + 10^{-14}} \quad \textbf{[28]}$$

Where:

- $RMR\ \%$: Percentage of variation of RMR according to Figure 28.

In this case the induced fractures need a reduced spacing rating from 20 to 10, and that means a spacing of 400 mm.

At this point, the trend line of Figure 25 is used to calculate the distance between the irradiated spots:

$$\boldsymbol{spa = 1.0582 * (DS) - 74.558} \quad \textbf{[29]}$$

Where:

- spa: Spacing in mm between the fractures on the rock (mm)
- DS: distance between the irradiated spots (mm)

$$\boldsymbol{DS} = \left(\frac{\boldsymbol{spa}}{\mathbf{1.0582}}\right) + \mathbf{74.558}$$

$$\boldsymbol{Distance\ between\ spots} = \mathbf{452.56}\ \boldsymbol{mm}$$

In order to know how many cracks per surface unit will be formed, the trend line of the Figure 26 is used:

$$\boldsymbol{NF} = \mathbf{39125} * (\boldsymbol{DS})^{-\mathbf{1.907}} \quad \textbf{[30]}$$

Where:

- NF:number of fractures

$$\boldsymbol{Number\ of\ fractures} = \mathbf{27.23} \rightarrow \mathbf{27}\ \boldsymbol{Fractures}$$

4 CALCULATIONS PROCEDURE

In this chapter the calculations or code in order to identify the behavior of the different parameters and all the possibilities that they form when combining them are explained in detail.

The code is described easily by flow diagrams and as well the background of the calculations is explained in deep. The parameters and ranges of the input data are also represented and extensively defined.

4.1 Input parameters

In order to define the applicability of the microwave technology as a pretreatment on the ground before it is dug out by a BWE, the calculation steps described in this chapter have been followed.

The main input parameters regarding the rock properties are displayed in Table 7. Additionally information related to the BWE dimensions was used and those values are collected in Table 13, Table 14 and Table 15.

4.1.1 Calculation of the RMR values of rocks

The parameters for these RMR values can be seen in the Table 7 The criteria when selecting the range of values as well as the steps is based on assumptions.

Ground water conditions, roughness, aperture, infilling and weathering conditions were selected as the most unfavorable conditions, thus the highest values of the rating. The main reason to do this type of parameter selection is rather simple: the lack of information about the conditions at the mine site regarding the rock mass. Due to this, the worst scenario is defined and calculated.

The UCS is limited due to the technical issues regarding the working regime of a BWE. Generally, a BWE will perform properly under 20 MPa. On the other side, above 100 MPa is unlikely to have adequate conditions for a BWE even after a treatment like microwave irradiation.

Table 7 shows the input values used in the calculations and the steps used for each parameter. The step defines the increment that each value in every stage of the

calculation loop. For example: if the UCS range is defined from 20 to 100 MPa and the step is 10 MPa, the first stage of the loop calculates with the UCS value of 10 MPa, the second UCS value will be 20 MPa, then 30 MPa and so on until 100 MPa is reached.

Table 7 Values of the input data for the RMR calculation

Parameter	Range of values	Step
UCS	20—100MPa	10
RQD	10—100 %	10
Spacing	25—2000 mm	25
Ground water	1	-
Persistence	1—5 m	1
Aperture	0—1 mm	1
Roughness	1	-
Infilling	1	-
Weathering	1	-

The persistence and the aperture are also limited by technical issues. The cracks induced by microwave irradiation did not perform a large aperture in the lab tests. The persistence was also limited by the unknown patterns of the cracks.

After calculation of the RMR, then the friction angle and the cohesion ranges are defined, which are needed for further calculations, such as the machine power among others. Additionally, the rock mass strength is calculated using the following procedure.

4.1.2 Rock mass strength

Many authors published equations and procedures to relate the damage on a rock to the unconfined compressive strength in order to predict the intact rock UCS. Some of them are shown in Table 8 (Ván and Vásárhelyi 2010):

In order to calculate the modified value of the rock strength once it has already been treated by the microwaves, the intact rock compressive strength will be used (UCS applied in the RMR rating) and the rock mass strength will be cleared.

The selected procedure for the calculations belongs to Kalamaras and Bieniawski (G.S. Kalamaras and Z. T. Bieniawski 1995), since the results present a lower variation ratio; this method is more conservative (see Figure 30 and Figure 29).

Table 8 Relation between the intact rock and the rock mass strength, including the RMR value

Authors	Formula	
Yudhbir et al. (1983)	$\frac{\sigma cm}{\sigma c} = exp(7.65((RMR - 100)/100)$	**[31]**
Ramamurthy et al. (1985)	$\frac{\sigma cm}{\sigma c} = exp((RMR - 100)/18.5)$	**[32]**
Kalamaras & Bieniawski (1993)	$\frac{\sigma cm}{\sigma c} = exp((RMR - 100)/25)$	**[33]**
Hoek et al. (1995)	$\frac{\sigma cm}{\sigma c} = \exp((RMR - 100)/18)$	**[34]**
Sheorey (1997)	$\frac{\sigma cm}{\sigma c} = \exp((RMR - 100)/20)$	**[35]**

Where:

- σcm: rock mass strength (MPa)
- σc: intact rock UCS (MPa)
- RMR: Rock Mass Rating

The reason behind this decision is simple: all the data and calculations are based on hypothesis and empirical procedures and so, the lower the variation ratio, the safer the results will be.

$$\sigma cm = \sigma c * (exp(\frac{RMR-100}{25})) \quad \textbf{[36]}$$

Figure 29 and Figure 30 reveal the comparison of the different procedures to relate the UCS and the rock mass strength; however the results are not realistic as a rock with a UCS value of 100 MPa might not have a value of 100 in the RMR scale, for example.

Thus, the only purpose of these two graphs is to illustrate the decision why the Kalamaras & Bieniawski procedure was chosen.

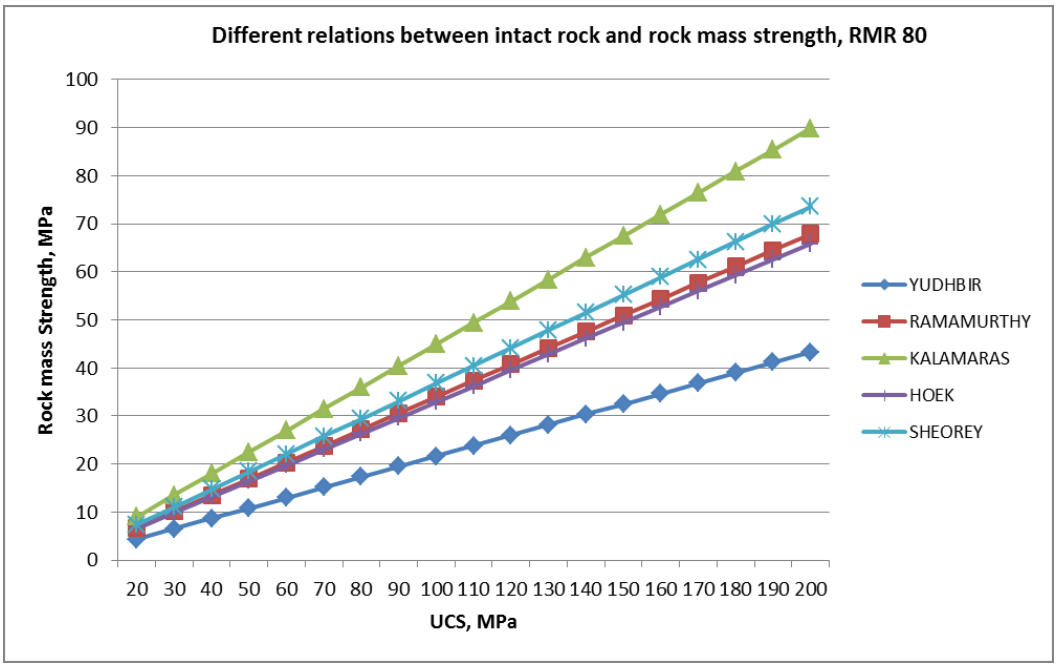

Figure 29 Comparison of the different rock mass strength calculations, regarding a fixed RMR of 80

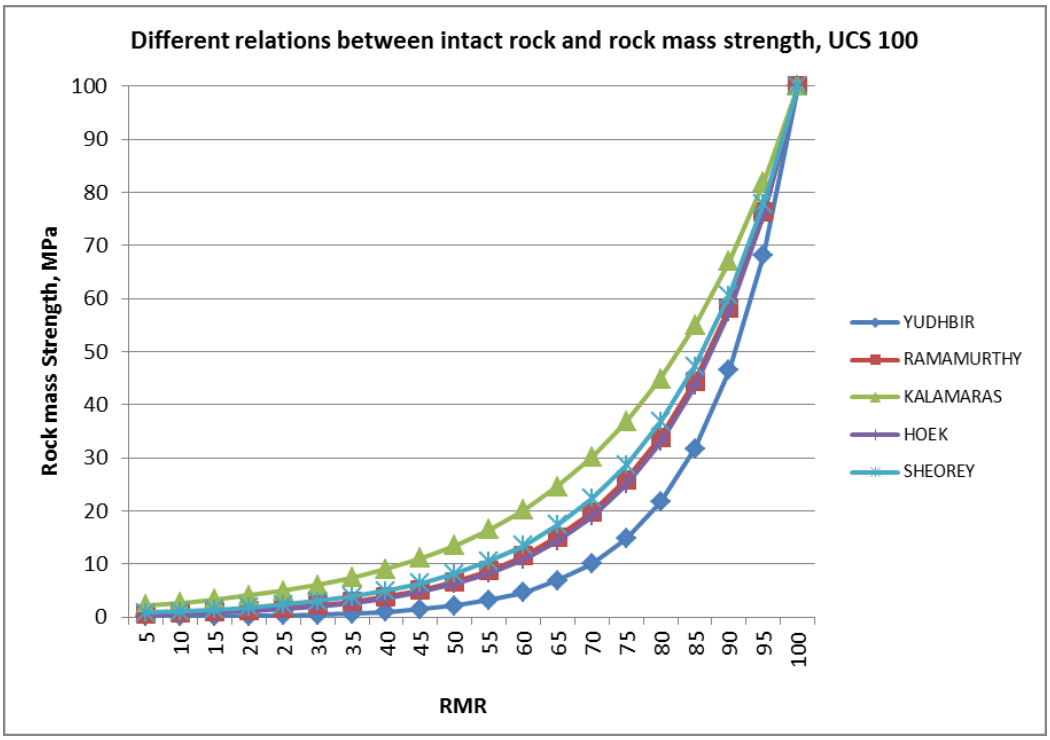

Figure 30 Comparison of the different procedures for rock mass strength calculation, regarding a fixed UCS value of 100 MPa

4.2 Machine regime and comparison

The machine working regime is defined by several parameters including the ones related to the rock mass. The UCS, cohesion and friction angle are the inputs for the specific cutting resistance, which was defined in equations [6] and [7].

$$A = 3.72432675\ \sigma rc^{1.592777} C^{0.348245478} \varphi^{-0,98134} \quad [6]$$

However, as the rest of the formulas are referred to the cutting resistance, Ke, this parameter will be used from now on:

$$Ke = \frac{A}{100 * to} \quad [7]$$

Where:

- Ke: cutting resistance (N/cm^2)
- A: specific cutting resistance (kN/m)

- to: cutting depth (cm)

Once the Ke has been defined, for situations before and after microwaving, the working regime parameters are calculated, and afterwards the power consumption and the extracted material volume.

4.3 Calculation code

The code for the calculations and the plots has been entirely done in *MATLAB*. The input data used has been provided by FL-Smidth or taken from the literature. Assumptions had to be made in order to simplify the calculations, as the data obtained was not enough for the calculations and to reach the target of this study. As the code is long and considers all the aspects explained in the previous chapter, it is explained step by step using flow diagrams to make it easier.

4.3.1 Description of the rating system code

The first step of the code calculates the RMR of the input data, which are: UCS, RQD, joint parameters—spacing, infilling, aperture…-. Figure 31explains the code behind the rating system, in this case for the UCS.

The input data in this case is the initial and final parameters of the UCS which are the first limit of the calculations which is input: “UCS_ini” and “UCS_end”. The step defines how many values of the UCS are calculated, other way to reduce or enhance the number of the values. This data is stored as a vector and is used later in further calculations. Once the values of the UCS are set up in a vector, the size of it is calculated:” ncol”.

Using a While loop, the values of UCS vector are rated according to the RMR system. This loop needs a counter, in this code is named “r” and has a starting value of one. The counter has two main functions:

- Restricting value: The counter increases every time that the process inside the loop is done: “r = r +1”. The While loop will work until the counter equals the size of the UCS vector and then the code will continue to the next rating process: RQD.

- Positioning: the rating system starts at the first position of the UCS vector and continues until the last. On one hand, the counter calls one UCS value or vector's position at the time to be rated. On the other, it orders the rating values on the UCS Rating vector at the same position.

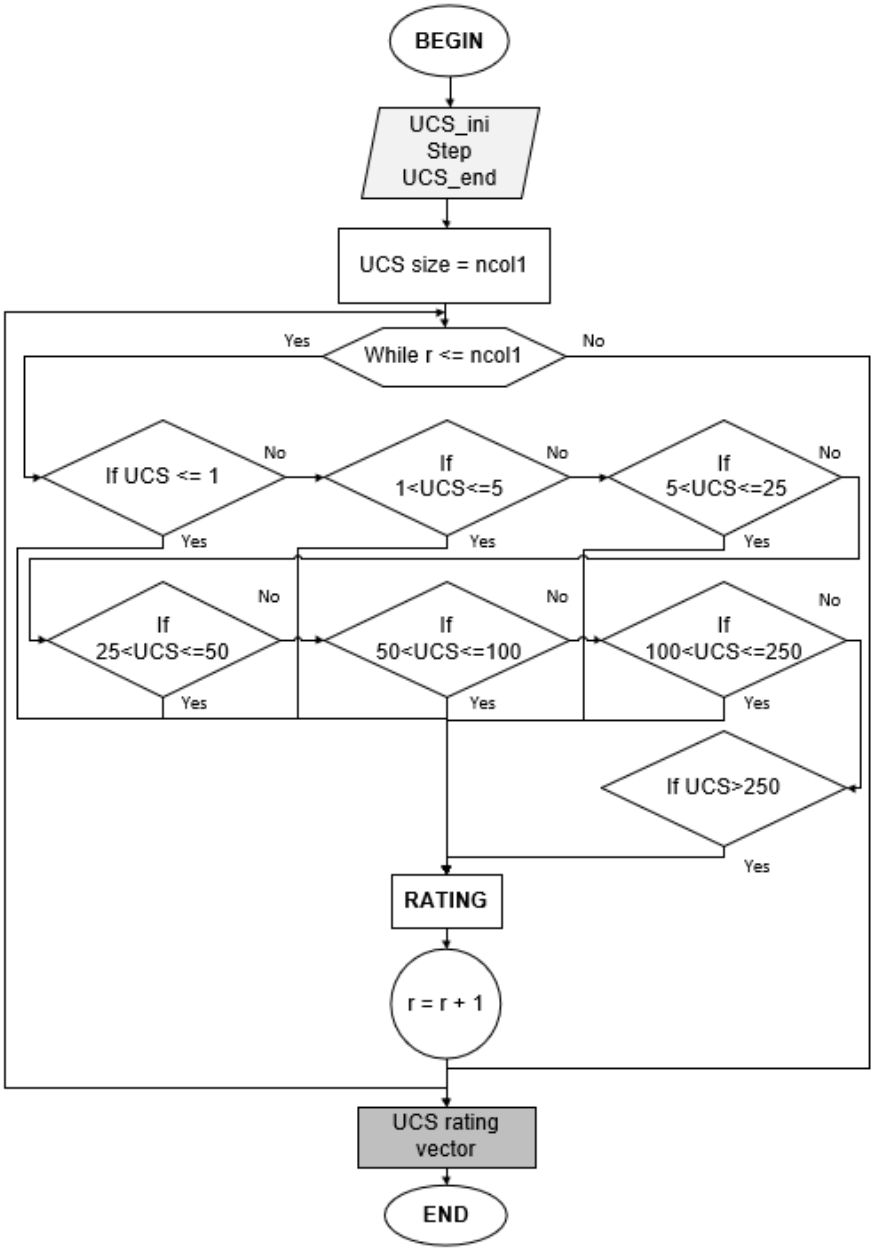

Figure 31 Flow diagram of the UCS rating system

The rating process is rather simple: the UCS values are evaluated by using an If / If else loop. If the value is contained in the range specified, the value gets rated. If the value does not fit in the range, it will be evaluated in the following If loop.

Finally, all the rating values are collected in a vector, which respects the positioning of the initial UCS vector. This fact is important for the storage of the information as it will be called for different proposes along the code and further calculations.

In the case of the spacing rating, the trend line is defined by the equation [27] and the Figure 27.

4.3.2 Description of the RMR code

After the rating of all the parameters of both rock and the joints, all the values are stored in different vectors which are collected in a matrix.

In order to contemplate all the possibilities, the matrix is created by using as many as For loops as parameters used in the RMR. These For loops take into account the size of every of the vectors of the initial data and create as many possibilities pivoting from each value. A simple example is given:

- UCS value = 30MPa
- RQD vector = (10:20:50) → starts at 10% until 50% and the step is 20MPa.

Table 9 Example of the pivoting system

UCS (MPa)	UCS rating	RQD (%)	RQD rating	Final Rating
30	4	10	2	6
30	4	30	8	12
30	4	50	13	17

The result of these considerations will be that, the value 30 MPa corresponding to the UCS will be related to 10%, 30% and 50% values corresponding to the RQD vector. All these considerations are calculated separately, and the final value is the RMR.

All the parameters are pivoted as explained including the rates. Since the matrix is created the rates are summed in order to get the final RMR value of each of the possibilities. The values of the final RMR are stored at RMR values vector.

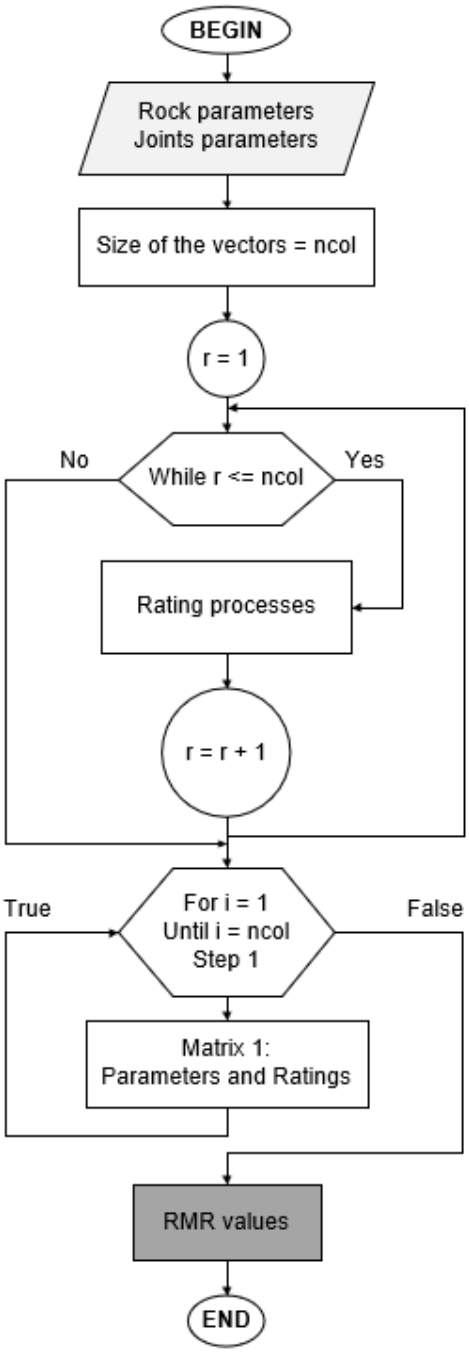

Figure 32 Flow diagram of the whole code for RMR calculation.

4.3.3 Assignation of rock parameters

The RMR rating procedure attributes some parameters to each range of RMR values. This part of the codes matches the cohesion and friction angle to each RMR value. Once again, the attribution of values is done by a While loop.

Additionally, the rock mass strength is calculated using Kalamaras' procedure (equation [33]).

The cutting resistance, Ke, is calculated in this step, as explained in the previous chapters (equation [7]).

As it was described in the previous steps, the results are stored in a matrix and each parameter in the corresponding vector.

I	II	III	IV	V
20 years for 15 m span	1 year for 10 m span	1 week for 5 m span	10 hours for 2.5 m span	30 minutes for 1.0 m span
> 400	300–400	200–300	100–200	< 100
45°	35°–45°	25°–35°	15°–25°	< 15°

Figure 33 Different RMR groups and the corresponding friction angle and cohesion. (Z. T. Bieniawski 1989)

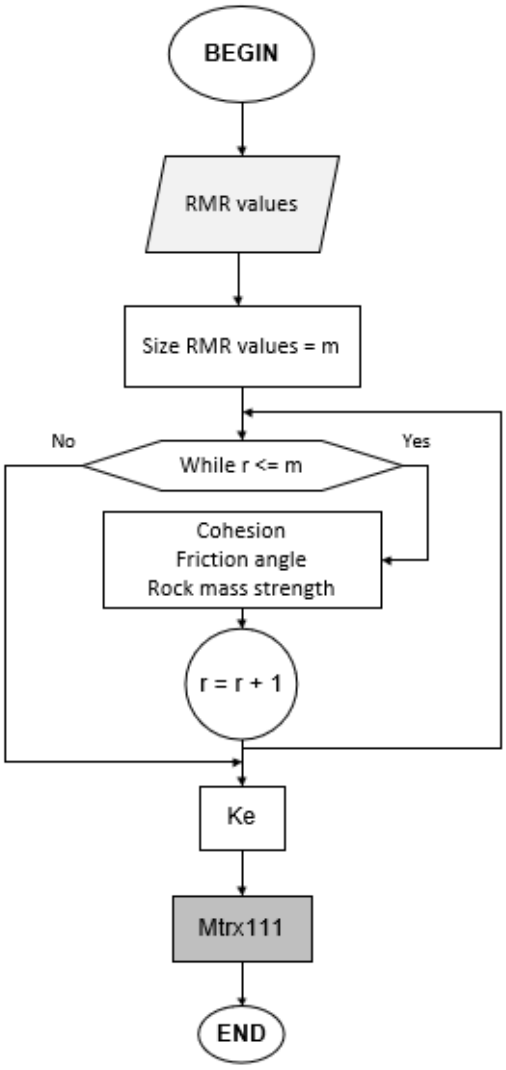

Figure 34 Flow diagram of the assignation of rock parameter from RMR values

4.3.4 Calculation of the BWE working regime

At this step the code is focused on the calculations related to the working regime of the machine. Power, volume of the material extracted as well as forces are calculated.

The calculations at this point need to load results of the previous steps and material properties, such as cutting resistance, cohesion, friction angle and the rock mass strength. After that, the machine parameters are input, mainly dimensions of the machine and the BW and working regime set up, such as linear velocity of the BW, performance of BW, and technical aspects like installed power and maximum

volume extracted. The data that was input regarding the BWE was taken from the technical file of the excavator target of the calculations.

Once again, a While loop is set up to calculate the force, power and volume of material extracted for each vector position as it was done in the previous steps.

The state of the cutting tools or bits is rather important as it was explained in previous chapters. The influence of this parameters is large, e.g. if the bit is worn out the power needed to extract the same amount of material with the same properties, must be increased by 20%. For this reason, the force, power and extracted volume were calculated three times, repeating the code:

1. Unworn cutting tool
2. Medium worn out tool
3. Worn out tool

Each of those situations are stored in different matrix, and for that reason the process of evaluating each situation is done separated in different loops which are alike, as it is illustrated in Figure 35.

Finally, some plots are printed in order to show the results and how the machine behaves in different environments and different conditions.

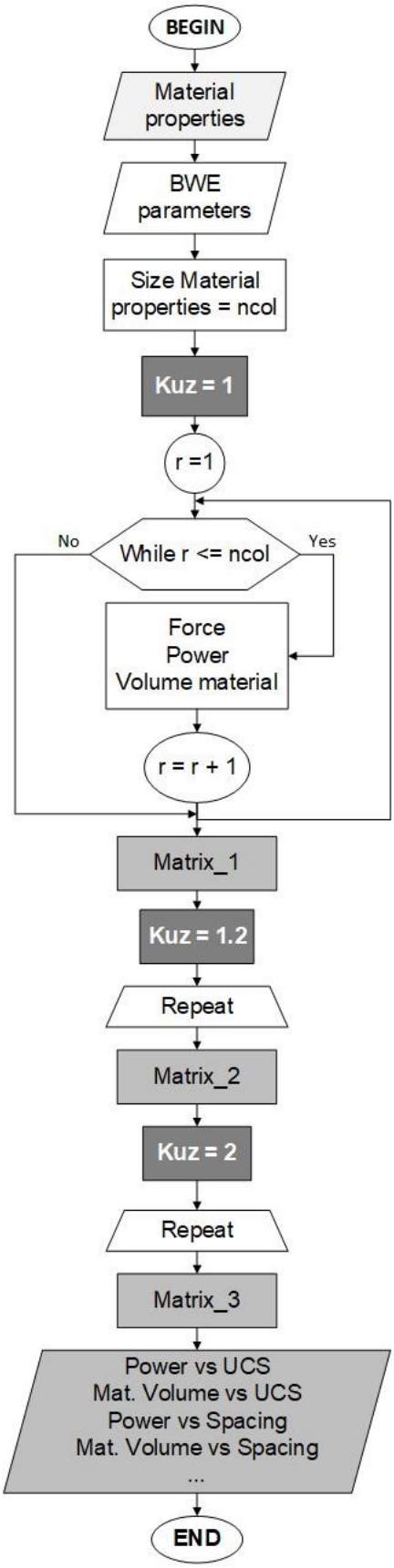

Figure 35 Flow diagram of the machine working regime.

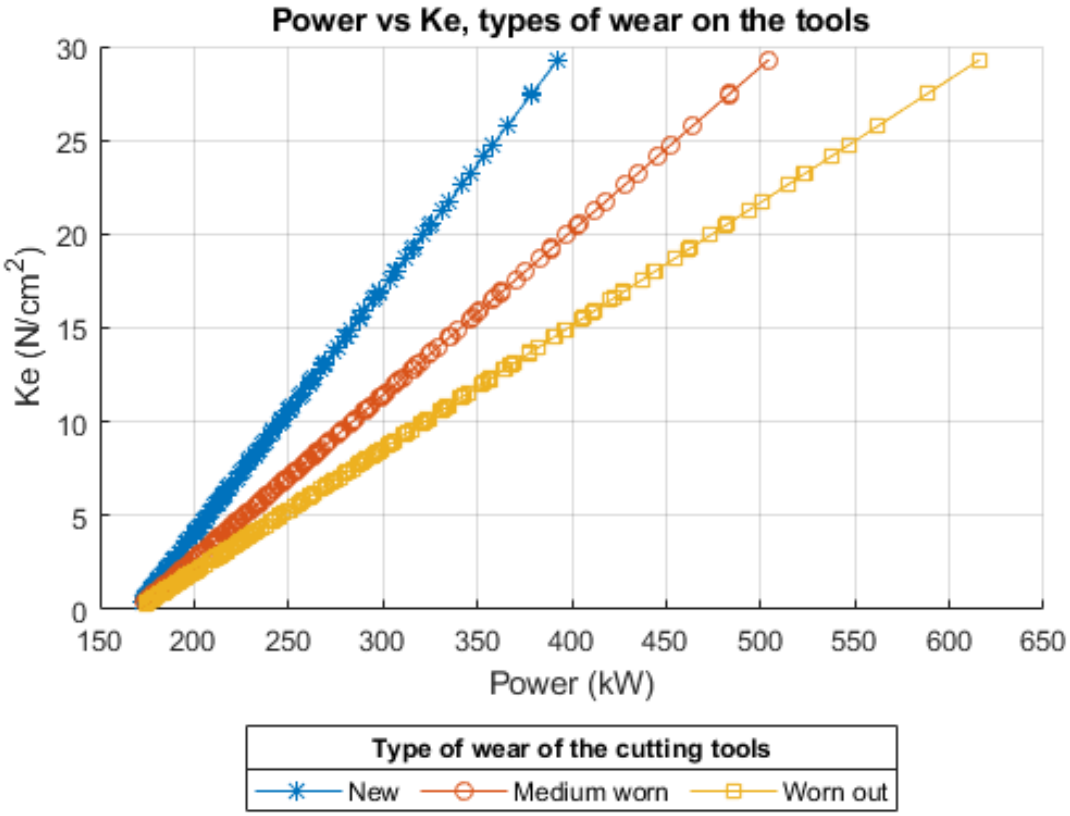

Figure 36 Ke (N/cm^2) range from 0 to 30 N/cm^2 related to the extraction power needed (kW) and the different types of wear of a cutting tool (Kuz value).

4.3.5 Results of the MATLAB code

The results of this part of the calculations reveal the trends of the different possibilities held in the RMR table and the varying parameters. About half a million possibilities were defined.

Figure 37, Figure 38 and Figure 39 display the results regarding the Ke, extraction power and the extracted material volume related to the spacing.

Figure 37 reveals a clear trend: the increasing spacing between the fractures is directly related to the increaseig Ke values. Due to the direct relation between the Ke and extracted power, it is reasonable that the Figure 38 has the same shape as Figure 37 (see equation[17]).

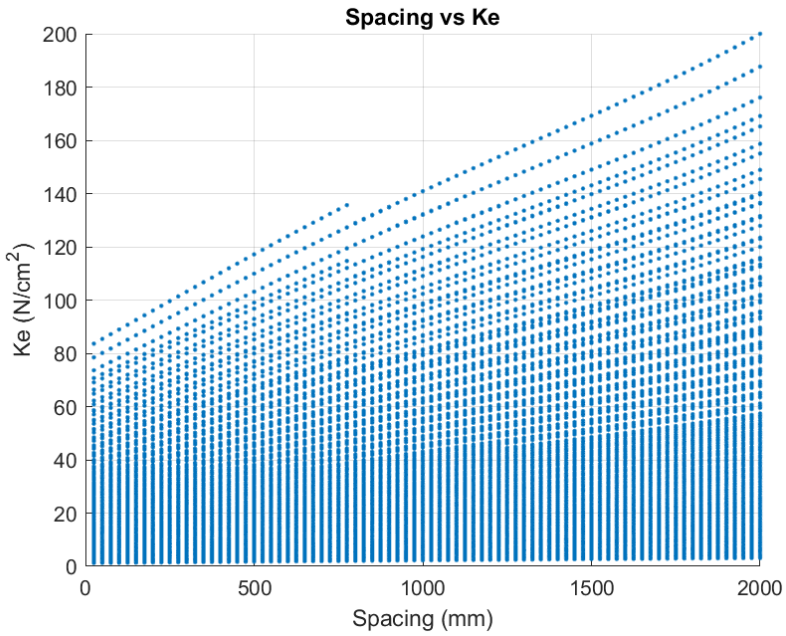

Figure 37 Relation between spacing (mm) and Ke (N/cm^2) that includes all the possible situations according to the RMR$_{89}$

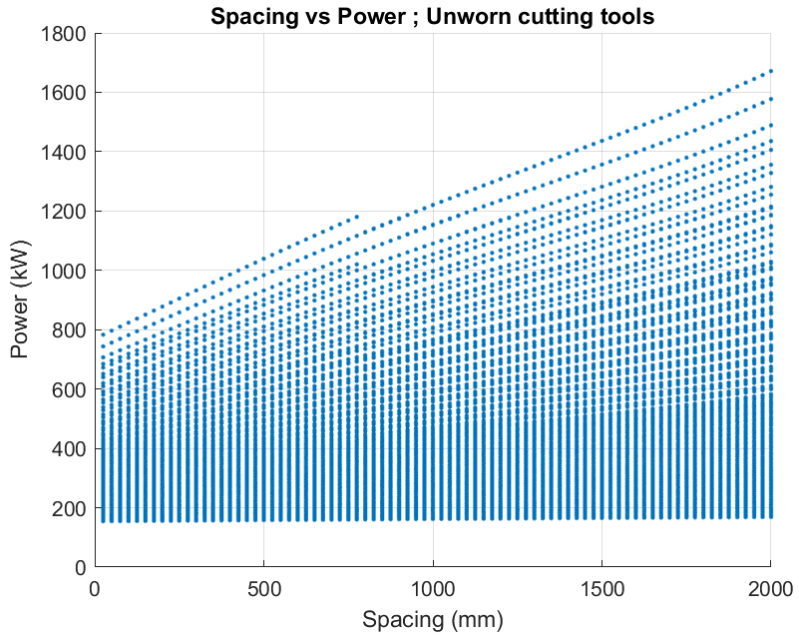

Figure 38 Relation between spacing (mm) and extraction power (kW) that includes all the possible situations according to the RMR$_{89}$

The volume extracted is also related directly with the Ke values and thus the spacing. Figure 29 defines that relation and also a clear trend is determined.

The volume extracted (m^3/h) decreases when the spacing increases. Therefore, the reduction in Ke, reduces the power needed to extract the material and as a direct consequence the volume that can be extracted increases.

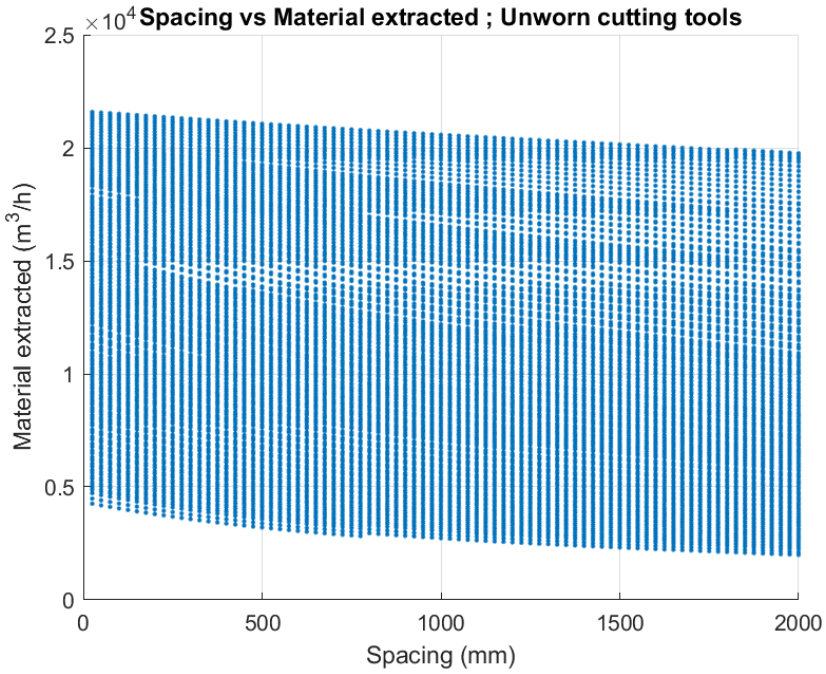

Figure 39 Relation between spacing (mm) and volume of material extracted (m^3/h) that includes all the possible situations according to the RMR_{89}

The state of the cutting tools determines the perfomance of the machine in terms of higher energy consumption (Figure 36). For the calculations in this chapter, the cutting tools wear was considered unexistent. However, this would not have a influence on the trends exposed. Applying other Kuz value would have resulted only in higher values of power consumption.

5 RESULTS ON THE BWE WORKING REGIME

FL-Smidth kindly provided data obtained by sensors assambled in a BWE. The data provided corresponds to the year 2018 and the measuring and storing frequency is 1Hz. The results regarding June and August are not included as there are no data available. The machine extracts the overburden of a coal mine in a continous regime.

In order to explain the procedure followed the only the data obtained in January 2018 is featured in this chapter to reduce the amount of graphs. However, all the data provided was used in the calculations and some plots for the entire year are also included.

Figure 40 Model of a BWE operating on an open pit cast. (FL-Smidth)

5.1 Data provided

Those sensors do not measure forces, which are the value needed in order to analyse the working regime of the machine, as it has been explained in previous chapters. Among other values, the voltage, torque, revolutions of the motor of the BW, material extracted at the dumping point of the conveyor belt, were given.

The torque was used to calculate the Fx force acting on the BW. The Ke was calculated using that Fx values. Afterwards, the power needed to extract the material was calculated. The power was calculated by using two methods:

- Equation [16]: $Pex = 10^{-3}\ FxR\ \ vt,\ kW$
- Equation [17]: $Pex = \frac{1}{360}\ Kuz\ \ Ke\ \ Qm,\ kW$

The propuse of that, is check that the method used fits with the data used. Other reason was that, by using these two methods the state of the teeth or cutting tools, Kuz parameter, can be established.

The equation [17] was calculated with a Kuz value of one, and after reckon the ratio between those two equations the real Kuz mean value was obtained. The difference between the results can be seen in Figure 41.

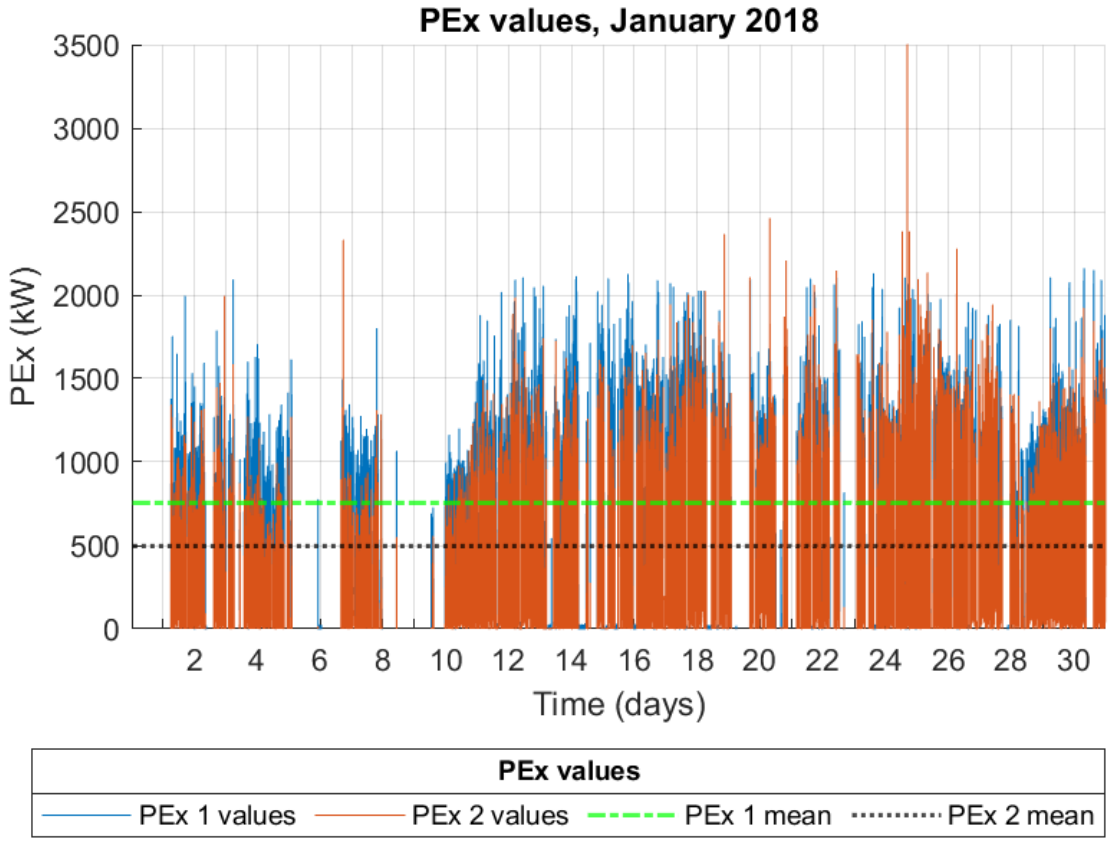

Figure 41 Extraction power of the object BWE using two different equations and showing the difference in power due to the wear condition of the cutting tools (Kuz value). Mean value PEx 1 = 750.75 kW, Mean value PEx 2 = 493.04 kW.

In this case Kuz, the wear condition parameter, is around 1.5, if calculated using the mean values of Pex 1 and PEx 2, which means that the cutting tools wear out easily, above the average, which is reasonable because of the type of operation the machine does. The overburden in the coal mine is a soft type of sandstone;

however, even the soft sandstone contains high levels of quartzite which turns this rock intro a rather abrasive one.

The figure above also relates the importance of replacing the cutting tools, thus the regular maintenance of the BWE. The difference between worn out picks (blue) and the brand-new ones (orange) is large in terms of necessary power to dig out the material.

There is no geotechnical study available of this specific mine. That is the reason why the Ke was caculated back from the torque and applied forces. Figure 42 displays the changing values of Ke during January 2018.

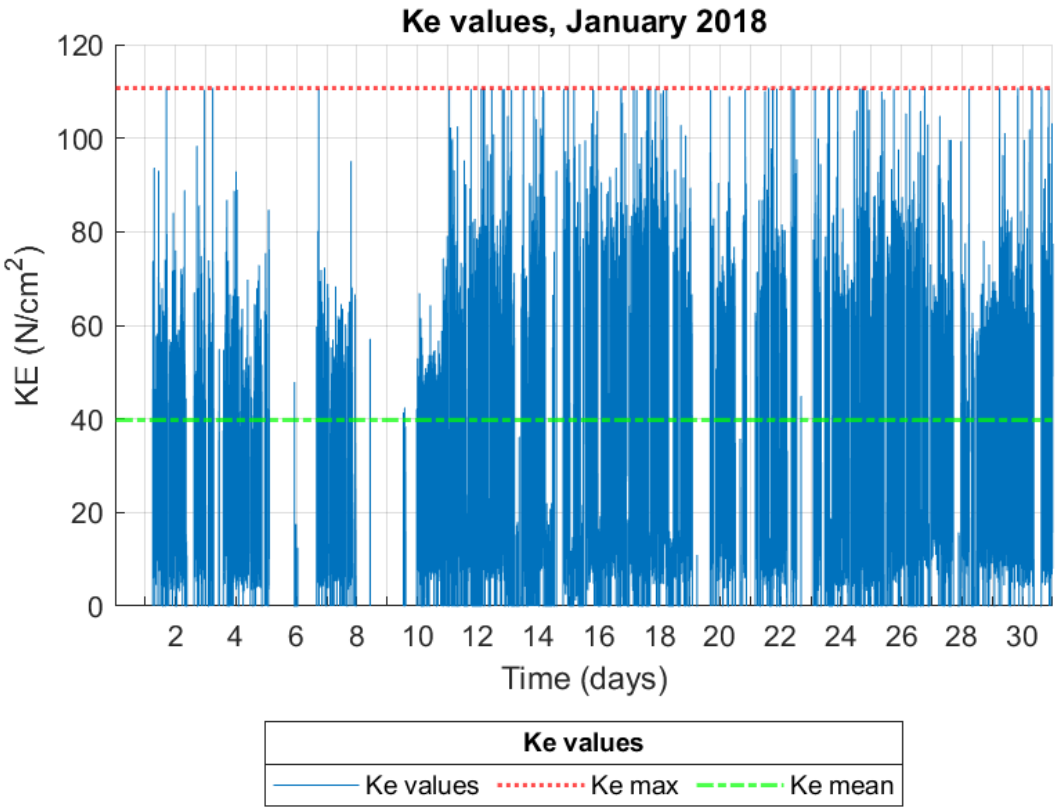

Figure 42 Cutting resistance values (Ke) of the BWE in January 2018 without any modification. Dashed line: mean value (39.09 N/cm^2) Maximum value: dotted line (109.26 N/ cm^2).

Unfortunatelly there are no values of June and August and these were removed from the charts and further calculations. The maximum values trend is easy to

notice: almost plain along the year with values up to 110 N/cm^2. The average values are slighly scattered; however the values also in the range of 30 to 40 N/cm^2.After analysing the results of the data (Figure 45) it is obvious that the machine does not work always in the proper working regime, as the Ke values are over the upper limit.

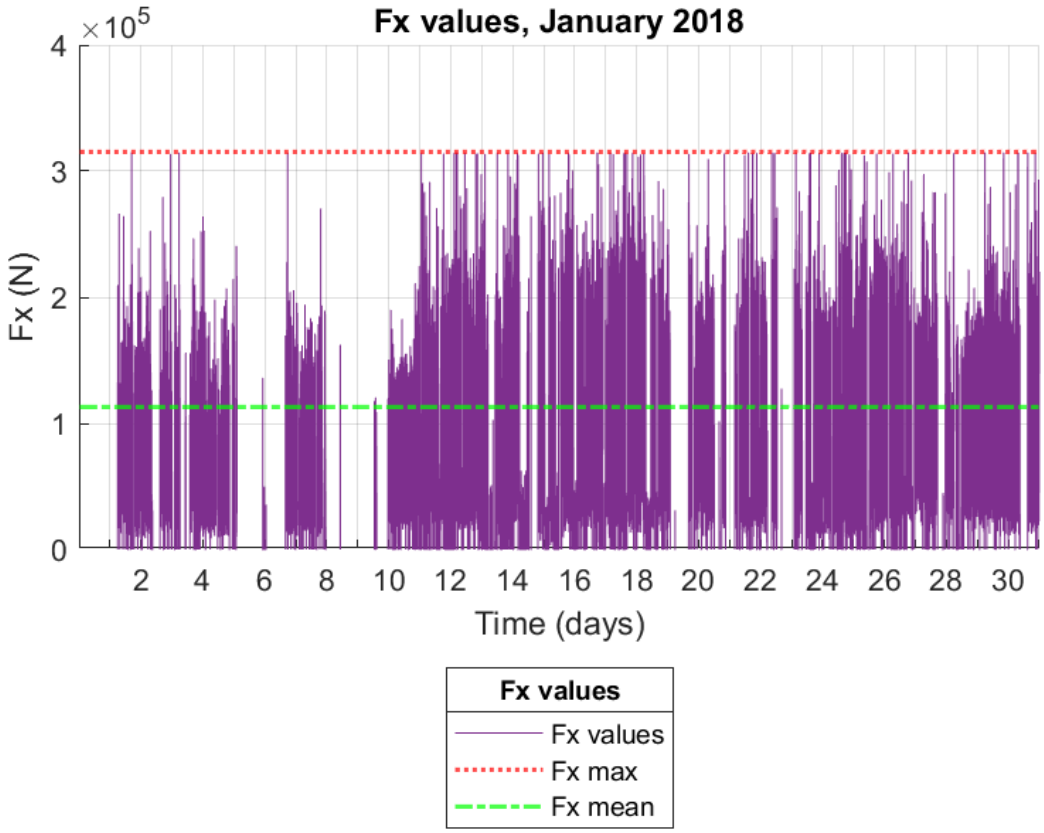

Figure 43 Fx force applied in January 2018 to extract the material. Fx mean, dashed line =1125.8 kW; Fx max value, dotted line = 3146.8 kW.

Figure 43 presents the data regarding the force needed to extract the material and it can be noticed that Figure 43 and Figure 42 reveal a similar pattern and trend due to the proportionality that the force applied formula and the calculation of the specific cuttting force have.

From this point, the comparison of the values and their reduction is going to be done just by comparing the Ke values and the power needed to achieve the extraction of the material.

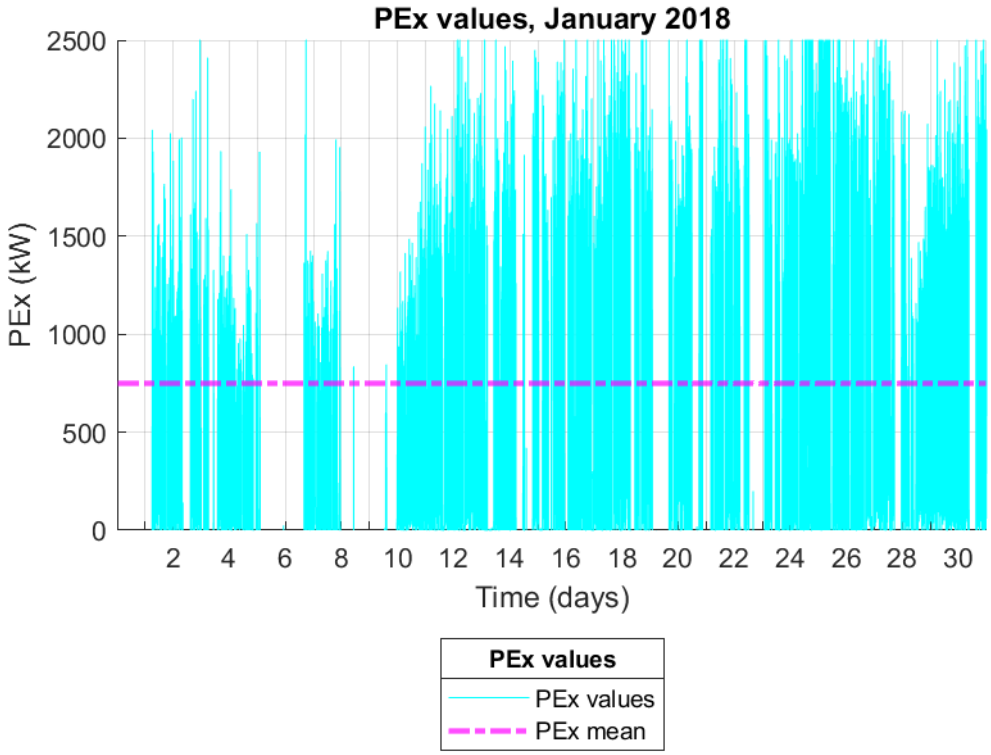

Figure 44 Initial Extraction power values during January 2018 without any modifications on the Ke. Dotted line: Mean value: 674.47 kW.

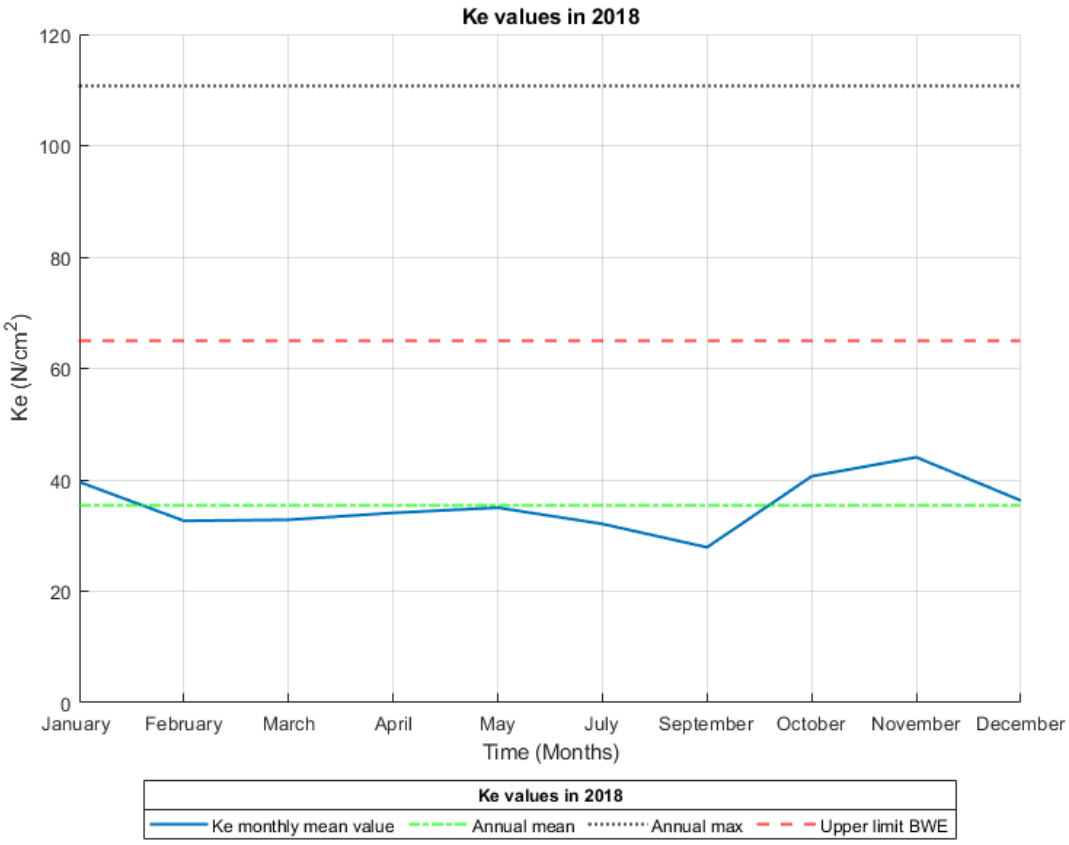

Figure 45 Ke monthly average values of the year, 2018. June and August are omitted due to the lack of data on those periods. Annual mean = 35.5 N/cm^2, Annual max = 110.82 N/cm^2, Upper limit BWE = 65 N/cm^2.

Figure 46 illustrates how the extraction power Pex 1 developed during the entire year 2018. If the Figure 46 is compared to Figure 45 there are similarities in the trend of both lines. In September the Ke mean value is dramatically reduced and so the extraction power Pex 1 experienced a large decrease too.

In absolute values, the BWE operates in a proper regime as the average value of Ke is below the Upper working limit Ke1 (65 N/cm^2); however, the maximum values are way above the average, in which cases the values are almost double the Upper BWE limit. This situation suggest that hard and unexpected materials occur in the deposit. Those harder materials might be the target of the microwave procedure.

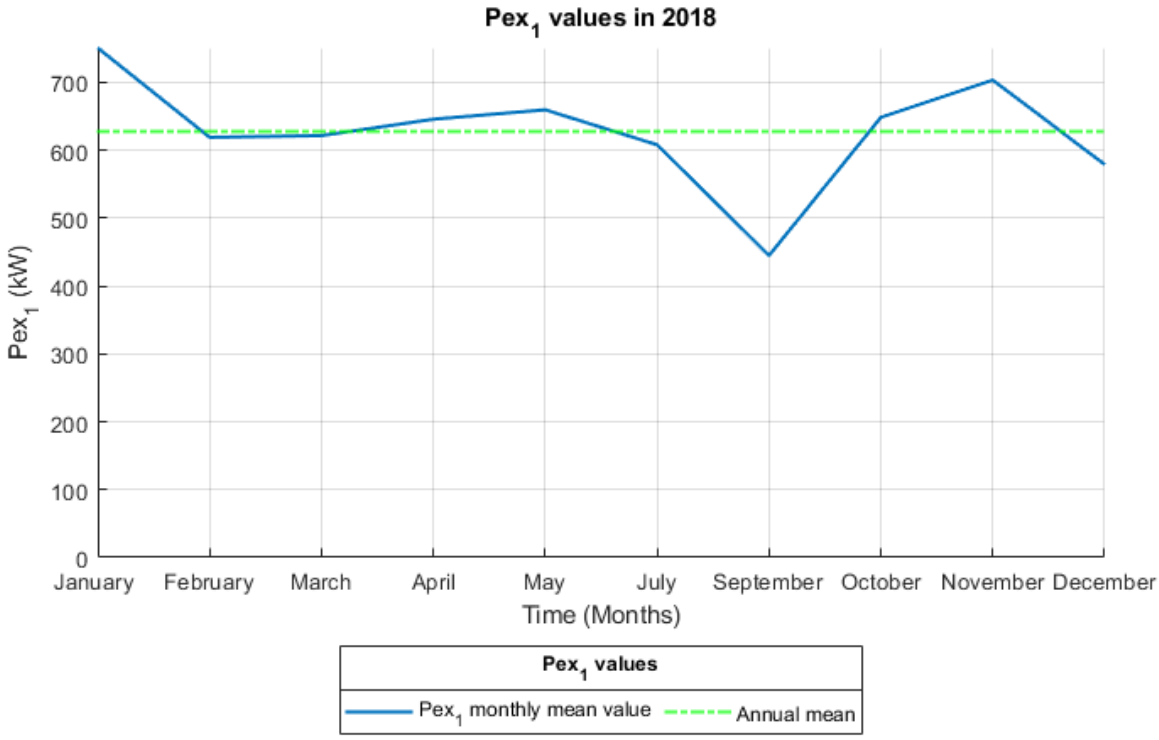

Figure 46 Pex 1 values in 2018. Pex 1 annual mean value = 628.06 kW.

Table 10 Summary of the 2018 Ke values of the object BWE of January and the whole year in order to compare the differences and BWE behavior forecast.

Parameter	Value (N/cm^2)
The average value of the Ke in January	39.61
The average value of the whole year	35.51
The maximum value of the Ke in January	110.72
The maximum value of the whole year	110.82
Upper limit of the working regime of the BWE, KE1	65

5.1.1 Reduction of the Ke values and response

The reduction of the Ke was defined in different stages in order to evaluate the different proposals for its application. The main discussion is focused on the Ke values and extraction power.

The following hypotheses, which apply a reduction of 10%, 15% and 20% of the Ke values on the whole area of extraction, show the reduction of the extraction power.

On the other side, the Ke parameter was also reduced until the working limit Ke1 and to 45 N/cm^2. Ke1 determines the maximum value of cutting resistance until which the BWE performs in the adequate regime. In this case the values above 65N/cm^2 were the only ones to be reduced, thus this calculation refers to a local treatment rather than an overall procedure. The other case when the Ke is reduced to 45 N/cm^2 follows the same local procedure but this time the cutting resistance is reduced to a value in the range of optimum performance, not just to its upper limit.

5.1.1.1 Reduction of Ke by 10%

The power needed to extract the material is directly proportional to the Ke (equation [17]). If all the values of the Ke are reduced by 10% the extraction power will also be decreased too. This effect can be seen in the Figure 47 and Figure 48.

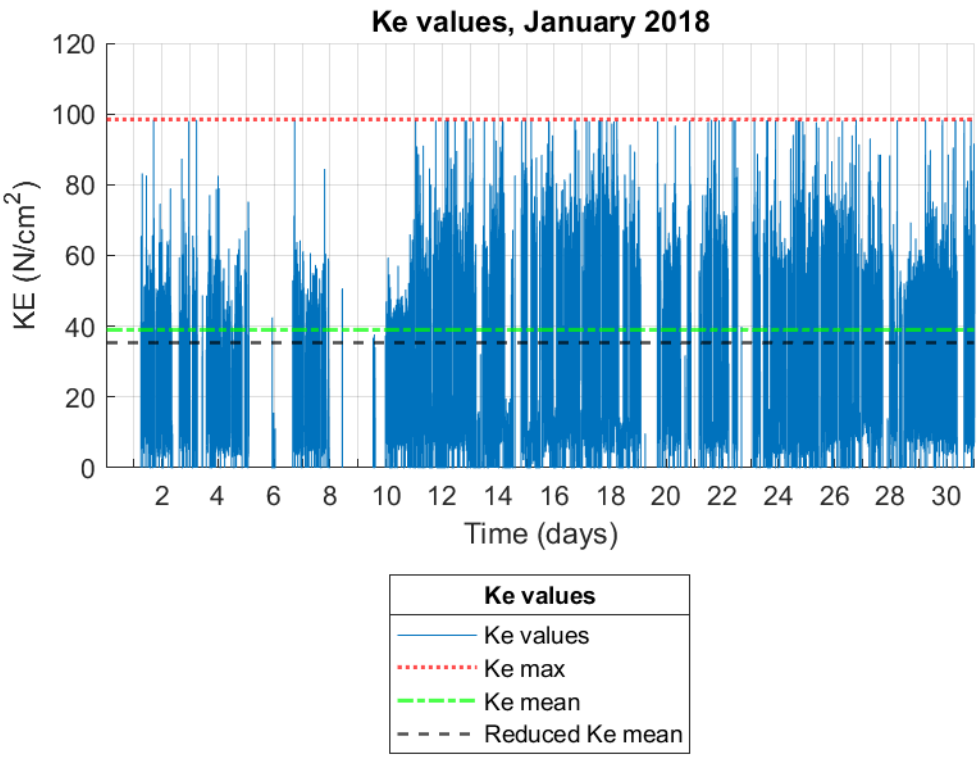

Figure 47 Ke decreased by of 10%, in January 2018 Wider line: year average value (39.09 N/cm^2) Maximum value: dotted line (109.26 N/cm^2). Dashed line: Reduced mean of Ke (35.18 N/cm^2)

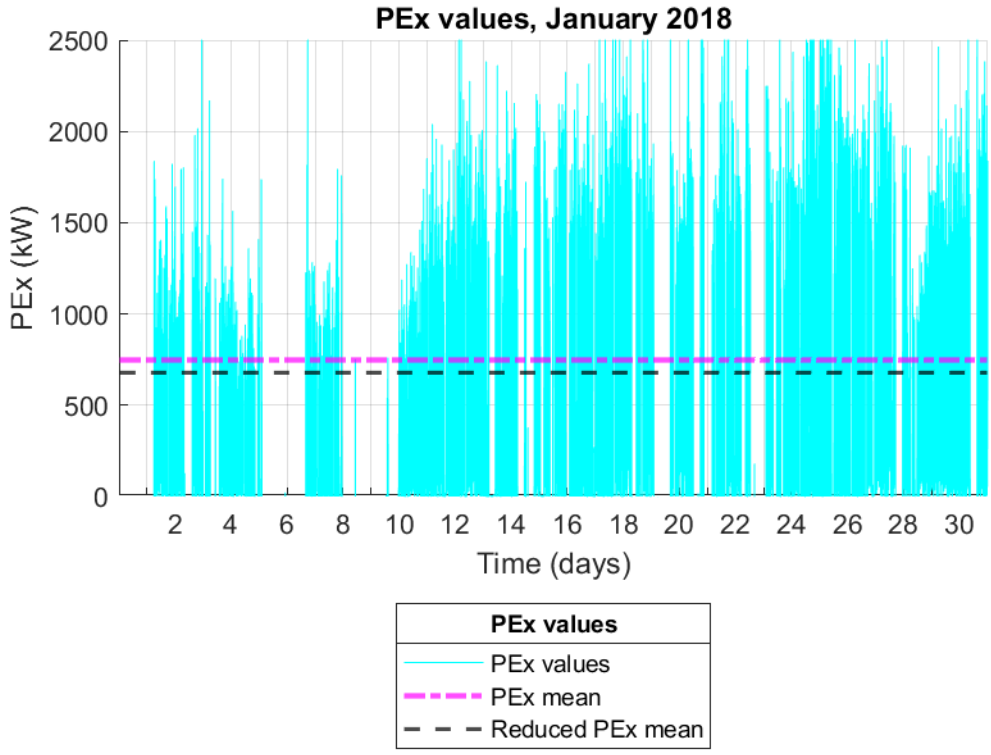

Figure 48 Extraction power after Ke is reduced 10%. Dotted line: extraction power mean value: 749.41 kW. Continuous line: Reduced Pex mean: 674.47 kW.

The reduction of power is confirmed after the reduction of Ke by the 10%. In absolute numbers, the extraction power has been reduced by 10% too.

The average value prior any modification is 582.96 kW and the average after the treatment has been decreased to 524.67 kW.

5.1.1.2 Reduction of Ke by 15%

The reduction of the Ke by 15% reveals also an improvement on the extraction (Figure 49 and Figure 50).

The reduction again shows a reduction by the same value. This time the average Ke value is 33.73 N/cm^2 and the reduced power after the treatment is 495.52 kW.

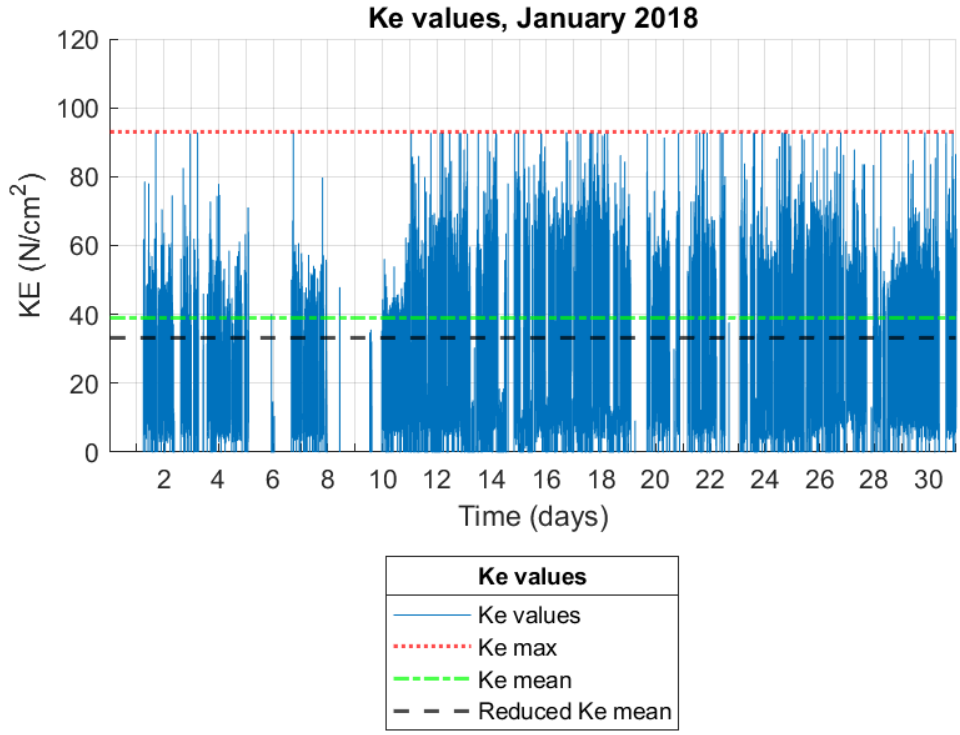

Figure 49 Ke decreased by of 15%, in January 2018 Wider line: year average value (39.09 N/cm^2) Maximum value: dotted line (109.26 N/ cm^2). Dashed line: Reduced mean of Ke (33.22 N/ cm^2).

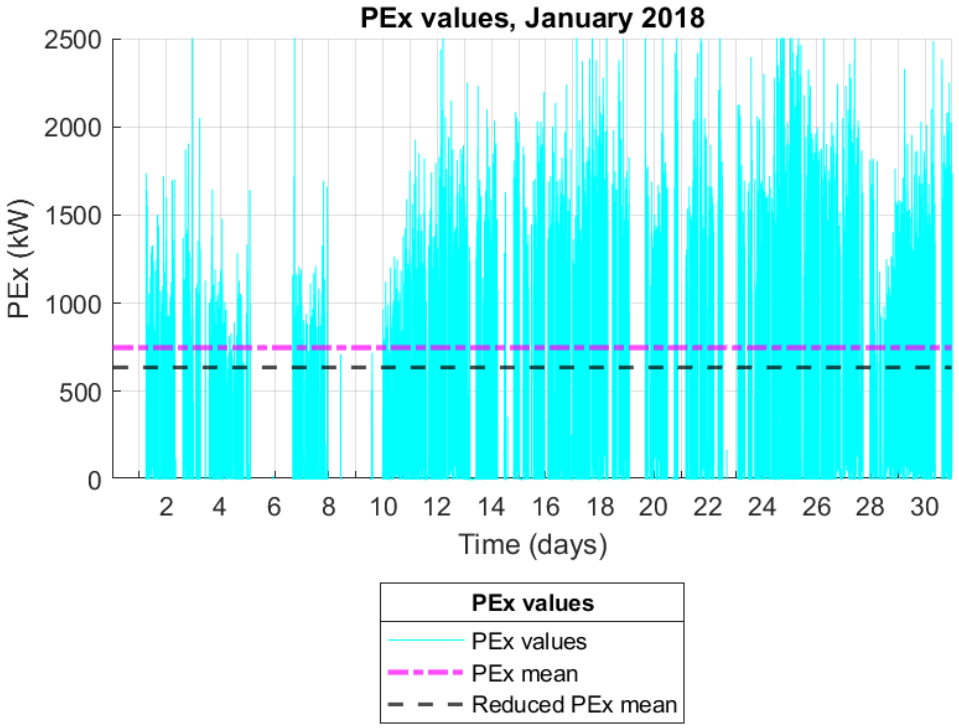

Figure 50 Extraction power after Ke is reduced 15%. Dotted line: extraction power mean value: 749.41 kW. Continuous line: Reduced Pex mean: 637.00 kW.

5.1.1.3 Reduction of Ke by 20%

A reduction of the 20% of the Ke value is again the trigger factor to reduce the extraction power to the same amount. Figure 51 and

Figure 52 confirm the concept. The Ke averaged value is 31.74 N/cm^2 and the extraction power was reduced to 466.38 kW.

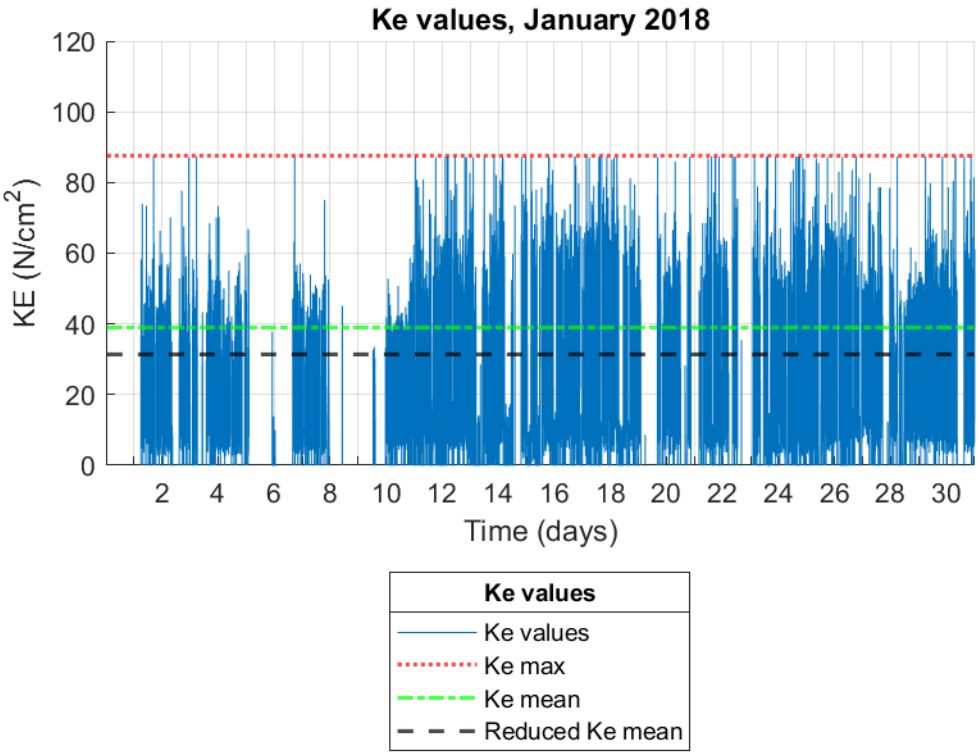

Figure 51 Ke decreased by of 20%. Wider line: year average value (39.09 N/cm^2) Maximum value: dotted line (109.26 N/ cm^2). Dashed line: Reduced mean of Ke (31.27 N/ cm^2).

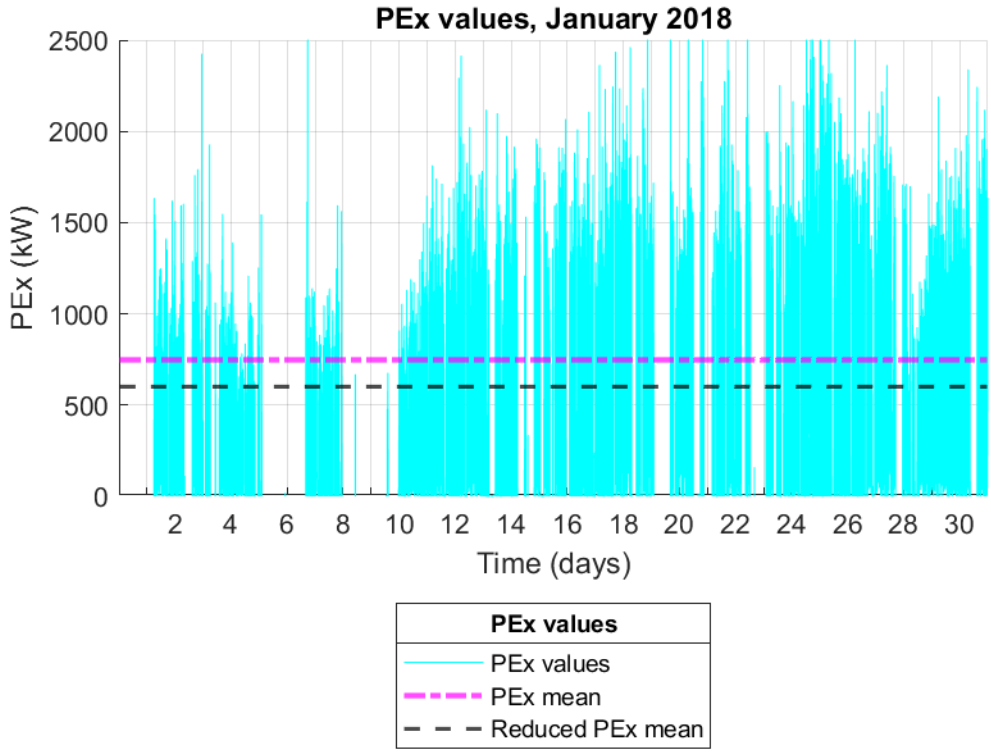

Figure 52 Extraction power after Ke is reduced 20%. Dotted line: extraction power mean value: 749.41 kW. Continuous line: Reduced mean: 599.53 kW.

5.1.1.4 Reduction the of Ke to upper limit Ke1, 65 N/cm2

This case displays a reduction of Ke to the Ke1, or upper limit, which determines the highest Ke value that the BWE excavates still being in the optimum performance range.

For this purpose, only the values higher than Ke1 will be affected. This reduction will not affect all the values, so it must be considered as a punctual or local treatment, for example for hard rock occurrences.

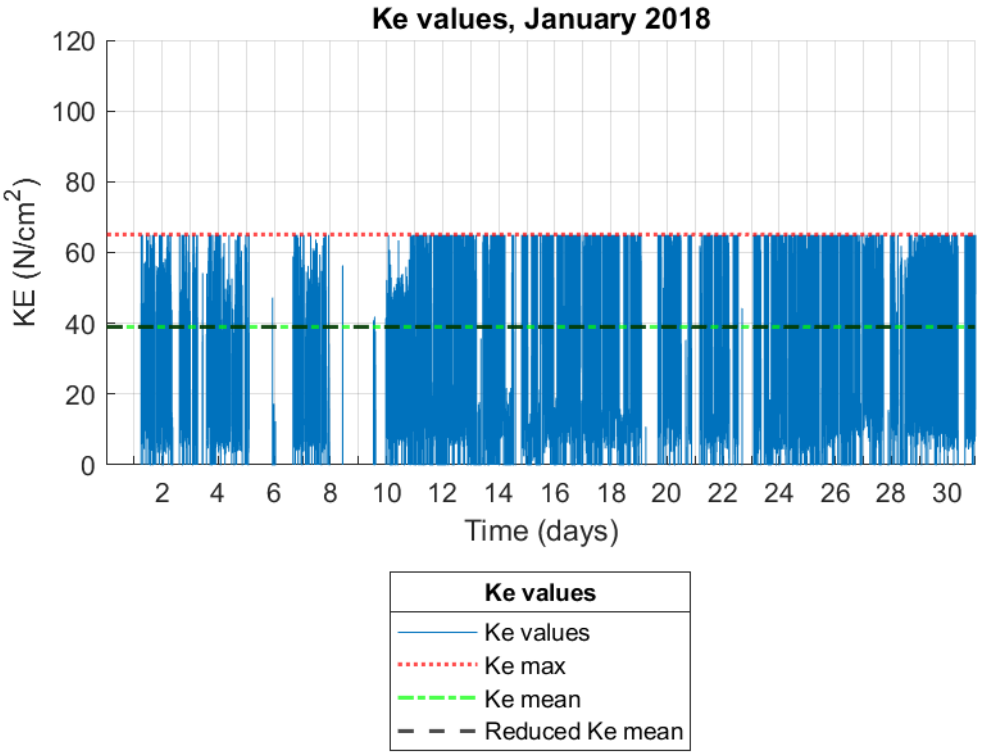

Figure 53 Ke decreased until reach Ke1 (65 N/cm^2). Wider line: year average value (39.09 N/cm^2) Maximum value: dotted line (109.26N/ cm^2). Dashed line: Reduced mean of Ke (38.96 N/ cm^2).

The results show that the average Ke value is close to the average value prior the treatment. The exact value of the average after the treatment is 39.53 N/cm^2 and the average prior the treatment is 39.68 N/cm^2, which is actually the effect expected. The same effect can be noticed on the extracted power: the after—treatment extraction power (580.96 kW) is almost the same value as the average value before the treatment (582.96 kW).

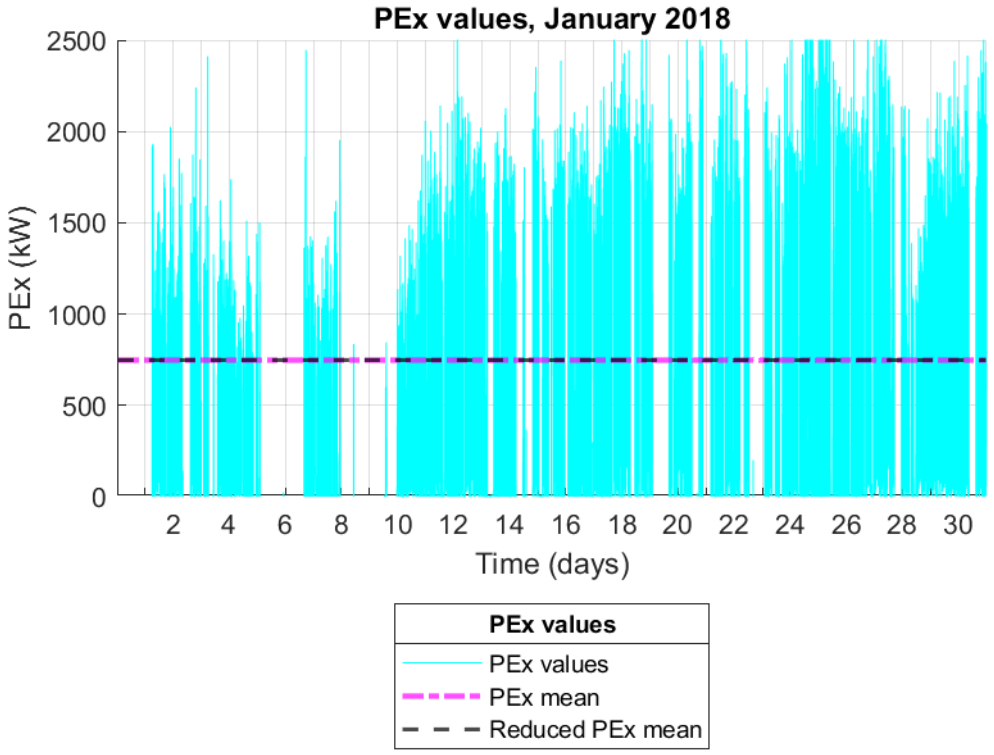

Figure 54 Extraction power after Ke is reduced to 65 N/cm^2. Dotted line: extraction power mean value: 749.41 kW. Reduced mean: 746.81 kW. Both means overlap in this graph.

5.1.1.5 Reduction of the Ke values if they are above 45 N/cm^2

The reduction of the Ke to 45 N/cm^2 must be considered also as a local procedure but this time the range of treated material is more extended, as it can be seen on Figure 55. The average Ke value after the treatment is 36.38 N/cm^2 and the extraction power is 528.32 kW.

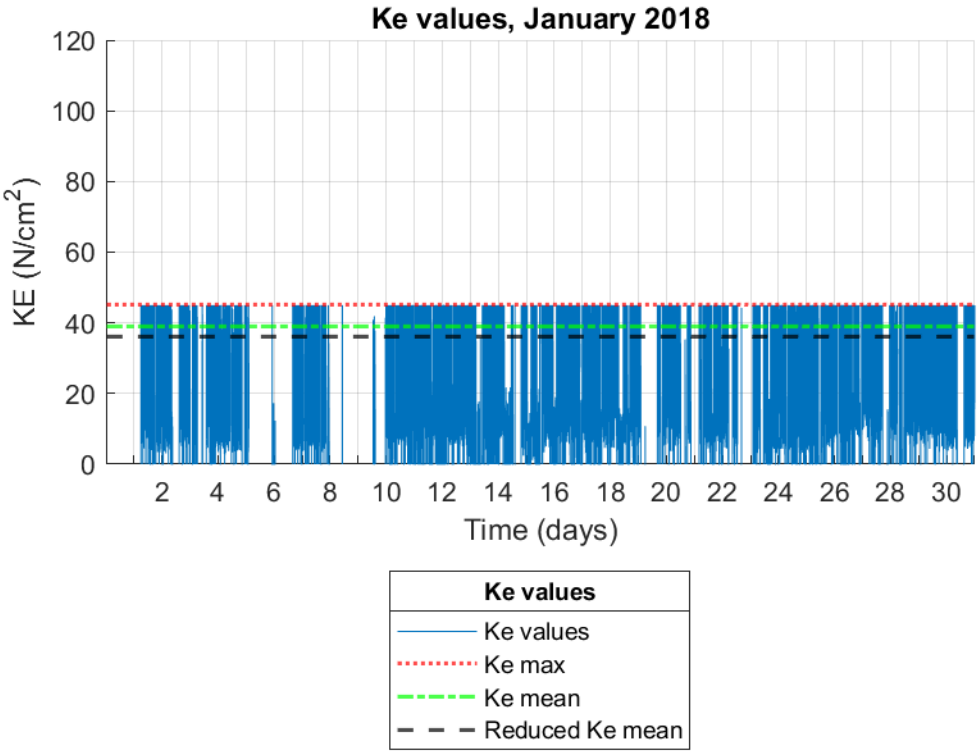

Figure 55 Ke decreased to maximum value of 45 N/cm^2 in January 2018. Wider line: year average value (39.09 N/cm^2) Maximum value: dotted line (109.26 N/ cm^2). Dashed line: Reduced mean of Ke (36.07 N/ cm^2).

In practice, the reduction to certain value (as explained in chapter 5.1.1.4 and this one) is the most suitable method because of the simplicity of the application. It is easier to set up a configuration or select a specific pattern for the whole area to treat rather than vary the pattern constantly.

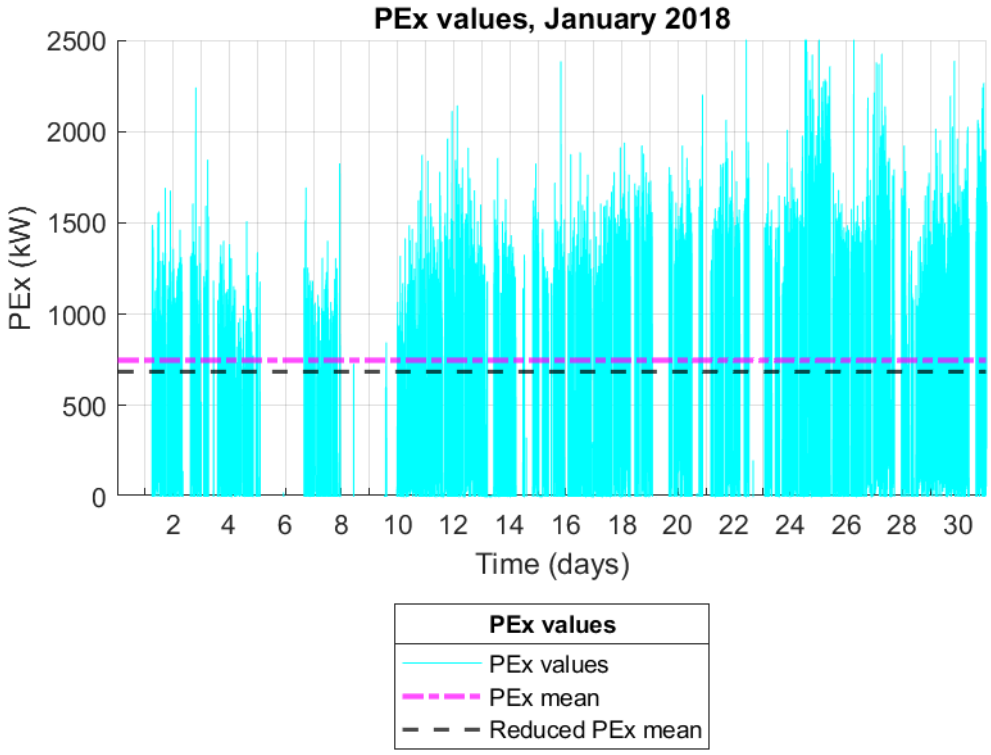

Figure 56 Extraction power after Ke to the maximum value of 45 N/cm^2. Dotted line: extraction power average value: 749.41 kW. Continuous line: Reduced mean: 684.08 kW.

5.2 Relation between Ke reduced values and the fracture patterns

It is necessary to establish some parameters by using assumptions and some cases, in order to determine how much the RMR value must be reduced and afterwards, determine the most suitable microwave irradiation pattern.

In order to evaluate these hypotheses, equations [6], [7] and [36] were used. Those equations relate the RMR, Ke, UCS and rock mass strength.

5.2.1 Soft material

The rock that the BWE digs out is soft material, and thus for this example the UCS is assumed to be 32 MPa, friction angle 10º and cohesion 4 MPa. The Ke initial value is 31.1 N/cm^2, which has been calculated after the established parameters: cohesion, friction angle, UCS.

It is also assumed that the RMR has a high value under those circumstances, so there are no fractures on the material which would reduce the RMR value. The

conditions of the rock are assumed to be the best, and the only parameter which reduces it of course is the UCS rating. For those reasons, the RMR obtained after the calculations is 87.29.

This first example has not been performed to reduce the values to a maximum of 45 or 65 N/cm^2 as the settled initial Ke value is below those values. The reduction of the values is established in each 5% until it reaches a reduction of 25%.

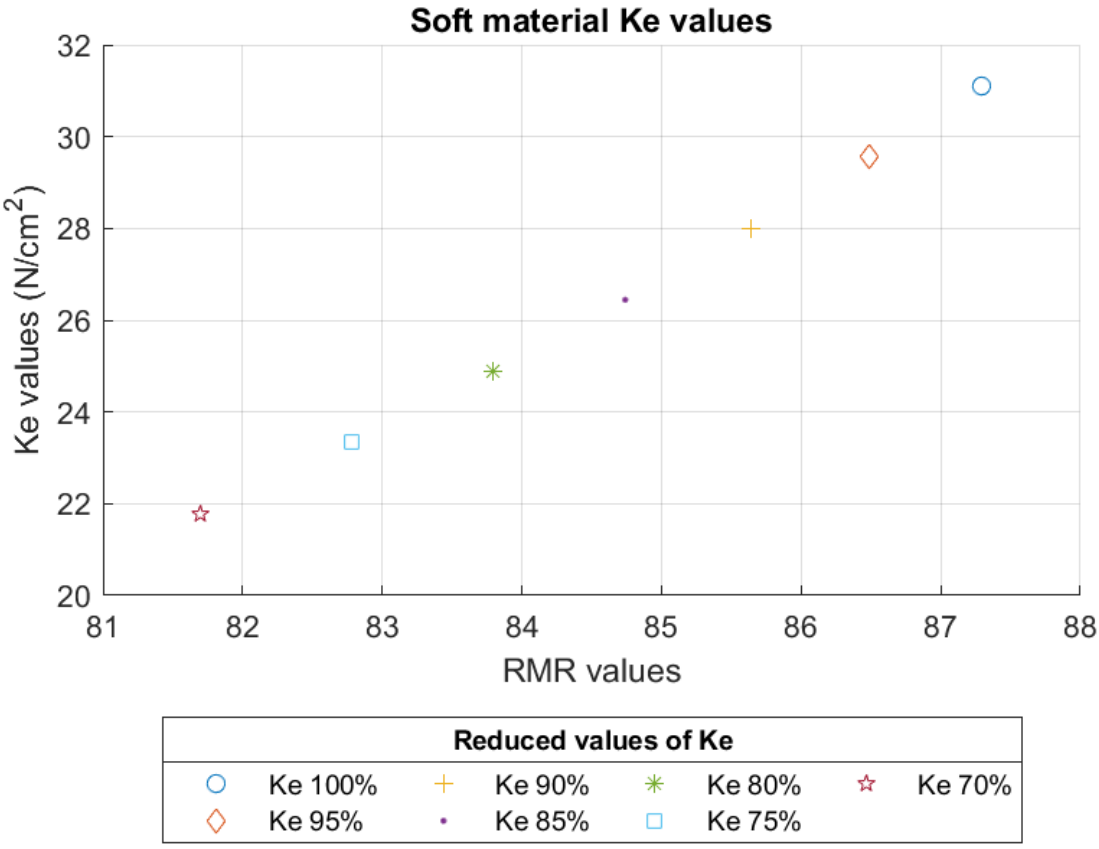

Figure 57 Relation between the Ke values and RMR absolute values needed for the initial Ke and each Ke reduced values in a soft material.

This first example gives an overview of how the reduction of the RMR produces a reduction in the Ke, although it does not make a lot of sense to pretreat this soft material as the maximum Ke value is below the Upper limit Ke 1 of the BWE which means that the machine can operate perfectly under these circumstances.

5.2.2 Hard material

If the material becomes harder, the rock parameters will change and to illustrate this situation the following rock parameters have been chosen: UCS is 100 MPa, friction angle is 30º, cohesion is 10 MPa and the initial Ke value (calculated after the settled rock parameters) is 111.1 N/cm^2. The RMR in this case is also calculated as the best rock conditions, which means that the only parameter that is taken into consideration is the UCS and for those reasons the initial RMR value is 90.7. The procedure followed is the same as in the soft material example.

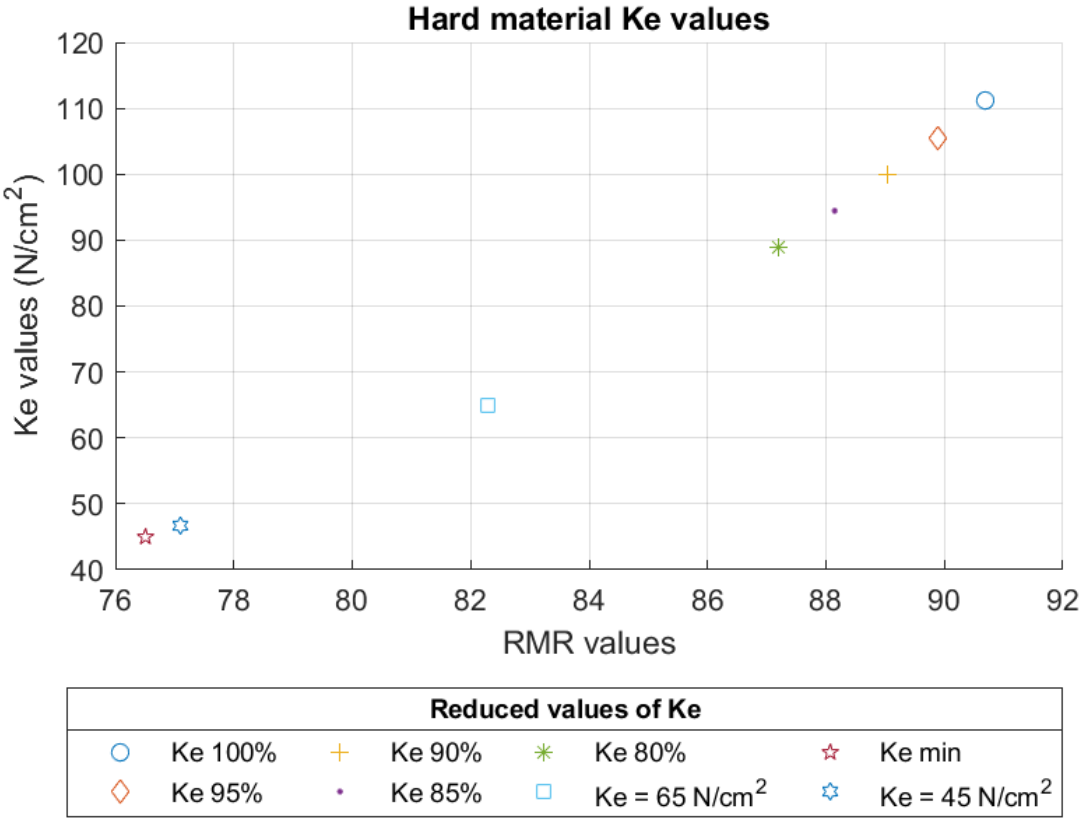

Figure 58 Relation between the Ke values and RMR absolute values needed for the initial Ke and each Ke reduced values in a hard material.

The results of the several reduction cases are illustrated in Figure 58. It can be noticed that the smallest reductions (from 5% until 20% of Ke value) do not decrease enough the Ke value and do not go below the upper BWE limit which has a value of 65 N/cm^2. However, the reduction until 65 N/cm^2 (RMR value = 82.28) is possible as the RMR must be reduced only by a 9.28%. on the other hand, the reduction until

45 N/cm^2 could not be reached as the maximum reduction by means of microwave irradiation pretreatment is 15%.

Thus, the maximum reduction of RMR is 15%, RMR = 77.095, which means that the minimum Ke value which might be performed is 46.70 N/cm^2.

As it was expected, the reduction of Ke to 45 N/cm^2 needs the highest reduction of the RMR to full fill that requirement (see Figure 58).

The pattern of the spots which would be irradiated with microwaves are calculated using the formulas [27], [29] and [30], which were obtained from Figure 25, Figure 26 and Figure 27.

This group of formulas and graphs which have been explained in previous chapters are the main relations between the Ke, RMR, fractures and fracture patterns. The results are given in the Table 11.

In the Table 11 the results show the trend as it was assumed since the beginning: the more fractures, the lower RMR and as a direct consequence, a reduction in the cutting resistance Ke.

Table 11 Results of the hypothesis in terms of reduction of RMR (%) fractures, fractures density and spacing (mm).

Ke values	RMR needed	RMR reduction (%)	Average spacing needed (mm)	Distance between spots (mm)	Fracture density (fractures/m2)
Ke reduced 10%	89.894	0.89%	1818.3	1789	2
Ke reduced 15%	88.148	2.81%	1458.7	1449	3
Ke reduced 20%	87.196	3.86%	1278.8	1279	4
Ke = 65 N/cm2	82.294	9.27%	519.0	561	17
Ke minimum = 46.7 N/cm2	77.095	15.00%	224.7	283	63
Ke = 45 N/cm2	76.512	15.64%	204.5	264	72

It can be noticed also that the reduction from 10 to 20% of Ke do not reveal a large reduction, which has been already discussed. The results also show that there is a huge difference between reaching 65 N/cm^2 and the minimum reachable value of Ke 46.7 N/cm^2 in which case the difference of the fracture density is almost 4 times.

In the following example, changes on the UCS have a high impact in the RMR needed in order to get a material which is diggable by a BWE.

Continuing with the procedure explain before, Table 12 displays the results of the varying UCS values and the decrease of RMR (%) needed, when the Ke value for the whole process remains constant with a value of 65 N/cm^2, which is actually the upper limit of the optimum range for the object BWE.

The average spacing needed in some of the hypotheses are negative (cases of reduction below 15%). The reason behind is that the RMR reduction cannot be greater than 15% and if that occurs then the average spacing turns negative.

Table 12 Relation between the UCS and the RMR reduction needed to be dug out by a BWE in an optimum working regime.

UCS (MPa)	RMR reduction (%)	Average spacing needed (mm)	Distance between spots (mm)	Fracture density (fractures/m^2)
30	9%	541	582	21
40	14%	73	140	317
50	18%	100	165	231
60	21%	100	165	231

As the fractures developed due to the microwave irradiation grow up to 100 mm from the irradiated spot and it is considered as the minimum distance between spots, the suggested distance is that one. After the determination of the distance between the spots, once again the fracture density is calculated.

The negative results in these calculations do not mean that the procedure would not increase the range of application of the BWE. The calculations depend on a large list of parameters. The possibilities are uncountable as well as the scenarios.

Additionally, the results are based on one specific machine and as the design and mechanical set up of it also influences the results.

CONCLUSIONS

- It was proven that the development of fractures by microwave irradiation affects directly the cutting resistance of the materials. Inducing fractures on the rock decreases the RMR value up to a 15%.

- The reduction of the RMR, thus the reduction of the cutting resistance, is a critical factor both to increase the performance of a machine and to increase the range of material diggable by a BWE. However, there are constrains related to the machinery technical characteristics and design.

- The study was based on a 2D problem, due to the lack of data regarding the penetration depth of the microwaves in different materials. It is suggested to research in deep this topic and invest in real cases, using samples of rocks which might be possible targets for this purpose.

- The calculations were based on a single machine, as well it is suggested to study a wider list of BWE in order to verify the method more extensively and to adjust the procedure followed in this study.

- It must be also considered the different designs, possibilities and versatility that BWE provide. More design parameter should be considered in further studies.

BIBLIOGRAPHY

Abdi, Hamdi; Rasouli Nezhad, Ramtin; Salehimaleh, Mohammad (2017): Fuel Cells. In *Electrochemical Energy Storage for Renewable Sources and Grid Balancing*, pp. 221–300. DOI: 10.1016/B978-0-12-804208-3.00005-4.

Andras, Iosif; Andras, Andrei; Stela, Dinescu (2016): On the Correlation of Cutting Resistance and Physical-mechanical Properties of Lignite and Overburden Rocks from Oltenia Coalfield. DOI: 10.26649/musci.2016.002.

Bölükbaşsi, Naci; Koncagül, Oğuz; Günhan Paşsamehmetoğlu, A. (1991): Material diggability studies for the assessment of bucket wheel excavator performance. In *Mining Science and Technology* 13 (3), pp. 271–277. DOI: 10.1016/0167-9031(91)90426-D.

Brady, B. H. G.; Brown, E. T. (2004): Rock mechanics. For underground mining. 3rd ed. Dordrecht, Boston: Kluwer Academic Publishers.

Celada, B.; Varona, P.; Rodríguez, A.; Bieniawski, Z. T. (2014): Proceedings of the World Tunnel Congress 2014 – Tunnels for a better Life. Foz do Iguaçu, Brazil.

G.S. Kalamaras; Z. T. Bieniawski (1995): A Rock Mass Strength Concept For Coal Seams Incorporating the Effect of Time. In *Rock Mech Rock Eng*.

Hartlieb, Philipp; Bock, Stefan (2018): Theoretical Investigations on the Influence of Artificially Altered Rock Mass Properties on Mechanical Excavation. In *Rock Mech Rock Eng* 51 (3), pp. 801–809. DOI: 10.1007/s00603-017-1355-3.

Hartlieb, Philipp; Grafe, Bruno (2017): Experimental Study on Microwave Assisted Hard Rock Cutting of Granite. In *Berg Huettenmaenn Monatsh* 162 (2), pp. 77–81. DOI: 10.1007/s00501-016-0569-0.

Hartlieb, Philipp; Grafe, Bruno; Shepel, Taras; Malovyk, Artem; Akbari, Behnam (2017): Experimental study on artificially induced crack patterns and their consequences on mechanical excavation processes. In *International Journal*

of Rock Mechanics and Mining Sciences 100, pp. 160–169. DOI: 10.1016/j.ijrmms.2017.10.024.

Hassani, Ferri; Nekoovaght, Pejman M.; Gharib, Nima (2016): The influence of microwave irradiation on rocks for microwave-assisted underground excavation. In *Journal of Rock Mechanics and Geotechnical Engineering* 8 (1), pp. 1–15. DOI: 10.1016/j.jrmge.2015.10.004.

López Jimeno, Carlos (1995): Manual de arranque, carga y transporte en minería a cielo abierto: Instituto Tecnológico Geominero.

Marin Silviu, Nan; Iosif, Kovacs; Iosif, Andras; Dumitru, Jula: Research Regarding the Establishment of Force and Energetic Characteristics of the Bucket Wheel Excavator in given Working Conditions WSEAS TRANSACTIONS on APPLIED and THEORETICAL MECHANICS.

Marin Silviu, Nan; Iosif, Kovacs; Iosif, Andras; Dumitru, Jula (2008): Study of the working regime of the bucket wheel excavators in the conditions of Romanian open pit lignite mines 8th WSEAS International Conference on SIMULATION, MODELLING and OPTIMIZATION (SMO '08).

Rasper, Ludwig (1975): The bucket wheel excavator. Bay Village, Ohio: Trans Tech (Series on bulk materials handling).

Santamarina, J. Carlos (1989): Rock Excavation with microwaves: a literature review. In *Foundation Engineering: Current Principles and Practices*, pp. 459–473.

Scott, Grant (2006): Microwave pretreatment of low grade copper ore to enhance milling performance and liberation.

U.S Department of Energy (1979): Bucket Wheel Excavator Study. Final Report.

Ván, P.; Vásárhelyi, B. (2010): Rock engineering in difficult ground conditions - soft rocks and karst. Mechanics, EUROCK 2009, Dubrovnik, Cavtat, Croatia, 29 - 31 October 2009. Boca Raton: CRC Press.

W. Durst; W. Vogt (1988): Bucket Wheel Excavator (7).

Z. T. Bieniawski (1989): Engineering Rock Mass Classifications.

LIST OF FIGURES

LIST OF TABLES

LIST OF ABBREVIATIONS

BWE	Bucket Wheel Excavator
BW	Bucket Wheel, spinning part of the machine
RQD	Drill core quality (%)
RMR	Rock Mass Rating, referring to RMR_{89}
UCS	Uniaxial Compression Strength (MPa)
A	Specific cutting resistance (N/cm)
Ke	Cutting resistance (N/cm^2)
Kuz	State of the cutting tools
Dp	Penetration depth

ANNEX I: INPUT DATA OF THE MACHINES

Parameters of the BWE

Table 13 Bucket wheel geometric parameters

BW diameter	d	12 m
Number of buckets	z	16
Frequency of the buckets	ns	70 l/min
Speed	n	4.38 l/min
	ω	0.46 rad/s
Circumferential speed	vs.	2.75 m/s
		< 4.4 m/s

Table 14 Buckets geometric parameters

Necessary volume of the bucket	J	1.637 m3
Width of the bucket	bo	900 mm
	bm	1012 mm
Height of the bucket wall	ho	100 mm
	hm	910 mm
Volume of the bucket	v	1830 l
Peak of conveying capacity		14022 to/h
		9002 m3/h

Table 15 BWE working parameters

Driving angle	φ	65.5°
BW height	hc	5.5 m
Cutting depth	to	800 mm
Cross sectional area of the cutting sickle	A	0.180 m2
Cutting width	b	0.225 m

Required swivel speed in the middle of the cutting sickle	vs 0	15.8m/min
Required swivel speed in other angles	vs φ	38.1m/min
Current Swing speed	V min	8 m/min
	V max	45 m/min
Propulsive power		1100 kW
Performance of the BW	η	0.92
Lifting power	Pl max	210 kW
	Pl min	129 kW
Lifting moment	Ml max	459 kNm
	Ml min	283 kNm
Lifting force	Fl max	109 kN
	Fl min	67 kN
Effective cutting power	Pc max	802 kW
	Pc min	883 kW
Effective cutting moment	Mc max	1750 kNm
	Mc min	1926 kNm
Effective cutting Force	Fc max	321 kN
	Fc min	292 kN
Specific cutting Force	Fc sp max	1107 N/cm
	Fc sp min	1006 N/cm
Maximum drive torque	M max	3601 kNm
Nominal motor speed		980 rpm
Required gear ratio		225

Esrc 1400·30/7·630 BWE parameters

Table 16 EsRc 1400·30/7·630 BWE (Marin Silviu et al.)

Cutting height	7.5	m
Number slices per step	4	-
Diameter BW	11.5	m
Power nominal	630	kW
Extraction volume (Average	3872	m^3/h
Transversal section of the chip	0.1—0.085	m^2

Srs 1300·26/3.5·500 BWE parameters

Table 17 SRs 1300·26/3,5·500 BWE (Marin Silviu et al.)

Cutting height	5	m
Number slices per step	4	-
Diameter BW	8.4	m
Power nominal	500	kW
Extraction volume (Average)	2830	m^3/h
Transversal section of the chip	0.068—0.053	m^2

ANNEX II: MATLAB CODE

- **Calculation of all the possibilities regarding the RMR values**

01

UCS VALUES AND RATING

```
%UNITS =MPa
mtrx1=[];
ucs_i = 20;
ncol1 = 100;
step1 = 10;

ucs=[ucs_i:step1:ncol1];
r = 1;
ncola = 1+(ncol1-ucs_i)/step1;
ucs_rat=zeros(1,ncol1);
aa=0;

while r <= ncola
if  aa+ucs_i <= 1
ucs_rat(1,r) = 0;
elseif aa+ucs_i>1 && aa+ucs_i<=5
ucs_rat(1,r) = 1;
elseif aa+ucs_i>5 && aa+ucs_i<= (25)
ucs_rat(1,r) = 2;
elseif aa+ucs_i>(25) && aa+ucs_i<= (50)
ucs_rat(1,r) = 4;
elseif aa+ucs_i>(50) && aa+ucs_i<=(100)
ucs_rat(1,r) = 7;
elseif aa+ucs_i>(100) && aa+ucs_i<(250)
ucs_rat(1,r) = 12;
elseif aa+ucs_i>=(250)
ucs_rat(1,r) = 15;
end
aa = aa + step1;
r = r + 1;
end
```

02

RQD VALUES AND RATING

```
%UNITS = %
rqd_i=20;
ncol2=100;
step2=10;

rqd=[rqd_i:step2:ncol2];
rr=1;
ncolb=1+(ncol2-rqd_i)/step2;
rqd_rat=zeros(1,ncolb);
bb=0;

while rr <= ncol2
if  bb+rqd_i <25
rqd_rat(1,rr) = 3;
elseif bb+rqd_i >=(25) && bb+rqd_i<(50)
rqd_rat(1,rr) = 8;
elseif bb+rqd_i >=(50) && bb+rqd_i<(75)
rqd_rat(1,rr) = 13;
elseif bb+rqd_i >=(75) && bb+rqd_i<(90)
rqd_rat(1,rr) = 17;
elseif bb+rqd_i >=(90) && bb+rqd_i<=(100)
rqd_rat(1,rr) = 20;
end
bb = bb + step2;
rr = rr + 1;
end
```

03

SPACING OF DISCONTINUITIES

```
%UNITS = mm
ncol211 = 2000;
spa_i1 = 25;
step211 = 25;

spa11=[spa_i1:step211:ncol211];
rr11=1;
rr111=25;
ncolc211=1+(ncol211-spa_i1)/step211;
spa_rat1=zeros(1,ncolc211);
```

```
while rr111 <= ncol211
spa_rat1(1,rr11)=  0.000000001*rr111^3 - 0.000005*rr111^2 + 0.0135*rr111 + 5;
rr111 = rr111+step211;
rr11=rr11+1;
end
```

04

GROUND WATER VALUE AND RATING

```
%UNITS = mm
gw =[1];
gw_rat=[10];
```

05

JOINT PERSISTANCE VALUES AN RATING

```
%UNITS = m
ncol3 = 5;
per_i = 0;
step3= 1;

per = [per_i:step3:ncol3];
rrr = 1;
ncolc = 1+(ncol3-per_i)/step3;
per_rat = zeros(1,ncolc);
cc=0;

while rrr <= ncolc
if  per_i + cc <=(1)
per_rat(1,rrr) = 6;
elseif per_i + cc >(1) && per_i+ cc<=(3)
per_rat(1,rrr) = 4;
elseif per_i + cc >(3) && per_i + cc<=(10)
per_rat(1,rrr) = 2;
elseif per_i + cc >(10) && per_i + cc<=(20)
per_rat(1,rrr) = 1;
elseif per_i + cc >(20)
per_rat(1,rrr) = 0;
end
cc = cc + 0.9;
rrr= rrr+1;
```

```
end
```

06

SEPARATION // APERTURE VALUES AN RATING

```
%UNITS = m

ape_i= 0;
ncol4 = 10;
step4= 1;
ape=[ape_i:step4:ncol4];
ncold=1+(ncol4-ape_i)/step4;
ape_rat=zeros(1,ncold);
s=1;
dd=0;

while s <=ncold
if  ape_i + dd <= 0
ape_rat(1,s) = 6;
ape(1,s)=ape_i+dd;
elseif ape_i + dd > 0 && ape_i + dd<=(0.1)
ape_rat(1,s) = 5;
ape(1,s)=ape_i+dd;
elseif ape_i + dd >=(0.1) && ape_i + dd<(1)
ape_rat(1,s) = 4;
ape(1,s)=ape_i+dd;
elseif ape_i + dd>=(1) && ape_i + dd<(5)
ape_rat(1,s) = 1;
ape(1,s)=ape_i+dd;
elseif ape_i + dd>=(5)
ape_rat(1,s) = 0;
ape(1,s)=ape_i+dd;
end
dd = dd + 0.1;
s= s + 1;
end
```

07

ROUGHNESS VALUES AN RATING

```
%UNITS = X
```

```
rou =[1];
rou_rat=[6];
```

08

INFILLING / GOUGE VALUES & RATINGS

```
%UNITS = X
gou = [1];
gou_rat= [6];
```

09

WEATHERING VALUES & RATINGS

```
%UNITS = X
wea = [1];
wea_rat = [6];
```

10

MATRIX OF RESULTS

```
for i = 1:size(ucs,2)
for ii= 1:size(rqd,2)
for ij = 1:size(spa11,2)
for iii = 1:size(gw,2)
for iiii = 1:size(per,2)
for j = 1:size(ape,2)
for jj = 1:size(rou,2)
for jjj= 1:size(gou,2)
for jjjj= 1:size(wea,2)
imtrx1(1)=ucs(i);
imtrx1(2)=ucs_rat(i);
imtrx1(3)=rqd(ii);
imtrx1(4)=rqd_rat(ii);
imtrx1(5)=spa11(ij);
imtrx1(6)=spa_rat1(ij);
```

```
imtrx1(7)=gw(iii);
imtrx1(8)=gw_rat(iii);
imtrx1(9)=per(iiii);
imtrx1(10)=per_rat(iiii);
imtrx1(11)=ape(j);
imtrx1(12)=ape_rat(j);
imtrx1(13)=rou(jj);
imtrx1(14)=rou_rat(jj);
imtrx1(15)=gou(jjj);
imtrx1(16)=gou_rat(jjj);
imtrx1(17)=wea(jjjj);
imtrx1(18)=wea_rat(jjjj);

mtrx1=[mtrx1;imtrx1];
end
end
end
end
end
end
end
end
end

RMR_matrix1 =
mtrx1(:,1);mtrx1(:,2);mtrx1(:,3);mtrx1(:,4);mtrx1(:,5);mtrx1(:,6);mtrx1(:,7);mtrx1(:,8);mtrx1(:,9);mtrx1(:,10);mtrx1
(:,11);mtrx1(:,12);mtrx1(:,13);mtrx1(:,14);mtrx1(:,15);mtrx1(:,16);mtrx1(:,17);mtrx1(:,18);

RMR_values1 =
mtrx1(:,2)+mtrx1(:,4)+mtrx1(:,6)+mtrx1(:,8)+mtrx1(:,10)+mtrx1(:,12)+mtrx1(:,14)+mtrx1(:,16)+mtrx1(:,18);
```

11

RMR COHESION FRICTION ANGLE AND ROCK MASS STRENGTH

```
RMR = RMR_values1;

[m,n] = size(RMR);
ucs_ = RMR_matrix1(:,1);
coh1 = zeros(m,1);
coh2 = zeros(m,1);
fri1 = zeros(m,1);
fri2 = zeros(m,1);
```

```
st_roc = zeros(m,1);
e = exp(1);
r=1;
mtrx111 =[];
Ke_1= zeros(m,1);
Ke_2= zeros(m,1);

while r <= m
if RMR(r,1)>80 && RMR(r,1)<=100
coh1(r,1) = 450;
coh2(r,1) = 400;
fri1(r,1) = 50;
fri2(r,1)= 45;
st_roc(r,1) = (ucs_(r,1))*e^((RMR(r,1)-100)/25);

Ke_i_1(r,1) = (3.72432675*ucs_(r,1)^(1.592777)*coh1(r,1)^(0.348245478)*fri1(r,1)^(-0.98134))*(10/22.5);
Ke_i_2(r,1) = (3.72432675*ucs_(r,1)^(1.592777)*coh2(r,1)^(0.348245478)*fri2(r,1)^(-0.98134))*(10/22.5);

Ke_1(r,1) = (3.72432675*st_roc(r,1)^(1.592777)*coh1(r,1)^(0.348245478)*fri1(r,1)^(-0.98134))*(10/22.5);
Ke_2(r,1) = (3.72432675*st_roc(r,1)^(1.592777)*coh2(r,1)^(0.348245478)*fri2(r,1)^(-0.98134))*(10/22.5);

elseif RMR(r,1)>60 && RMR(r,1)<=80
coh1(r,1) = 400;
coh2(r,1) = 300;
fri1(r,1) = 45;
fri2(r,1)= 35;
st_roc(r,1) = (ucs_(r,1))*e^((RMR(r,1)-100)/25);

Ke_i_1(r,1) = (3.72432675*ucs_(r,1)^(1.592777)*coh1(r,1)^(0.348245478)*fri1(r,1)^(-0.98134))*(10/22.5);
Ke_i_2(r,1) = (3.72432675*ucs_(r,1)^(1.592777)*coh2(r,1)^(0.348245478)*fri2(r,1)^(-0.98134))*(10/22.5);

Ke_1(r,1) = (3.72432675*st_roc(r,1)^(1.592777)*coh1(r,1)^(0.348245478)*fri1(r,1)^(-0.98134))*(10/22.5);
Ke_2(r,1) = (3.72432675*st_roc(r,1)^(1.592777)*coh2(r,1)^(0.348245478)*fri2(r,1)^(-0.98134))*(10/22.5);

elseif RMR(r,1)>40 && RMR(r,1)<=60
coh1(r,1) = 300;
coh2(r,1) = 200;
fri1(r,1) = 35;
fri2(r,1)= 25;
st_roc(r,1) = (ucs_(r,1))*e^((RMR(r,1)-100)/25);
```

```
Ke_i_1(r,1) = (3.72432675*ucs_(r,1)^(1.592777)*coh1(r,1)^(0.348245478)*fri1(r,1)^(-0.98134))*(10/22.5);
Ke_i_2(r,1) = (3.72432675*ucs_(r,1)^(1.592777)*coh2(r,1)^(0.348245478)*fri2(r,1)^(-0.98134))*(10/22.5);

Ke_1(r,1) = (3.72432675*st_roc(r,1)^(1.592777)*coh1(r,1)^(0.348245478)*fri1(r,1)^(-0.98134))*(10/22.5);
Ke_2(r,1) = (3.72432675*st_roc(r,1)^(1.592777)*coh2(r,1)^(0.348245478)*fri2(r,1)^(-0.98134))*(10/22.5);

elseif RMR(r,1)>20 && RMR(r,1)<=40
coh1(r,1) = 200;
coh2(r,1) = 100;
fri1(r,1) = 25;
fri2(r,1)= 15;
st_roc(r,1) = (ucs_(r,1))*e^((RMR(r,1)-100)/25);

Ke_i_1(r,1) = (3.72432675*ucs_(r,1)^(1.592777)*coh1(r,1)^(0.348245478)*fri1(r,1)^(-0.98134))*(10/22.5);
Ke_i_2(r,1) = (3.72432675*ucs_(r,1)^(1.592777)*coh2(r,1)^(0.348245478)*fri2(r,1)^(-0.98134))*(10/22.5);

Ke_1(r,1) = (3.72432675*st_roc(r,1)^(1.592777)*coh1(r,1)^(0.348245478)*fri1(r,1)^(-0.98134))*(10/22.5);
Ke_2(r,1) = (3.72432675*st_roc(r,1)^(1.592777)*coh2(r,1)^(0.348245478)*fri2(r,1)^(-0.98134))*(10/22.5);

elseif RMR(r,1)<=20
coh1(r,1) = 100;
coh2(r,1) = 50;
fri1(r,1) = 15;
fri2(r,1)= 5;
st_roc(r,1) = (ucs_(r,1))*e^((RMR(r,1)-100)/25);

Ke_i_1(r,1) = (3.72432675*ucs_(r,1)^(1.592777)*coh1(r,1)^(0.348245478)*fri1(r,1)^(-0.98134))*(10/22.5);
Ke_i_2(r,1) = (3.72432675*ucs_(r,1)^(1.592777)*coh2(r,1)^(0.348245478)*fri2(r,1)^(-0.98134))*(10/22.5);

Ke_1(r,1) = (3.72432675*st_roc(r,1)^(1.592777)*coh1(r,1)^(0.348245478)*fri1(r,1)^(-0.98134))*(10/22.5);
Ke_2(r,1) = (3.72432675*st_roc(r,1)^(1.592777)*coh2(r,1)^(0.348245478)*fri2(r,1)^(-0.98134))*(10/22.5);

end
r = r + 1;
end
mtrx111 = [RMR, coh1, coh2, fri1, fri2, ucs_, st_roc, Ke_1, Ke_2,Ke_i_1,Ke_i_2];
12
*BWE WORKING REGIME INPUT DATA*
*Input data needed for the further BWE working regime calculations*

% Transversal section of the chip in cm2, ro angle = 0 rad
```

```
Stm = 0.18*100^2;
% Transversal section of the chip in cm2, ro angle =/ 0 rad
%St(ro)=
% Number of buckets
nc = 16;
% Cutting height = height mined out slice, m
H= (2/3)*12;
% Diameter of the rotor, m
D = 12;
% Cutting radius, m
R = D/2;
% *Ratio between the penetration force Fy and diggin force Fx,
% experimentally*
Ky = 0.3;
% *Ratio between lateral force Fz and digginf force Fx, experimentally*
Kz = 0.3;
% Cutting speed m/s
Vt= 2.75;
% Swelling speed m/s
Vp = 15.8/60;
% Number of unloading operation performed by the buckets, s^-1
z = 70/60;
% Maximum cutting thickness, width of the chip, m
h_0 = 0.3;
% Width of the chip removed by the bucket, m
b = 0.225;
% Density of the massive material, t/m3
ddd = 25.7/9.81;
% Gravity constant, m/s2
gg= 9.81;
% Active height of the bucket
hc = 0.91;
% Performance of the loading / unloading process, btwn 0.6/0.7 according to literature
nr = 0.65;
% Bulk coefficient
Ka = 1.65;
% Theoretical excavation capacity, m3/h
Qt = 4167;
% Transmission output btwn rotor and bucket wheel
nt = 0.92;
% theoretical excavation power, kW
```

```
Pt = 800;
```

13

BWE WORKING REGIME CALCULATIONS

```
%%                *Calculations Of Parameters*

nca = nc*(acos(1-H/R))/(2*pi);              % Active buckets in a given period of time
Va = hc*h_0*b;                              % Volume of a chip cut by the bucket, m3
%K1 = Kuz/(3.6*10^2*Ka*nt);
%K2 = (grav)*dens*(D-H/2-2/3*hc)/(3.6*10^3*Ka*nt);
%Ce =(10*Kuz*Ke)*((1/n_r)*Hr*dens(grav)      % Extraction factor, kW
dens_a = ddd/Ka;                            % Bulk material density, t/m3
Ga = ddd * gg * Va;                         % Weight of the chip material, KN

Qm = 3600 * Va * z;                         % Momentary excavating capacity, m3/h


%%        *Calculations for the working regime of the machine*
Fxm1 = zeros(m,1);
FxR1= zeros(m,1);
Fym1= zeros(m,1);
FyR1 = zeros(m,1);
Fzm1 = zeros(m,1);
FzR1 = zeros(m,1);
Pex1 = zeros(m,1);
P1 = zeros(m,1);
Pp1 = zeros(m,1);
Pt1 = zeros(m,1);
Qt1= zeros(m,1);
Fxm2 = zeros(m,1);
FxR2 = zeros(m,1);
Fym2 = zeros(m,1);
FyR2 = zeros(m,1);
Fzm2 = zeros(m,1);
FzR2 = zeros(m,1);
Pex2 = zeros(m,1);
P2 = zeros(m,1);
Pp2 = zeros(m,1);
Pt2 = zeros(m,1);
Qt2 = zeros(m,1);
Ce_2 = zeros(m,1);
Ce_1 = zeros(m,1);
```

```
qqt1 = zeros(m,1);
qqt2 = zeros(m,1);
r_1 =1;

matrix_1=[];
matrix_2=[];
matrix_3=[];

%%              * Wear of the teeth in the bucket *

%   kuz = 1-> new cutting tools
%   kuz = 1,2-1,5 -> average worn cutting tools
%   kuz >= 2 -> very worn cutting tools

[m,n] = size(RMR);
r_1=1;
r1=1;
while r_1<=m
Kuz =1;
K1 = Kuz/(3.6*10^2*Ka*nt);
K2 = gg*(ddd)*(D-H/2-2/3*hc)/(3.6*10^3*Ka*nt);
ce1= gg*(10*Kuz)*((1/nr)*hc*(ddd));
Ce_1(r_1,1) =  Ke_1(r_1,1).*ce1;
Ce_2(r_1,1) =  Ke_2(r_1,1).*ce1;

Fxm1(r_1,1) =  Ke_1(r_1,1) * Kuz * Stm;
FxR1(r_1,1) = nca * Fxm1(r_1,1);

Fym1(r_1,1) = Ky * Kuz * Ke_1(r_1,1) * Stm;
FyR1(r_1,1) = Ky * Kuz * Ke_1(r_1,1) * Stm * nca;
Fzm1(r_1,1) = Kz*Ke_1(r_1,1)*Stm*Kuz;
FzR1(r_1,1) = FxR1(r_1,1)*Kz;

Pex1(r_1,1) = (1/360)*Kuz*Ke_1(r_1,1)*Qm;

Pp1(r_1,1) = (10^-3)*FzR1(r_1,1)*Vp;
Pt1(r_1,1) = ((K1*Ke_1(r_1,1))+K2)*Qt;

qqt1(r_1,1)=((K1*Ke_1(r_1,1))+K2);
Qt1(r_1,1) = Pt*qqt1(r_1,1)^-1;
```

```
Fxm2(r_1,1) =  Ke_2(r_1,1) * Kuz * Stm;
FxR2(r_1,1) = nca * Fxm1(r_1,1);

Fym2(r_1,1) = Ky * Kuz * Ke_2(r_1,1) * Stm;
FyR2(r_1,1) = Ky * Kuz * Ke_2(r_1,1) * Stm * nca;
Fzm2(r_1,1) = Kz*Ke_1(r_1,1)*Stm*Kuz;
FzR2(r_1,1) = FxR2(r_1,1)*Kz;

Pex2(r_1,1) = (1/360)*Kuz*Ke_2(r_1,1)*Qm;

Pp2(r_1,1) = (10^-3)*FzR2(r_1,1)*Vp;
Pt2(r_1,1) = ((K1*Ke_2(r_1,1))+K2)*Qt;
qqt2(r_1,1)=((K1*Ke_2(r_1,1))+K2);
Qt2(r_1,1) = Pt*qqt2(r_1,1)^-1;

r_1 = r_1 +1;

matrix_1 = [Ke_1,Fxm1,Fym1,Fzm1,Pt1,Qt1,Ke_2,Fxm2,Fym2,Fzm2,Pt2,Qt2];

end
r_1=1;
while r_1<=m
Kuz=1.5;
K1 = Kuz/(3.6*10^2*Ka*nt);
K2 = gg*(ddd)*(D-H/2-2/3*hc)/(3.6*10^3*Ka*nt);
ce1= gg*(10*Kuz)*((1/nr)*hc*(ddd));
Ce_1(r_1,1) =  Ke_1(r_1,1).*ce1;
Ce_2(r_1,1) =  Ke_2(r_1,1).*ce1;

Fxm1(r_1,1) =  Ke_1(r_1,1) * Kuz * Stm;
FxR1(r_1,1) = nca * Fxm1(r_1,1);

Fym1(r_1,1) = Ky * Kuz * Ke_1(r_1,1) * Stm;
FyR1(r_1,1) = Ky * Kuz * Ke_1(r_1,1) * Stm * nca;
Fzm1(r_1,1) = Kz*Ke_1(r_1,1)*Stm*Kuz;
FzR1(r_1,1) = FxR1(r_1,1)*Kz;

Pex1(r_1,1) = (1/360)*Kuz*Ke_1(r_1,1)*Qm;

Pp1(r_1,1) = (10^-3)*FzR1(r_1,1)*Vp;
Pt1(r_1,1) = ((K1*Ke_1(r_1,1))+K2)*Qt;
```

```
qqt1(r_1,1)=((K1*Ke_1(r_1,1))+K2);
Qt1(r_1,1) = Pt*qqt1(r_1,1)^-1;

Fxm2(r_1,1) =  Ke_2(r_1,1) * Kuz * Stm;
FxR2(r_1,1) = nca * Fxm1(r_1,1);

Fym2(r_1,1) = Ky * Kuz * Ke_2(r_1,1) * Stm;
FyR2(r_1,1) = Ky * Kuz * Ke_2(r_1,1) * Stm * nca;
Fzm2(r_1,1) = Kz*Ke_1(r_1,1)*Stm*Kuz;
FzR2(r_1,1) = FxR2(r_1,1)*Kz;

Pex2(r_1,1) = (1/360)*Kuz*Ke_2(r_1,1)*Qm;

Pp2(r_1,1) = (10^-3)*FzR2(r_1,1)*Vp;
Pt2(r_1,1) = ((K1*Ke_2(r_1,1))+K2)*Qt;
qqt2(r_1,1)=((K1*Ke_2(r_1,1))+K2);
Qt2(r_1,1) = Pt*qqt2(r_1,1)^-1;

r_1 = r_1 +1;

matrix_2 = [Ke_1,Fxm1,Fym1,Fzm1,Pt1,Qt1,Ke_2,Fxm2,Fym2,Fzm2,Pt2,Qt2];
end
r_1=1;
while r_1<=m
Kuz=2;
K1 = Kuz/(3.6*10^2*Ka*nt);
K2 = gg*(ddd)*(D-H/2-2/3*hc)/(3.6*10^3*Ka*nt);
ce1= gg*(10*Kuz)*((1/nr)*hc*(ddd));
Ce_1(r_1,1) =  Ke_1(r_1,1).*ce1;
Ce_2(r_1,1) =  Ke_2(r_1,1).*ce1;

Fxm1(r_1,1) =  Ke_1(r_1,1) * Kuz * Stm;
FxR1(r_1,1) = nca * Fxm1(r_1,1);

Fym1(r_1,1) = Ky * Kuz * Ke_1(r_1,1) * Stm;
FyR1(r_1,1) = Ky * Kuz * Ke_1(r_1,1) * Stm * nca;
Fzm1(r_1,1) = Kz*Ke_1(r_1,1)*Stm*Kuz;
FzR1(r_1,1) = FxR1(r_1,1)*Kz;

Pex1(r_1,1) = (1/360)*Kuz*Ke_1(r_1,1)*Qm;
```

```
Pp1(r_1,1) = (10^-3)*FzR1(r_1,1)*Vp;
Pt1(r_1,1) = ((K1*Ke_1(r_1,1))+K2)*Qt;

qqt1(r_1,1)=((K1*Ke_1(r_1,1))+K2);
Qt1(r_1,1) = Pt*qqt1(r_1,1)^-1;

Fxm2(r_1,1) =  Ke_2(r_1,1) * Kuz * Stm;
FxR2(r_1,1) = nca * Fxm1(r_1,1);

Fym2(r_1,1) = Ky * Kuz * Ke_2(r_1,1) * Stm;
FyR2(r_1,1) = Ky * Kuz * Ke_2(r_1,1) * Stm * nca;
Fzm2(r_1,1) = Kz*Ke_1(r_1,1)*Stm*Kuz;
FzR2(r_1,1) = FxR2(r_1,1)*Kz;

Pex2(r_1,1) = (1/360)*Kuz*Ke_2(r_1,1)*Qm;

Pp2(r_1,1) = (10^-3)*FzR2(r_1,1)*Vp;
Pt2(r_1,1) = ((K1*Ke_2(r_1,1))+K2)*Qt;
qqt2(r_1,1)=((K1*Ke_2(r_1,1))+K2);
Qt2(r_1,1) = Pt*qqt2(r_1,1)^-1;

r_1 = r_1 +1;

matrix_3 = [Ke_1,Fxm1,Fym1,Fzm1,Pt1,Qt1,Ke_2,Fxm2,Fym2,Fzm2,Pt2,Qt2];
end
```

- **Code to calculate the graphs to understand the behavior of the method used**

01

GRAPH FOR Ke AND Es = All possibilities

```
%% From 200 to 0 MPa

sig1 = [95:200];
coh1 = [3:4];
phi1 = [30:45];

sig2 = [45:100];
coh2 = [2:3];
phi2 = [20:35];

sig3 = [20:50];
coh3 = [1:2];
phi3 = [15:25];

sig4 = [0:25];
coh4 = [0:1];
phi4 = [5:20];

mtrx1 = [];

for i= 1:size(sig1,2)
for ii= 1:size(coh1,2)
for iii= 1:size(phi1,2)
imtrx1(1)=sig1(i);
imtrx1(2)=coh1(ii);
imtrx1(3)=phi1(iii);

mtrx1=[mtrx1;imtrx1];
end
end
end

r = 1;
vctr = mtrx1(:,1);
```

```
[mm,nn]=size(vctr);
KE1 = zeros(mm,nn);
sig11 = mtrx1(:,1);
coh11 = mtrx1(:,2);
phi11 = mtrx1(:,3);
while r <= mm
KE1(r,1) = (3.72432675*sig11(r,1)^(1.592777)*coh11(r,1)^(0.348245478)*phi11(r,1)^(-0.98134))*(10/22.5);

r = r + 1;
end

%% From 100 to 50 MPa
mtrx2 = [];
for i= 1:size(sig2,2)
for ii= 1:size(coh2,2)
for iii= 1:size(phi2,2)
imtrx2(1)=sig2(i);
imtrx2(2)=coh2(ii);
imtrx2(3)=phi2(iii);

mtrx2=[mtrx2;imtrx2];
end
end
end
r = 1;
vctr = mtrx2(:,1);
[mm,nn]=size(vctr);
KE2 = zeros(mm,nn);
sig22 = mtrx2(:,1);
coh22 = mtrx2(:,2);
phi22 = mtrx2(:,3);
while r <= mm
KE2(r,1) = (3.72432675*sig22(r,1)^(1.592777)*coh22(r,1)^(0.348245478)*phi22(r,1)^(-0.98134))*(10/22.5);
r = r + 1;
end

%% From 50 to 25 MPa
mtrx3 = [];
for i= 1:size(sig3,2)
for ii= 1:size(coh3,2)
for iii= 1:size(phi3,2)
```

```
imtrx3(1)=sig3(i);
imtrx3(2)=coh3(ii);
imtrx3(3)=phi3(iii);

mtrx3=[mtrx3;imtrx3];
end
end
end

r = 1;
vctr = mtrx3(:,1);
[mm,nn]=size(vctr);
KE3 = zeros(mm,nn);
sig33 = mtrx3(:,1);
coh33 = mtrx3(:,2);
phi33 = mtrx3(:,3);
while r <= mm
KE3(r,1) = (3.72432675*sig33(r,1)^(1.592777)*coh33(r,1)^(0.348245478)*phi33(r,1)^(-0.98134))*(10/22.5);
r = r + 1;
end
%% From 25 to 0 MPa
mtrx4 = [];
for i= 1:size(sig4,2)
for ii= 1:size(coh4,2)
for iii= 1:size(phi4,2)
imtrx4(1)=sig4(i);
imtrx4(2)=coh4(ii);
imtrx4(3)=phi4(iii);

mtrx4=[mtrx4;imtrx4];
end
end
end

r = 1;
vctr = mtrx4(:,1);
[mm,nn]=size(vctr);
KE4 = zeros(mm,nn);
sig44 = mtrx4(:,1);
coh44 = mtrx4(:,2);
phi44 = mtrx4(:,3);
```

```
while r <= mm
KE4(r,1) = (3.72432675*sig44(r,1)^(1.592777)*coh44(r,1)^(0.348245478)*phi44(r,1)^(-0.98134))*(10/22.5);
r = r + 1;
end

%% Max and Min of the function A
sig5 = [0:10:200];
coh5 = [0:20:400];
phi5 = [0:2:40];
mtrx5 = [];
for i= 1:size(sig5,2)
for ii= 1:size(coh5,2)
for iii= 1:size(phi5,2)
imtrx5(1)=sig5(i);
imtrx5(2)=coh5(ii);
imtrx5(3)=phi5(iii);

mtrx5=[mtrx5;imtrx5];
end
end
end

r = 1;
vctr5 = mtrx5(:,1);
[mm5,nn5]=size(vctr5);
A5 = zeros(mm5,nn5);
sig55 = mtrx5(:,1);
coh55 = mtrx5(:,2);
phi55 = mtrx5(:,3);

while r <= mm5
A5(r,1) = (3.72432675*sig55(r,1)^(1.592777)*coh55(r,1)^(0.348245478)*phi55(r,1)^(-0.98134))*(10/22.5);
r = r + 1;
end


%% scatterS

h=figure;
xlabel ('Cohesion (MPa)')
ylabel ('Ke (N/cm^2)')
```

```
grid on
title ('Cohesion vs Ke')
hold on
scatter (coh11,KE1,50,'*')
scatter (coh22,KE2,50,'o')
scatter (coh33,KE3,50,'s')
scatter (coh44,KE4,50,'.')
title(legend,'Range of values (RMR)')
legend('location','eastoutside')
legend('Range 1','Range 2','Range 3','Range 4')
%scatter (coh55,A5)
saveas(h,'all_poss1','png');

h=figure;
xlabel ('Friction angle (deg)')
ylabel ('Ke (N/cm^2)')
grid on
title ('Friction vs Ke')
hold on
scatter (phi11,KE1,50,'*')
scatter (phi22,KE2,50,'o')
scatter (phi33,KE3,50,'s')
scatter (phi44,KE4,50,'.')
title(legend,'Range of values (RMR)')
legend('location','eastoutside')
legend('Range 1','Range 2','Range 3','Range 4')
%scatter (phi55,A5)
saveas(h,'all_poss2','png');

h=figure;
xlabel ('UCS (MPa)')
ylabel ('Ke (N/cm^2)')
grid on
title ('UCS vs Ke')
hold on
scatter (sig11,KE1,50,'*')
scatter (sig22,KE2,50,'o')
scatter (sig33,KE3,50,'s')
scatter (sig44,KE4,50,'.')
%scatter (sig55,A5)
title(legend,'Range of values (RMR)')
```

```
legend('location','eastoutside')
legend('Range 1','Range 2','Range 3','Range 4')
saveas(h,'all_poss3','png');
```

02

GRAPH FOR Ke AND Es = UCS constant

```
clc
% From 100 MPa

sig1 = [100];
coh1 = [0:4];
phi1 = [0:45];
mtrx1 = [];

for i= 1:size(sig1,2)
for ii= 1:size(coh1,2)
for iii= 1:size(phi1,2)
imtrx1(1)=sig1(i);
imtrx1(2)=coh1(ii);
imtrx1(3)=phi1(iii);

mtrx1=[mtrx1;imtrx1];
end
end
end

r = 1;
vctr = mtrx1(:,1);
[mm,nn]=size(vctr);
KE1 = zeros(mm,nn);
sig11 = mtrx1(:,1);
coh11 = mtrx1(:,2);
phi11 = mtrx1(:,3);
while r <= mm
KE1(r,1) = (3.72432675*sig11(r,1)^(1.592777)*coh11(r,1)^(0.348245478)*phi11(r,1)^(-0.98134))*(10/22.5);

r = r + 1;
end
```

```
%%                  scatterS

h=figure;
xlabel ('Cohesion (MPa)')
ylabel ('Ke (N/cm^2)')
grid on
title ('Cohesion vs Ke')
hold on
scatter (coh11,KE1,50,'.')
saveas(h,'ucs_cte1','png');

h=figure;
xlabel ('Friction angle (deg)')
ylabel ('Ke (N/cm^2)')
grid on
title ('Friction vs Ke')
hold on
scatter (phi11,KE1,50,'.')
saveas(h,'ucs_cte2','png');

h=figure;
xlabel ('UCS (MPa)')
ylabel ('Ke (N/cm^2)')
grid on
title ('UCS vs Ke')
hold on
scatter (sig11,KE1,50,'.')
saveas(h,'ucs_cte3','png');
```

03

GRAPH FOR Ke AND Es = Cohesion constant

```
%_____________________________________________________________________
clc
% From 200 MPa

sig2 = [0:250];
coh2 = [2];
phi2 = [0:45];
mtrx2 = [];

for i= 1:size(sig2,2)
```

```
for ii= 1:size(coh2,2)
for iii= 1:size(phi2,2)
imtrx2(1)=sig2(i);
imtrx2(2)=coh2(ii);
imtrx2(3)=phi2(iii);

mtrx2=[mtrx2;imtrx2];
end
end
end

r = 2;
vctr = mtrx2(:,1);
[mm,nn]=size(vctr);
KE2 = zeros(mm,nn);
sig22 = mtrx2(:,1);
coh22 = mtrx2(:,2);
phi22 = mtrx2(:,3);
while r <= mm
KE2(r,1) = (3.72432675*sig22(r,1)^(1.592777)*coh22(r,1)^(0.348245478)*phi22(r,1)^(-0.98134))*(10/22.5);

r = r + 1;
end


%%                  scatterS

h=figure;
xlabel ('Cohesion (MPa)')
ylabel ('Ke (N/cm^2)')
grid on
title ('Cohesion vs Ke')
hold on
scatter (coh22,KE2,50,'.')
saveas(h,'coh_cte1','png');

h=figure;
xlabel ('Friction angle (deg)')
ylabel ('Ke (N/cm^2)')
grid on
title ('Friction vs Ke')
```

```
hold on
scatter (phi22,KE2,50,'.')
saveas(h,'coh_cte2','png');

h=figure;
xlabel ('UCS (MPa)')
ylabel ('Ke (N/cm^2)')
grid on
title ('UCS vs Ke')
hold on
scatter (sig22,KE2,50,'.')
saveas(h,'coh_cte3','png');
```

04

GRAPH FOR Ke AND Es = Friction angle constant

```
clc
%% From 22 deg

sig3 = [0:250];
coh3 = [0:4];
phi3 = [22];
mtrx3 = [];

for i= 1:size(sig3,2)
for ii= 1:size(coh3,2)
for iii= 1:size(phi3,2)
imtrx3(1)=sig3(i);
imtrx3(2)=coh3(ii);
imtrx3(3)=phi3(iii);

mtrx3=[mtrx3;imtrx3];
end
end
end

r = 2;
vctr = mtrx3(:,1);
[mm,nn]=size(vctr);
KE3 = zeros(mm,nn);
sig33 = mtrx3(:,1);
```

```
coh33 = mtrx3(:,2);
phi33 = mtrx3(:,3);
while r <= mm
KE3(r,1) = (3.72432675*sig33(r,1)^(1.592777)*coh33(r,1)^(0.348245478)*phi33(r,1)^(-0.98134))*(10/22.5);

r = r + 1;
end


%%                  scatterS

h=figure;
xlabel ('Cohesion (MPa)')
ylabel ('Ke (N/cm^2)')
grid on
title ('Cohesion vs Ke')
hold on
scatter (coh33,KE3,50,'.')
saveas(h,'fri_cte1','png');

h=figure;
xlabel ('Friction angle (deg)')
ylabel ('Ke (N/cm^2)')
grid on
title ('Friction vs Ke')
hold on
scatter (phi33,KE3,50,'.')
saveas(h,'fri_cte2','png');

h=figure;
xlabel ('UCS (MPa)')
ylabel ('Ke (N/cm^2)')
grid on
title ('UCS vs Ke')
hold on
scatter (sig33,KE3,50,'.')
saveas(h,'fri_cte3','png');
```